

# Analog Circuit Design

Harald Pretl  
Johannes Kepler University  
harald.pretl@jku.at

Michael Koefinger

Simon Dorrer

2026-01-08

## Table of contents

1	Introduction .....	3
1.1	IHP's SG13G2 130nm CMOS Technology .....	4
1.2	Schematic Entry Using Xschem .....	5
1.3	Circuit Simulation Using ngspice .....	5
1.4	Integrated IC Design Environment (IIC-OSIC-TOOLS) .....	5
1.5	Setting up the Design Directory .....	5
1.5.1	Creating Backups .....	6
1.5.2	Updating the Repository .....	6
2	First Steps .....	6
2.1	The Metal-Oxide-Semiconductor Field-Effect-Transistor (MOSFET) .....	7
2.1.1	Large-Signal MOSFET Model .....	10
2.1.2	Small-Signal MOSFET Model .....	12
2.2	Conclusion .....	17
3	Transistor Sizing Using gm/ID Methodology .....	18
3.1	MOSFET Characterization Testbench .....	18
3.2	NMOS Characterization in Saturation .....	21
3.3	PMOS Characterization in Saturation .....	29
3.4	Tradeoffs in Saturation .....	34
3.5	NMOS and PMOS Characterization in Triode .....	35
3.6	Tradeoffs in Triode .....	37
4	First Circuit: MOSFET Diode .....	38
4.1	MOSFET Diode Sizing .....	40
4.2	MOSFET Diode Large-Signal Behavior .....	41
4.3	MOSFET Diode Small-Signal Analysis .....	42
4.4	MOSFET Diode Stability Analysis .....	44
4.5	MOSFET Diode Noise Calculation .....	47
4.6	Conclusion .....	51
5	Common-Source Amplifier .....	51
5.1	Sense Amplifier Driving 50 Ohm Matched Load .....	52
6	Current Mirror .....	55
7	Differential Pair .....	56
7.1	Differential Operation of the Diffpair .....	57
7.2	Common-Mode Operation of the Diffpair .....	57
8	A Basic 5-Transistor OTA .....	59
8.1	Voltage Buffer with OTA .....	60

8.2	Large-Signal Analysis of the OTA .....	61
8.3	Small-Signal Analysis of the OTA .....	63
8.3.1	OTA Small-Signal Transfer Function .....	63
8.3.2	OTA Noise .....	66
8.4	5T-OTA Sizing .....	68
8.5	5T-OTA Simulation .....	70
8.6	Component Mismatch .....	70
8.6.1	MOSFET Mismatch .....	70
8.6.2	Resistor Mismatch .....	72
8.6.3	Capacitor Mismatch .....	72
8.7	5T-OTA Simulation versus PVT and MC .....	72
8.7.1	PVT Simulation Analysis .....	75
8.7.2	Monte Carlo Simulation Analysis .....	75
8.8	OTA Variants .....	75
9	Cascode Stage .....	78
9.1	Cascode Output Impedance .....	80
9.2	Cascode Input Impedance .....	81
10	Improved Current Mirrors .....	82
10.1	Low-Voltage Regulated Current Mirror .....	89
10.2	Current Source Variations Summary .....	90
10.3	Current Mirror Matching .....	91
11	Improved (Telescopic) OTA .....	95
11.1	Sizing the Improved OTA .....	96
11.2	Designing the Improved OTA .....	98
11.2.1	Discussion of the OTA Design .....	98
11.3	Simulation of Improved OTA .....	99
11.4	Corner Simulation of Improved OTA .....	101
12	Biasing .....	103
12.1	Bandgap Reference .....	104
12.2	Banba Bandgap Reference .....	109
13	Differential OTAs .....	111
13.1	Miller Compensation .....	112
13.2	Common-Mode Regulation .....	115
13.3	Final Differential OTA .....	118
13.4	Differential OTA Variants .....	120
14	An RC-OPAMP Filter .....	121
15	Summary & Conclusion .....	121
16	Appendix: Middlebrook's Method .....	122
17	Appendix: Useful Circuit Theorems .....	123
17.1	Miller's Theorem .....	123
17.2	Bode's Noise Theorem .....	124
18	Appendix: 5T-OTA Small-Signal Output Impedance .....	124
18.1	Open-Loop Configuration .....	125
18.2	Closed-Loop Configuration .....	126
19	Appendix: Linux Cheatsheet .....	127
20	Appendix: Xschem Cheatsheet .....	127

21	Appendix: ngspice Cheatsheet .....	128
21.1	Commands .....	128
21.2	Options .....	129
21.3	Convergence Helper .....	130
21.4	Internal Variables .....	130
22	Appendix: Circuit Designer's Etiquette .....	130
22.1	Prolog .....	130
22.2	Pins .....	130
22.3	Schematics .....	131
22.4	Symbols .....	133
22.5	Design Robustness .....	133
22.6	Rules for Good Mixed-Signal and RF Circuits .....	133
22.7	VHDL/Verilog Coding Guide .....	134
22.8	Further Reading .....	135
	Bibliography .....	135

## 1 Introduction

This is the material for an intermediate-level MOSFET analog circuit design course, held at JKU under course number 336.009 (“KV Analoge Schaltungstechnik”).

The course makes heavy use of circuit simulation, using **Xschem** for schematic entry and **ngspice** for simulation. The 130nm CMOS technology **SG13G2** from IHP Microelectronics is used.

Tools and PDK are integrated in the **IIC-OSIC-TOOLS** Docker image, which will be used during the coursework.

### **! Important**

All course material (source code of this document, Jupyter notebooks for calculations, Xschem circuits, etc.) is made publicly available on GitHub (follow this link) and shared under the Apache-2.0 license.

Please feel free to submit pull requests on GitHub to fix errors and omissions!

The production of this document would be impossible without these (and many more) great open-source software products: **VS Code**, **Quarto**, **Pandoc**, **TexLive**, **Jupyter Notebook**, **Python**, **Xschem**, **ngspice**, **CACE**, **pygmid**, **schemdraw**, **Numpy**, **Scipy**, **Matplotlib**, **Pandas**, **Git**, **Docker**, **Ubuntu**, **Linux**, ...

### **! Important**

Please use the **IIC-OSIC-TOOLS** image with tag **2025.09** or later!

## Further Reading

These notes are considered to be self-contained, although some explanations are kept short and probably lack depth. To dive into details, there are many excellent textbooks on analog circuit design available. Among them, we can recommend the following ones:

- [1] is a classic book and a definitive read.
- [2] is an excellent introduction into CMOS analog circuit design.
- [3] is a book with a lot of very useful information hard to find elsewhere.
- [4] is a great reference for MOSFET device physics and modeling.
- [5] is the in-depth reference for MOSFET device operation.

## 1.1 IHP's SG13G2 130nm CMOS Technology

SG13G2 is the name of a 130nm CMOS technology (strictly speaking BiCMOS) from IHP Microelectronics. It features low-voltage (thin-oxide) core MOSFET, high-voltage (thick-oxide) I/O MOSFET, various types of linear resistors, and 7 layers of Aluminum metallization (5 thin plus 2 thick metal layers). This PDK is open-source, and the complete process specification can be found at SG13G2 process specification. While we will not do layouts in this course, the layout rules can be found at SG13G2 layout rules.

For our circuit design, the most important parameters of the available devices are summarized in the following table. Matching properties are summarized in Table 3.

Table 1: IHP SG13G2 devices

Component	Device Name	Specifications
Low-voltage NMOS	(LV) sg13_lv_nmos	operating voltage (nom.) $V_{DD} = 1.5$ V, $L_{min} = 0.13 \mu\text{m}$ , $V_{th} \approx 0.5$ V; isolated NMOS available
Low-voltage PMOS	(LV) sg13_lv_pmos	operating voltage (nom.) $V_{DD} = 1.5$ V, $L_{min} = 0.13 \mu\text{m}$ , $V_{th} \approx -0.47$ V
High-voltage NMOS	(HV) sg13_hv_nmos	operating voltage (nom.) $V_{DD} = 3.3$ V, $L_{min} = 0.45 \mu\text{m}$ , $V_{th} \approx 0.7$ V; isolated NMOS available
High-voltage PMOS	(HV) sg13_hv_pmos	operating voltage (nom.) $V_{DD} = 3.3$ V, $L_{min} = 0.45 \mu\text{m}$ , $V_{th} \approx -0.65$ V
Silicided poly resistor	r <sub>sil</sub>	$R_s = 7 \Omega \pm 10\%$ , $\text{TC}_1 = 3100 \text{ ppm/K}$
Poly resistor	r <sub>ppd</sub>	$R_s = 260 \Omega \pm 10\%$ , $\text{TC}_1 = 170 \text{ ppm/K}$
Poly resistor high	r <sub>high</sub>	$R_s = 1360 \Omega \pm 15\%$ , $\text{TC}_1 = -2300 \text{ ppm/K}$
MIM capacitor	cap_cmim	$C' = 1.5 \text{ fF} / \mu\text{m}^2 \pm 10\%$ , $\text{VC}_1 = -26 \text{ ppm/V}$ , $\text{TC}_1 = 3.6 \text{ ppm/K}$ , breakdown voltage > 15 V
MOM capacitor	n/a	The metal stack is well-suited for MOM capacitors due to 5 thin metal layers, but no primitive capacitor device is available at this point.

## 1.2 Schematic Entry Using Xschem

Xschem is an open-source schematic entry tool with emphasis on integrated circuits. For up-to-date information of the many features of Xschem and the basic operation of it please look at the available online documentation. Usage of Xschem will be learned with the first few basic examples, essentially using a single MOSFET. The usage model of Xschem is that the schematic is hierarchically drawn, and the simulation and evaluation statements are contained in the schematics. Further, Xschem offers embedded graphing, which we will mostly use.

A summary of important Xschem keyboard shortcuts is provided in Section 20.

## 1.3 Circuit Simulation Using ngspice

ngspice is an open-source circuit simulator with SPICE dependency [6]. Besides the usual simulated types like op (operating point), dc (dc sweeps), tran (time domain), ac (small-signal frequency sweeps), and noise (small-signal noise analysis), ngspice offers a script-like control interface, where many different simulation controls and result evaluations can be done. For detailed information please refer to the latest online manual.

Important ngspice simulation commands and options (e.g., how to control convergence settings) are listed in Section 21.

## 1.4 Integrated IC Design Environment (IIC-OSIC-TOOLS)

In order to make use of the various required components (tools like Xschem and ngspice, PDKs like SG13G2) easier, we will use the **IIC-OSIC-TOOLS**. This is a pre-compiled Docker image which allows to do circuit design on a virtual machine on virtually any type of computing equipment (personal PC, Raspberry Pi, cloud server) on various operating systems (Windows, macOS, Linux). For further information like installed tools, how to setup a VM, etc., please look at IIC-OSIC-TOOLS GitHub page.

### ⚠ Preparation

Please make sure to receive information about your personal VM access ahead of the course start.

Experienced users can install this image on their personal computer, for JKU students the IIC will host a VM on our compute cluster and provide personal login credentials.

### ⚠ Linux

In this course, we assume that students have a basic knowledge of Linux and how to operate it using the terminal (shell). If you are not yet familiar with Linux (which is basically a must when doing integrated circuit design as many tools are only available on Linux), then please check out a Linux introductory course or tutorial online, there are many resources available.

A summary of important Linux shell commands is provided in Section 19.

## 1.5 Setting up the Design Directory

- Open your VM by entering the URL in your browser.

- Open a terminal (third icon in the taskbar at the bottom). You should get the following prompt: `/foss/designs >`
- Clone the git repository into the current directory: `git clone https://github.com/iic-jku/analog-circuit-design.git`
- This GitHub repository includes a file called `.designinit`, which sets the PDK and certain paths. However, this must be located in `/foss/designs/`
- Therefore, we first need to copy it there: `cp analog-circuit-design/.designinit .`
- Then we adjust the variable `XSCHEM_USER_LIBRARY_PATH` by opening the file in an editor e.g. `nano .designinit`
  - Change the last line from `export XSCHEM_USER_LIBRARY_PATH=$DESIGNS/xschem` to `export XSCHEM_USER_LIBRARY_PATH=$DESIGNS/analog-circuit-design/xschem`
- To apply the changes, we need to close the current terminal window: `exit`
- Open again a terminal
- Test if the correct PDK gets selected: `echo $PDK` (you should get `sg13g2` as the answer)
- Change into the GitHub repository: `cd analog-circuit-design`
- Start xschem using `xschem` or directly open a specific schematic using `xschem xschem/dc_lv_nmos.sch`

### 1.5.1 Creating Backups

You can easily create backups of your work by creating a zip archive of the complete directory:

- Change to the parent directory: `cd /foss/designs`
- Create a zip archive from the complete design folder: `zip backup.zip analog-circuit-design -r`

### 1.5.2 Updating the Repository

- **Create a backup!**
- Go to directory: e.g. `cd /foss/designs/analog-circuit-design`
- Fetch newest changes from the origin: `git fetch origin`
- Merge changes from the origin into local branch ‘master’: `git merge origin/main`

#### Git Merge Conflicts

It is possible that `git merge` does not complete successfully. Either you are able to resolve the merge conflict manually, or it may be easier to make a fresh clone of the repository and adding your local changes manually from the backup.

#### Important

Please think twice before executing any git command without a backup, as this could lead to permanent loss of data!

## 2 First Steps

In this first chapter we will learn to use Xschem for schematic entry, and how to operate the ngspice SPICE simulator for circuit simulations. Further, we will make ourself familiar with the transistor and other passive components available in the IHP Microelectronics SG13G2

technology. While this is strictly speaking a BiCMOS technology offering MOSFETs as well as SiGe heterojunction bipolar transistors (HBTs), we will use it as a pure CMOS technology, which is available from IHP under the name SG13C.

## 2.1 The Metal-Oxide-Semiconductor Field-Effect-Transistor (MOSFET)

In this course, we will **not** dive into semiconductor physics and derive the device operation bottom-up starting from a fundamental level governed by quantum mechanics or a simplified solid-state physics based approach resulting in the well-known square-law model. Instead, we will treat the MOSFET behaviorally by assuming a 4-terminal device, and the performance of this device regarding its terminal voltages and currents we will largely derive from the simulation model.

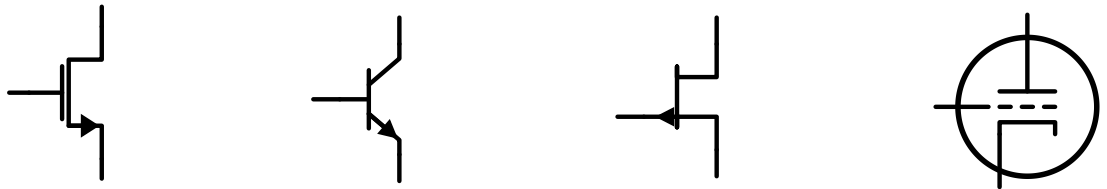


Figure 1: Circuit symbols for different voltage-controlled amplifiers (from left to right: MOSFET, bipolar junction transistor, junction FET, triode).

Look at the transistor symbols shown in Figure 1. By treating them as a black box, where the output current is controlled by an input voltage, we can design circuits with all of them, even vacuum tubes would work in the same way.

Since we have an emphasis on integrated circuit design in this course the size of the MOSFET can be adapted by changing its width  $W$  and its length  $L$ . As we will see later,  $L$  has a profound impact on the MOSFET performance allowing to trade-off speed versus output conductance versus device-to-device matching. The width  $W$  is more of a scaling parameter to adapt the current **density** (strictly speaking charge density) forming in the MOSFET channel to a desired current. More about this later.

The circuit symbol that we will use for the n-channel MOSFET is shown in Figure 2, and for the p-channel MOSFET it is shown in Figure 3. A control voltage between gate (“G”) and source (“S”) controls the current flow between drain (“D”) and source. The MOSFET is a 4-terminal device, so the bulk (“B”) can also control the drain-source current flow. Often, the bulk is connected to source, and then the bulk terminal is not shown to declutter the schematics.

## i MOSFET Background

Strictly speaking is the drain-source current of a MOSFET controlled by the voltage between gate and bulk ( $V_{GB}$ ) and the voltage between drain and source ( $V_{DS}$ ). Since bulk is often connected to source anyway, and many circuit designers historically were already familiar with the operation of the bipolar junction transistor (BJT), it is common to consider the gate-source voltage (besides the drain-source voltage) as the controlling voltage.

This focus on gate-source suggests that the source is special compared to the drain. In a typical physical MOSFET, however, the drain and source are constructed exactly the same (i.e., the MOSFET is a symmetric device), and which terminal is drain, and which terminal is source, is only determined by the applied voltage potentials, and can change dynamically during operation (think of a MOSFET operating as a switch... which side is the drain, which side is the source?).

Unfortunately, this focus on a “special” source has made its way into some MOSFET compact models. The model that is used in SG13G2 luckily uses the PSP model, which is formulated symmetrically with regards to drain and source, and is thus very well suited for analog and RF circuit design. For a detailed understanding of the PSP model please refer to the model documentation.

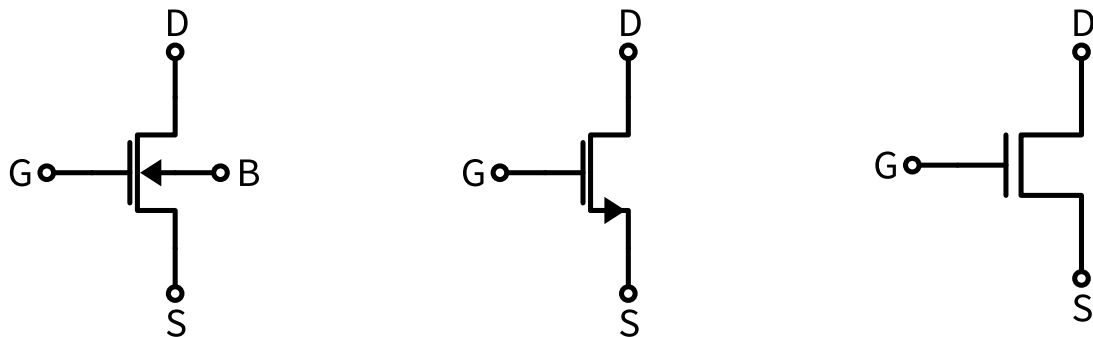


Figure 2: Circuit symbol of n-channel MOSFET. For circuit design in this course, we will mostly use the middle symbol without bulk connection and an arrow indicating the source terminal.

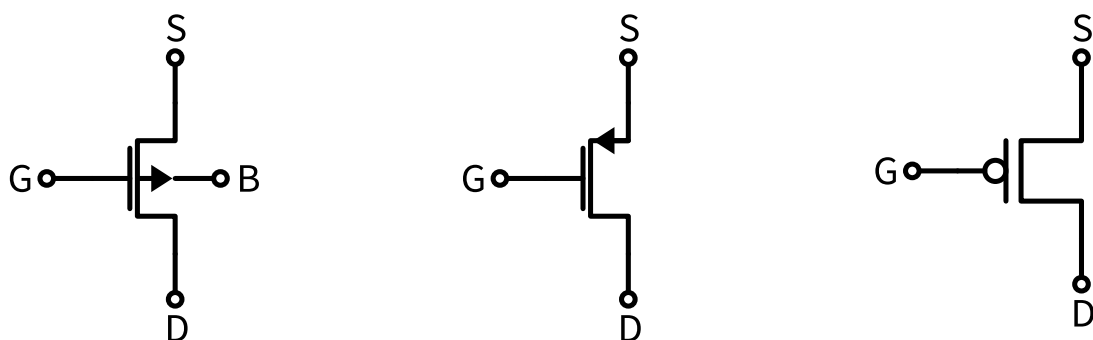


Figure 3: Circuit symbol of p-channel MOSFET. As for n-channel MOSFETs, we will mostly use the middle symbol without bulk connection and an arrow indicating the source terminal.

For hand calculations and theoretical discussions we will use the following simplified large-signal model, shown in Figure 4. A current source  $I_D$  models the current flow between drain and source, and it is controlled by the three control voltages  $V_{GS}$ ,  $V_{DS}$ , and  $V_{SB}$ . Note that in this way (since  $I_D = f(V_{DS})$ ) also a resistive behavior between D and S can be modelled. In case that B and S are shorted then simply  $V_{SB} = 0$  and  $C_{SB}$  is shorted.

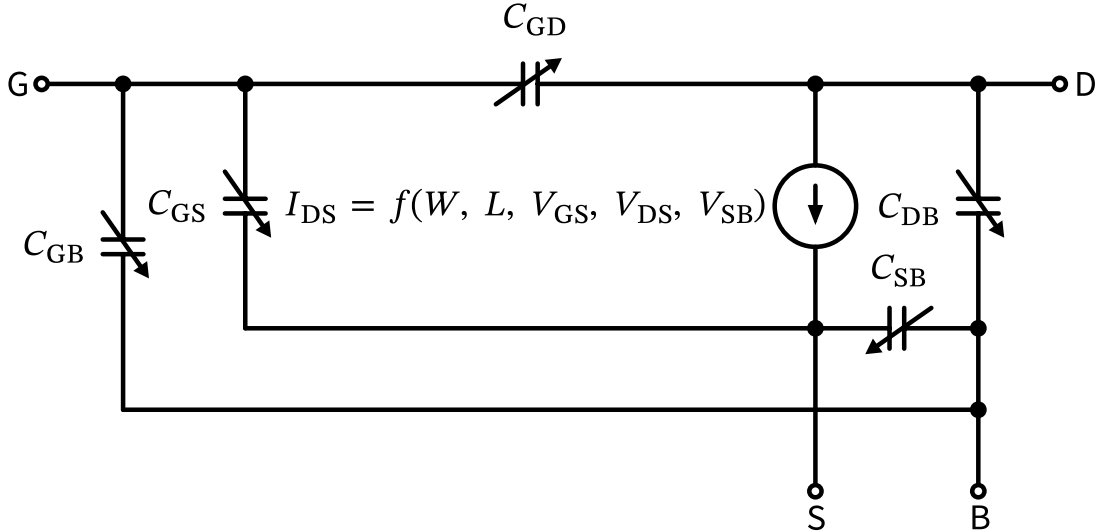


Figure 4: The MOSFET large-signal model. In general, all capacitors are nonlinear, i.e., they depend on their terminal voltages.

In an ideal MOSFET no dc current is flowing into the gate, the behavior is purely capacitive. We model this by two capacitors:  $C_{GG} = C_{GS} + C_{GD} + C_{GB}$  is the total capacitance when looking into the gate of the MOSFET.  $C_{GS}$  is usually the dominant capacitance, and  $C_{GD}$  models the capacitive feedback between D and G, usually induced by a topological overlap capacitance in the physical construction of the MOSFET. This capacitance is often small compared to  $C_{GS}$ , but in situations where we have a large voltage swing at the drain this capacitance will be affected by the Miller effect (see Section 17.1). In hand calculations we will often set  $C_{GD} = C_{GB} = C_{DB} = C_{SB} = 0$ .

To model a physical MOSFET there will be also a requirement for resistors in the model to account for terminal access resistances ( $R_G$ ,  $R_D$ , and  $R_S$ ) as well as resistors to model second-order effects like non-quasistatic operation. For lower frequencies and bulk MOSFETs we will not consider these resistors, and just deal with the capacitive behavior.

### i MOSFET Bulk Terminal

In many situations we will connect the bulk and source terminals of a MOSFET together, which results in a simplified large-signal model. As an exercise, look at Figure 4 and draw this simplified model (hint: look at Figure 6 and Figure 7 for inspiration).

Now, as we are skipping the bottom-up approach of deriving the MOSFET large-signal behavior from basic principles, we need to understand the behavior of the elements of the large-signal model in Figure 4 by using a circuit simulator and observing what happens. And generally, a first step in any new IC technology should be to investigate basic MOSFET

performance, by doing simple dc sweeps of  $V_{GS}$  and  $V_{DS}$  and looking at  $I_D$  and other large- and small-signal parameters.

As a side note, the students who want to understand MOSFET behavior from a physical angle should consult the MOSFET chapter from the JKU course “Design of Complex Integrated Circuits” (VL 336.048). A great introduction into MOSFET operation and fabrication is given in [4], which is available freely online and is a recommended read. A very detailed description of the MOSFET (leaving usually no question unanswered) is provided in [5].

Now, in order to get started, basic Xschem testbenches are prepared, and first simple dc sweeps of various voltages and currents will be done. But before that, please look at the import note below!

### ! Mathematical Notation

Throughout this material, we will largely stick to the following notation standardized by IEEE:

- A **dc quantity** is shown with an upper-case variable name with upper-case subscripts, like  $V_{GS}$ .
- Double-subscripts denote **dc sources**, like  $V_{DD}$  and  $V_{SS}$ .
- An **ac (small-signal) quantity** (incremental quantity) has a lower-case variable name with a lower-case subscript, like  $g_m$ .
- A **total quantity** (dc plus ac) is shown as a lowercase variable name with upper-case subscript, like  $i_{DS}$ .
- An upper-case variable name with a lower-case subscript is used to denote **RMS quantities**, like  $I_{ds}$ .

### i A Comment on Active and Passive Devices and Linear vs. Nonlinear

In contrast to the **passive** devices resistor  $R$ , inductor  $L$ , and capacitor  $C$ , which can only dissipate energy (and are often treated in a linearized fashion), transistors (like the MOSFET) are called “**active**”, since they can provide signal power amplification. However, transistors can not create energy out of thin air, but merely convert **dc** energy (supplied by the power supply) into **ac** energy. They have to have nonlinear transfer characteristics to do this, but it has been shown that a piecewise-linear characteristic is sufficient [7]. This is very good news for circuit design, as usually we strive for linear behaviour!

#### 2.1.1 Large-Signal MOSFET Model

We start with an investigation into the large-signal MOSFET model shown in Figure 4 by using the simple testbench for the LV NMOS shown in Figure 5.



Figure 5: Testbench for NMOS dc sweeps.

## i MOSFET Simulation Model

For modelling the MOSFET behavior in a circuit simulator like ngspice different models are available. Some of these models have been widely adopted, like the BSIM (Berkeley Short-channel IGFET Model) or PSP (Philips Penn State) model. The PSP model version 103.6 is used in the IHP SG13G2 PDK for the LV and HV MOSFET. This model has several advantages:

- Physics-based surface-potential model
- Symmetric formulation with respect to drain and source
- Support for mobility reduction, velocity saturation, DIBL, gate current, lateral doping gradient effects, STI stress, NQS, etc.

The PSP 103.6 model documentation can be found here. In chapter 8 the dc operating point output of the model (these parameters can be queried in ngspice) is explained, which is helpful to interpret the simulation output.

### 💡 Exercise: MOSFET Investigation

Please try to execute the following steps and answer these questions:

1. Get the LV NMOS testbench (available at [https://github.com/iic-jku/analog-circuit-design/blob/main/xschem/dc\\_lv\\_nmos.sch](https://github.com/iic-jku/analog-circuit-design/blob/main/xschem/dc_lv_nmos.sch)) working in your IIC-OSIC-TOOLS environment.
2. Make yourself familiar with Xschem (change the schematic in various ways, run a simulation, graph the result).
3. Make yourself familiar with ngspice (run various simulations, save nets and parameters, use the embedded Xschem graphing, explore the interactive ngspice shell to look at MOSFET model parameters).
4. Explore the LV NMOS `sg13_lv_nmos`:
  1. How is  $I_D$  affected by  $V_{GS}$  and  $V_{DS}$ ?
  2. Change  $W$  and  $L$  of the MOSFET. What is the impact on the above parameters? Can you explain the variations?
  3. Look at the capacitance values for  $C_{GS}$ ,  $C_{GB}$ ,  $C_{GD}$ , and  $C_{DB}$ . How are they affected by  $W$  and  $L$  and by changing the bias conditions (play with  $V_{GS}$  and  $V_{DS}$ )?
  4. When looking at the model parameters in ngspice, you see that there is a  $C_{GD}$  and a  $C_{DG}$ . Why is this, what could be the difference? Sometimes these capacitors show a negative value, why? (Hint: Study Note 1)
5. Build testbenches in Xschem for the LV PMOS, the HV NMOS, and the HV PMOS. Explore the different results.
  1. For a given  $W$  and  $L$ , which device provides more drain current? How are the capacitances related?
  2. If you would have to size an inverter, what would be the ideal ratio of  $W_p/W_n$ ? Will you exactly design this ratio, or are the reasons to deviate?
  3. There are LV and HV MOSFETs, and you investigated the difference in performance. What is the rationale when designing circuits for selection either an LV type, and when to choose an HV type?
6. Build a test bench to explore the body effect, start with LV NMOS.
  1. What happens when  $V_{SB} \neq 0$ ?

#### 2.1.2 Small-Signal MOSFET Model

As you have seen in the previous investigations, the large-signal model of Figure 4 describes the behavior of the MOSFET across a wide range of voltages applied at the MOSFET terminals. Unfortunately, for hand analysis dealing with a nonlinear model is close to impossible, at the very least it is quite tedious.

However, for many practical situations, we bias a MOSFET with a set of dc voltages applied to its terminal, and only apply small signal excursions during operation. If we do this, we can linearize the large-signal model in this dc operating point, and resort to a small-signal model which can be very useful for hand calculations. Many experienced designers analyze their circuits by doing these kind of hand calculations and describing the circuit analytically, which is a great way to understand fundamental performance limits and relationships between parameters.

We will use the small-signal MOSFET model shown in Figure 6 for this course. The current-source  $i_d = g_m v_{gs}$  models the drain current  $I_D$  as a function of  $V_{GS}$  with

$$g_m = \frac{\partial I_D(V_{GS}, V_{DS}, V_{SB})}{\partial V_{GS}},$$

and the resistor  $g_{ds}$  models the dependency of the drain current by  $V_{DS}$ :

$$g_{ds} = \frac{\partial I_D(V_{GS}, V_{DS}, V_{SB})}{\partial V_{DS}}$$

The drain current dependency on the source-bulk voltage (the so-called “body effect”) is introduced by the current source  $i_d = g_{mb} v_{sb}$ :

$$g_{mb} = \frac{\partial I_D(V_{GS}, V_{DS}, V_{SB})}{\partial V_{SB}}$$

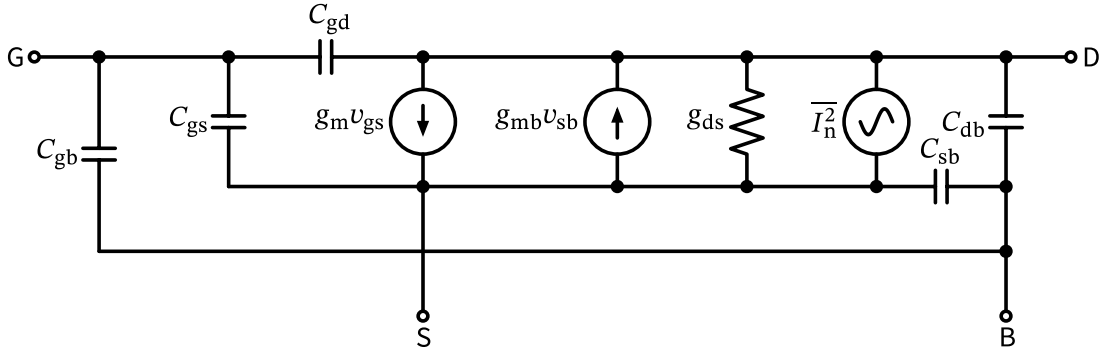


Figure 6: The MOSFET small-signal model.

As has been mentioned before, in many situations (and whenever we want to use a simplified model) we connect source and bulk of the MOSFET together. This results in the much simplified small-signal model shown in Figure 7.

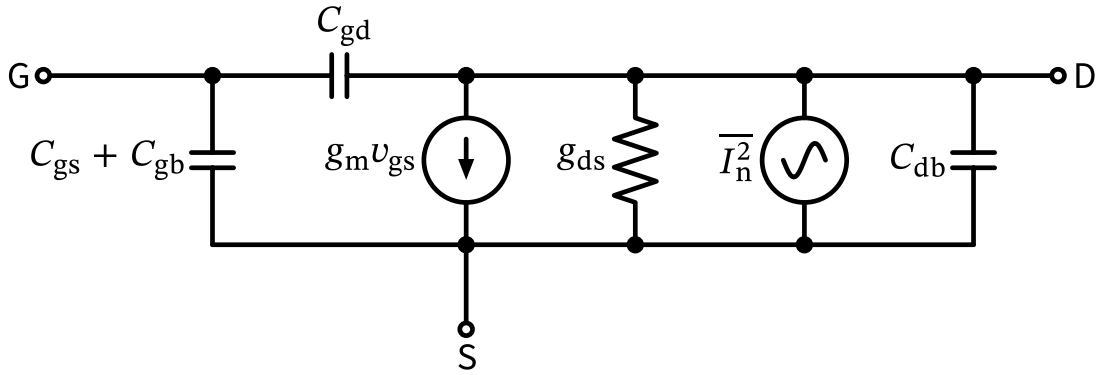


Figure 7: The MOSFET small-signal model when source and bulk are shorted.

As any electronic device the MOSFET introduces noise into the circuit. In this course we will only consider the **drain-source current noise** of the MOSFET, given by

$$\overline{I_n^2} = 4kT\gamma g_{d0}, \quad (1)$$

where  $\overline{I_n^2}$  is the one-sided power-spectral density of the noise in  $A^2/\text{Hz}$ ;  $k$  is the Boltzmann constant;  $T$  is the absolute temperature;  $\gamma$  is a (fitting) parameter in simplified theory changing between  $\gamma = 2/3$  in saturation and  $\gamma = 1$  for triode operation;  $g_{d0}$  is equal to  $g_m$  in saturation and  $g_{ds}$  in triode).

### i MOSFET Triode and Saturation Region

Sometimes we will refer to different operating modes of the MOSFET like “saturation” or “triode.” Generally speaking, when the drain-source voltage is small, then the MOSFET acts as a voltage-controlled resistor (since the impact of both  $V_{GS}$  and  $V_{DS}$  on  $I_D$  is large), and this mode of operation we call “**triode**” mode.

When the drain-source voltage  $V_{DS}$  is increased, at some point the drain-source current saturates and is only a weak function of the drain-source voltage, while still being well controlled by  $V_{GS}$ . This mode is called “**saturation**” mode.

As you can see in the large-signal investigations, these transitions happen gradually, and it is difficult to define a precise point where one operating mode switches to the other one. In this sense we use terms like “triode” and “saturation” only in an approximate sense.

We can also consider an even more reduced small-signal MOSFET model compared to Figure 7, which is shown in Figure 8. In this, we just consider the transconductance  $g_m$ , the input capacitor  $C_{gg}$ , as well as the output conductance  $g_{ds}$ . Note that we can redraw the pi-model of Figure 8 into the  $\tau$ -model of Figure 9. Depending on the circuit configuration, either the first or the second form results in simpler calculations of the circuit equations.



Figure 8: The MOSFET small-signal basic pi-model.

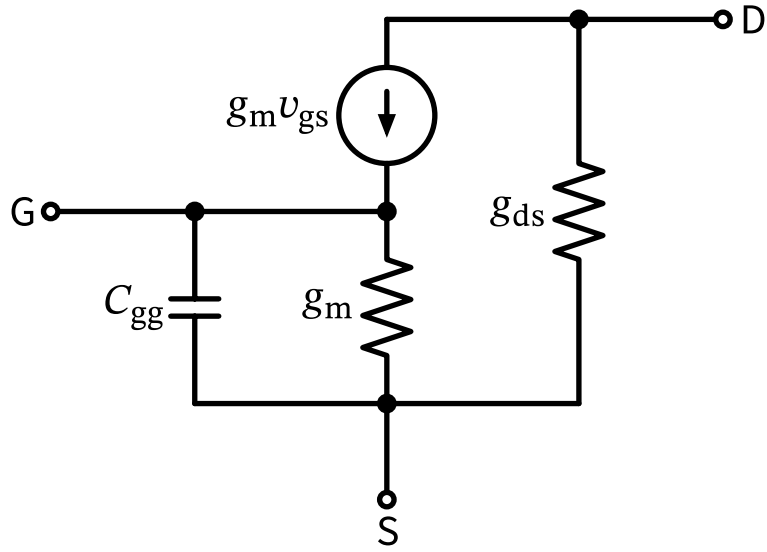


Figure 9: The MOSFET small-signal basic T-model.

Exercise: MOSFET Model Transformation

Can you show, with which circuit manipulations you can transform the pi-model of Figure 8 into the T-model of Figure 9?

A metric which is useful to assess the speed of a MOSFET is the so-called **transit frequency**  $f_T$ . It is defined as the frequency where the small-signal current gain (output current divided by the input current) of a MOSFET driven by a voltage-source at the input and loaded by a voltage source at the output drops to unity (reaches one). It can easily be derived using the simplified MOSFET small-signal model of Figure 7 by driving it with a voltage source and shorting the output to (neglecting the feed-forward current introduced by  $C_{gd}$ )

$$\omega_T = 2\pi f_T \approx \frac{g_m}{C_{gg}} = \frac{g_m}{C_{gs} + C_{gd} + C_{gb}}. \quad (2)$$

This frequency is an extrapolated frequency where the MOSFET operation is dominated by several second-order effects (hence Equation 2 is not valid any longer). A rule-of-thumb is to use a MOSFET up to approximately  $f_T/10$ . In any case,  $f_T$  is a proxy of the speed of a MOSFET; in other words, how much input capacitance  $C_{gg}$  is incurred when creating a certain  $g_m$ .

Exercise: MOSFET Transit Frequency

As a home exercise, try to derive Equation 2 starting from Figure 7. By showing this transformation you can proof that indeed both circuits are electrically equivalent.

Now we need to see how the small-signal parameters seen in Figure 6 can be investigated and estimated using circuit simulation.

### 💡 Exercise: MOSFET Small-Signal Parameters

Please try to execute the following steps and answer the following questions:

1. Reuse the LV NMOS testbench (available at [https://github.com/iic-jku/analog-circuit-design/blob/main/xschem/dc\\_lv\\_nmos.sch](https://github.com/iic-jku/analog-circuit-design/blob/main/xschem/dc_lv_nmos.sch)).
2. Explore the LV NMOS `sg13_lv_nmos`:
  1. How are  $g_m$  and  $g_{ds}$  changing when you change the dc node voltages?
  2. What is the ratio of  $g_m$  to  $g_{mb}$ ? What is the physical reason behind this ratio (you might want to revisit MOSFET device physics at this point)?
  3. Take a look at the device capacitances  $C_{gs}$ ,  $C_{gd}$ , and  $C_{gb}$ . Why are they important? What is the  $f_T$  of the MOSFET?
  4. Look at the drain noise current according to the MOSFET model and compare with a hand calculation of the noise. In the noise equation there is the factor  $\gamma$ , which in triode is  $\gamma = 1$  and in saturation is  $\gamma = 2/3$  according to basic text books. Which value of  $\gamma$  are you calculating? Why might it be different?
3. Go back to your testbench for the LVS PMOS `sg13_lv_pmos`:
  1. What is the difference in  $g_m$ ,  $g_{ds}$ , and other parameters between the NMOS and the PMOS? Why could they be different?

### **i** Note 1: Maxwell Capacitance Matrix

A Maxwell capacitance matrix [8] provides the relation between voltages on a set of conductors and the charges on these conductors. For a given conductor set with  $N$  conductors (and thus  $N$  terminals) the relation is

$$\mathbf{Q} = \mathbf{C} \cdot \mathbf{V}$$

where  $\mathbf{Q}$  is a vector of the charges on the  $N$  conductors,  $\mathbf{C}$  is a  $N \times N$  capacitance matrix, and  $\mathbf{V}$  is the potential vector. In the case of two conductors and physical capacitances between them,  $\mathbf{C}$  is given by

$$\mathbf{C} = \begin{pmatrix} C_{11} + C_{12} & -C_{12} \\ -C_{21} & C_{21} + C_{22} \end{pmatrix}$$

where  $C_{xx} = \partial Q_x / \partial V_x$  is the auto capacitance from a conductor  $x$  towards infinity (ground), and  $C_{xy} = \partial Q_x / \partial V_y$  is the mutual capacitance from node/conductor  $x$  to node/conductor  $y$ . For a physical capacitor  $C_{xy} = C_{yx}$ .

Using the above equation to calculate  $Q_1$  (the charge on conductor 1) results in

$$Q_1 = (C_{11} + C_{12})V_1 - C_{12}V_2 = C_{11}(V_1 - 0) + C_{12}(V_1 - V_2)$$

which is the expected result.

Such a Maxwell capacitance formulation is also used in the MOSFET model to describe the charge at a terminal as a function of potential at another terminal. So,

$$C_{GD} = \frac{\partial Q_G}{\partial V_D}$$

or

$$C_{GG} = \frac{\partial Q_G}{\partial V_G}$$

with  $Q_G$  the charge at terminal G in response to either  $V_D$  or  $V_G$ . Note that in a MOSFET, generally  $C_{xy} \neq C_{yx}$ !

## 2.2 Conclusion

Congratulations for making it thus far! By now you should have a solid grasp of the tool handling of Xschem and ngspice, and you should be familiar with the large- and small-signal operation of both NMOS and PMOS, and the parameters describing these behaviors. If you feel you are not sufficiently fluent in these things, please go back to the beginning of Section 2.1 and revisit the relevant sections, or dive into further reading about the MOSFET operation, like in [4].

### 3 Transistor Sizing Using $g_m/I_D$ Methodology

When designing integrated circuits it is an important question how to select various parameters of a MOSFET, like  $W$ ,  $L$ , or the bias current  $I_D$ . In comparison to using discrete components in PCB design, or also compared to a bipolar junction transistor (BJT), we have these degrees of freedom, which make integrated circuit design so interesting.

Often, transistor sizing in entry-level courses is based on the square-law model, where a simple analytical equation for the drain current can be derived. However, in nanometer CMOS, the MOSFET behavior is much more complex than these simple models. Also, this highly simplified derivations introduce concepts like the threshold voltage or the overdrive voltage, which are interesting from a theoretical viewpoint, but bear little practical use.

#### MOSFET Square-Law Model

One of the many simplifications of the square-law model is that the mobility of the charge carriers is assumed constant (it is not). Further, the existence of a threshold voltage is assumed, but in fact this voltage is just existing given a certain definition, and depending on definition, its value changed. In addition, in nm CMOS, the threshold voltage is a function on many thing, like  $W$  and  $L$ .

An additional shortcoming of the square-law model is that it is only valid in strong inversion, i.e. for large  $V_{GS}$  where the drain current is dominated by the drift current. As soon as the gate-source voltage gets smaller, the square-law model breaks, as the drain current component based on diffusion currents gets dominant. Modern compact MOSFET models (like the PSP model used in SG13G2) use hundreds of parameters and fairly complex equations to somewhat properly describe MOSFET behavior over a wide range of parameters like  $W$ ,  $L$ , and temperature. A modern approach to MOSFET sizing is thus based on the thought to use exactly these MOSFET models, characterize them, put the resulting data into tables and charts, and thus learn about the complex MOSFET behavior and use it for MOSFET sizing.

Being a well-established approach we select the  $g_m/I_D$  methodology introduced by P. Jespers and B. Murmann in [9]. A brief introduction is available here as well.

The  $g_m/I_D$  methodology has the huge advantage that it catches MOSFET behavior quite accurately over a wide range of operating conditions, and the curves look very similar for pretty much all CMOS technologies, from micrometer bulk CMOS down to nanometer FinFET devices. Of course the absolute values change, but the method applies universally.

#### 3.1 MOSFET Characterization Testbench

In order to get the required tabulated data we use a testbench in Xschem which sweeps the length  $L$  and the terminal voltages ( $V_{GS}$ ,  $V_{DS}$  and  $V_{SB}$ ) for a fixed device width  $W = 5 \mu\text{m}$  and records various large- and small-signal parameters, which are then stored in large tables. The testbench for the LV NMOS is shown in Figure 10, and the TB for the LV PMOS is shown in Figure 11.

## i Note on Characterization Testbench

The testbenches are relatively straightforward, with one exception: The drain current noise is sensed via the drain voltage source  $v_d$  and converted to a noise voltage (node  $n$ ) using a current-controlled voltage source (CCVS). This is necessary as the `.noise` simulation statement works with voltages.

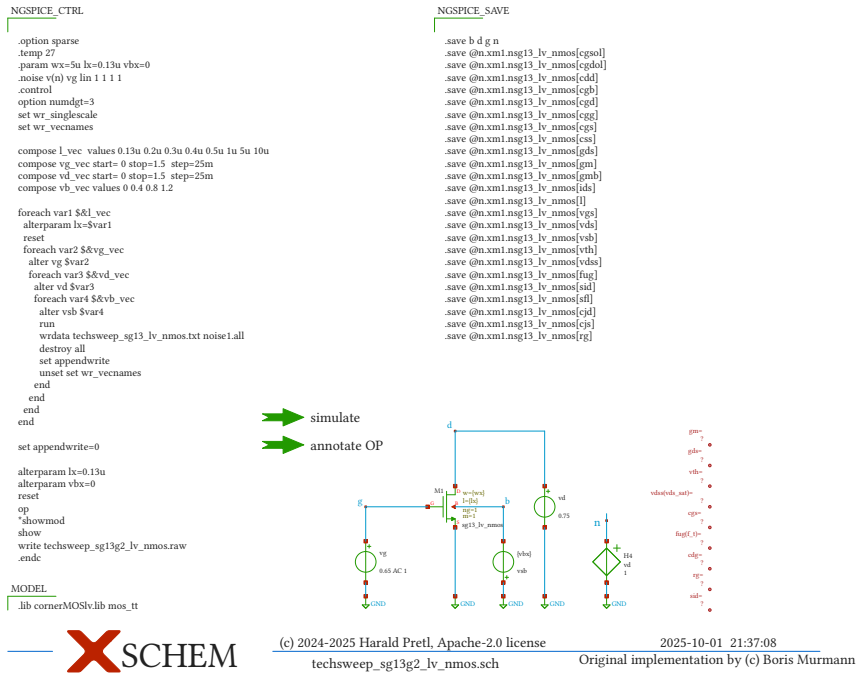


Figure 10: Testbench for LV NMOS  $g_m/I_D$  characterization.

```

NGSPICE_CTRL
.option sparse
.param wxe=5u b=6.13u vbx=0
.noise v(n) vg ln 1 1 1 1
control
option numdgt=3
set wr_singlecase
set wr_vclassnames
compose Lyce values 0.13u 0.2u 0.3u 0.4u 0.5u 1u 5u 10u
compose vq_vec start= 0 stop=1.5 step=25m
compose vd_vec start= 0 stop=1.5 step=25m
compose vb_vec values 0.4 0.8 1.2
foreach var1 $s&1_vec
altparam lx=$var1
reset
foreach var2 $&vqg_vec
alter vg $var2
foreach var3 $&vd_vec
alter vd $var3
foreach var4 $&vb_vec
alter vb $var4
run
writedata techsweep_sg13_lv_pmos.txt noise1.all
destroy all
set appendwrite
unset set wr_vclassnames
end
end
end
end
set appendwrite=0
altparam lx=0.13u
altparam vbx=0
reset
op
*showmod
show
write techsweep_sg13g2_lv_pmos.raw
endc

MODEL
.lib cornerMOSIV.lib mos_tt

NGSPICE_SAVE
.save b d g n
.save @nxml1.ngs13_lv_pmos(cgsd)
.save @nxml1.ngs13_lv_pmos(cgd)
.save @nxml1.ngs13_lv_pmos(cdd)
.save @nxml1.ngs13_lv_pmos(cgh)
.save @nxml1.ngs13_lv_pmos(cgd)
.save @nxml1.ngs13_lv_pmos(cgg)
.save @nxml1.ngs13_lv_pmos(cgs)
.save @nxml1.ngs13_lv_pmos(css)
.save @nxml1.ngs13_lv_pmos(vds)
.save @nxml1.ngs13_lv_pmos(vds)
.save @nxml1.ngs13_lv_pmos(vch)
.save @nxml1.ngs13_lv_pmos(vds)
.save @nxml1.ngs13_lv_pmos(fug)
.save @nxml1.ngs13_lv_pmos(sid)
.save @nxml1.ngs13_lv_pmos(sdl)
.save @nxml1.ngs13_lv_pmos(cjs)
.save @nxml1.ngs13_lv_pmos(rg)

simulate
annotate OP


```

Schematic (c) 2024-2025 Harald Pretl, Apache-2.0 license  
techsweep\_sg13g2\_lv\_pmos.sch 2025-10-01 21:38:53  
Original implementation by (c) Boris Murmann

Figure 11: Testbench for LV PMOS  $g_m/I_D$  characterization.

We will use Jupyter notebooks to inspect the resulting data, and interpret some important graphs. This will greatly help to understand the MOSFET behavior.

### Note on width $W$

In general, the device width could be included as a fifth sweep variable. However, this is not necessary since the parameters scale approximately linearly with  $W$  across the typical range encountered in analog design. For  $W > 2 \mu\text{m}$  the error lies within about 1.5% for  $g_m/I_D$ ,  $g_m/g_{ds}$  and  $g_m/C_{gg}$  as described in [9].

The resulting four-dimensional data is saved into a .txt file and imported into two Jupyter notebooks as visualized in Figure 12. The first notebook outputs .mat files, which are compatible with the pygmid Python package used for sizing. The second notebook generates vector graphic characterization plots, which are shown in Section 3.2 for LV NMOS and Section 3.3 for LV PMOS. With these plots, an immediate understanding of the tradeoffs for the given transistor can be acquired. Furthermore, they can be used for fast hand calculations in small circuits.



Figure 12: Overview of the  $g_m/I_D$  MOSFET characterization procedure [10].

### 3.2 NMOS Characterization in Saturation

First, we will start looking at the LV NMOS. In Section 3.3 we have the corresponding graphs for the LV PMOS. In this lecture, we will only use the LV MOSFETs. While there are also the HV types available, they are mainly used for high-voltage circuits, like circuits connecting to the outside world. Here, we only will design low-voltage circuits running at a nominal supply voltage of 1.5 V, so only the LV types are of interest to us.

In the plots that follow we will set  $V_{DS} = V_{DD}/2$  to keep the MOSFET in saturation (as this is the region of operation where most MOSFET are operated when working in class-A). We will later also look at the MOSFET performance in triode operation, as this is the operation mode where the MOSFET is used as a switch. While the  $g_m/I_D$  method is primarily intended to be used for circuits where the MOSFETs are held in saturation and are biased by a certain bias current (usually referred to class-A), the generated tables using the testbenches of Section 3.1 contain the data for all MOSFET bias points.

The first import graph is the plot of  $g_m/I_D$  and  $f_T$  versus the gate-source voltage  $V_{GS}$ . First let us answer the question why  $g_m/I_D$  is a good parameter to look at, and actually this is also the central parameter in the  $g_m/I_D$  methodology. In many circuits we want to get a large amplification from a MOSFET, which corresponds to a large  $g_m$ . We want to achieve this by spending the minimum biasing current possible (ideally zero), as we almost always design for lowest power consumption. Thus, a high  $g_m/I_D$  ratio is good.

### **i** Power Consumption

Designing for minimum power consumption is pretty much always mandated. For battery-operated equipment it is a paramount requirement, but also in other equipment electrical energy consumption is a concern, and often severely limited by the cooling capabilities of the electrical system.

However, as can be seen in the below plot, there exists a strong and unfortunate trade-off with device speed, characterized here by the transit frequency  $f_T$ . It would be ideal if there exists a design point where we get high transconductance per bias current concurrently to having the fastest operation, but unfortunately, this is clearly not the case. The  $g_m/I_D$  peaks for  $V_{GS} < 0.3$  V, and the highest speed we get at  $V_{GS} \approx 1.2$  V. The dashed vertical line plots the nominal threshold voltage, as you can see in this continuum of parameter space, it marks not a particularly special point.

Note that

$$\frac{g_m}{I_D} = \frac{1}{nV_T} \quad (3)$$

for a MOSFET in weak inversion (i.e., small gate-source voltage).  $n$  is the subthreshold slope, and  $V_T = kT/q$  which is 25.8 mV at 300 K. We thus have  $n \approx 1.38$  for this LV NMOS, which falls nicely into the usual range for  $n$  of 1.3 to 1.5 for bulk CMOS (FinFET have  $n$  very close to 1).

For the classical square-law model of the MOSFET in strong inversion,  $g_m/I_D$  is given as

$$\frac{g_m}{I_D} = \frac{2}{V_{GS} - V_{th}} = \frac{2}{V_{od}} \quad (4)$$

with  $V_{th}$  the threshold voltage and  $V_{od}$  the so-called “overdrive voltage.” The latter is sometimes also dubbed the effective gate-source voltage  $V_{eff}$  [11].

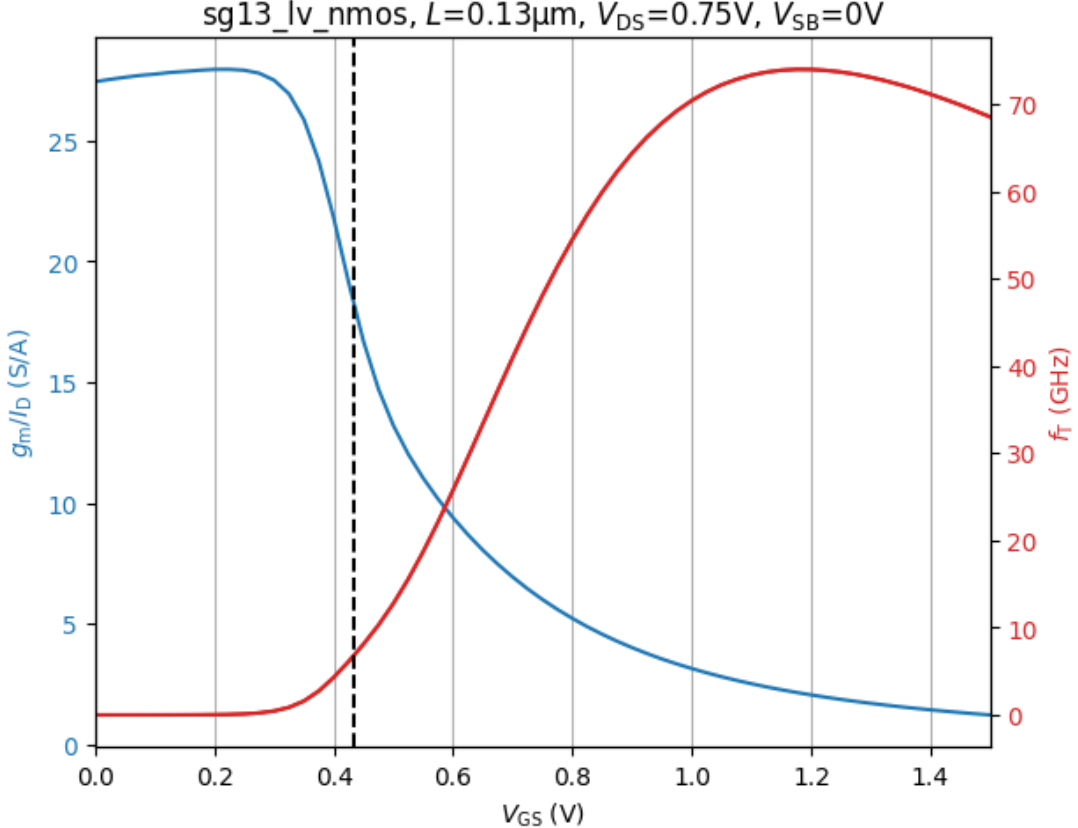
### **i** Why 300K?

Why are we so often using a temperature of 300 K for a typical condition? As this corresponds to roughly 27°C, this accounts for some self heating compared to otherwise cooler usual room temperatures. Further, engineers like round numbers which are easy to remember, so 300 K is used as a proxy for room temperature.

As we can also see from belows plot, the peak transit frequency of the LV NMOS is about 75 GHz, which allows building radio-frequency circuits up to ca.  $f_T/10 = 7.5$  GHz, which is a respectable number. It is no coincidence, that the transition for RF design in the GHz-range switched from BJT-based technologies to CMOS roughly in the time frame when 130nm CMOS became available (ca. 2000).

Note that  $f_T$  saturates and even decreases again at around  $V_{GS} = 1.2$  V due to second-order effects of the transistor like velocity saturation and DIBL. Velocity saturation describes the saturation of the velocity of the electrons at a certain  $V_{GS}$ . As a consequence, also  $g_m$  saturates.

Since  $f_T \propto g_m/C_{gs}$ ,  $f_T$  can not further increase. DIBL explains the effect when a too high  $V_{GS}$  is applied and therefore the channel is confined to a narrow region at the surface, leading to more carrier scattering and thus lower mobility.



The following figure plots  $f_T$  against  $g_m/I_D$  for several different  $L$ . As you can see, device speed maximizes for a low  $g_m/I_D$  and a short  $L$ . Note, that the drain-source voltage is kept at  $V_{DS} = 0.75$  V =  $V_{DD}/2$ , which is a typical value keeping the MOSFET in saturation across the characterization sweeps. Further, the source-bulk voltage is kept at  $V_{SB} = V_S - V_B = 0$  V, which means bulk and source terminals are connected. If  $V_{SB} \neq 0$  V, then the so-called body effect, bulk effect or back-gate effect occurs.

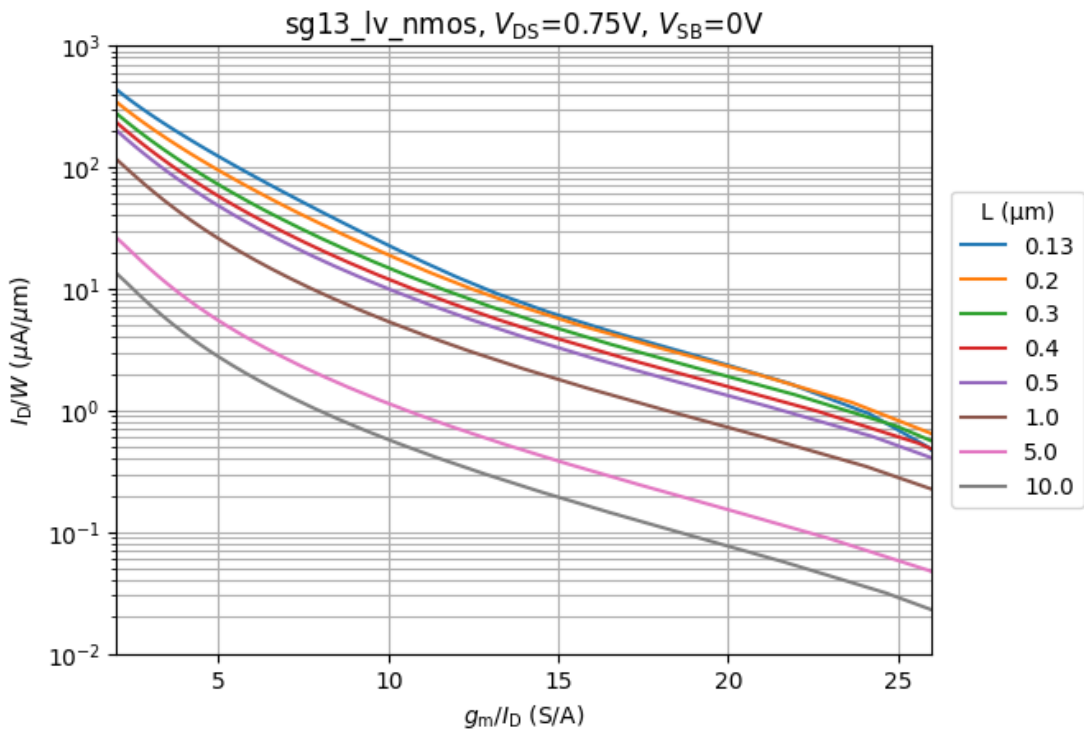
If  $V_{SB} > 0$  V, then  $V_{th}$  increases. If  $V_{SB} < 0$  V, then  $V_{th}$  decreases. At first glance, this effect may sound unwanted (and often also is), however, improved circuit designs by changing the bulk potential can be realized. For example, circuit 16 in [12] shows an implementation of a current mirror by exploiting the body effect. However, keep in mind that a deep-n-well (DNW), also called triple-well, is needed for NMOS transistors when the bulk is not tied to GND. This DNW may not be supported by the used PDK or can add additional costs to the wafer processing.



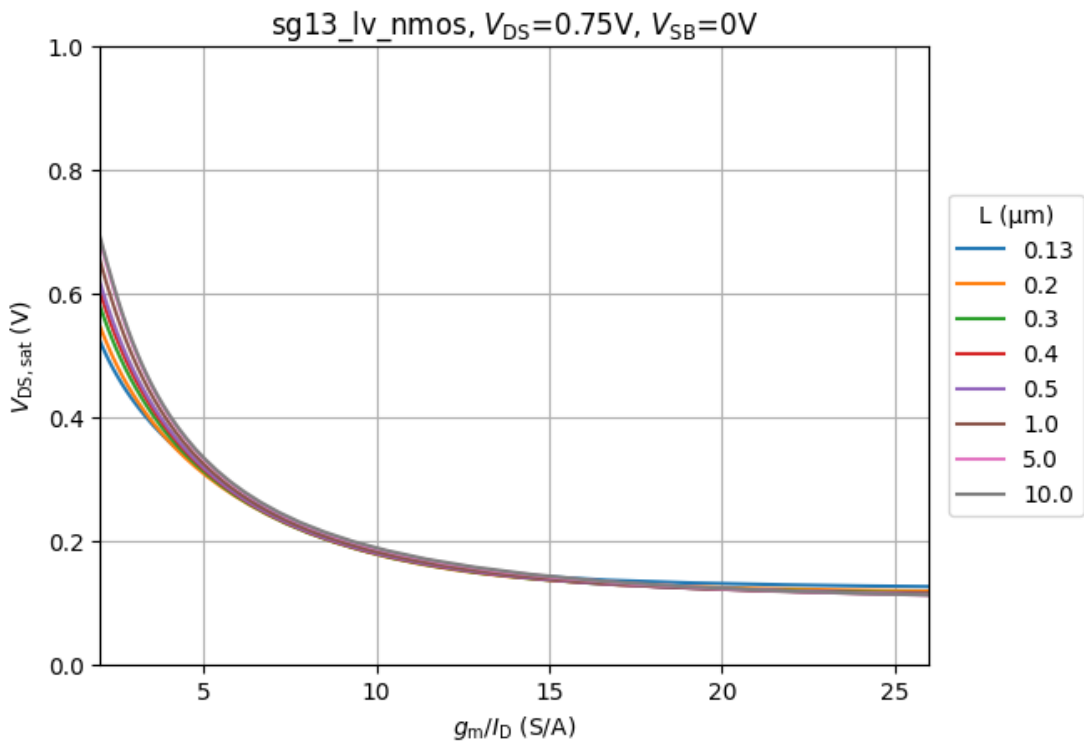
The next plot shows the ratio of  $g_m/g_{ds}$  versus  $g_m/I_D$ . The ratio  $g_m/g_{ds}$  is the so-called **“self-gain”** of the MOSFET, and shows the maximum voltage gain we can achieve in a single transistor configuration. As one can see the self gain increases for increasing  $L$ , but this also gives a slower transistor, so again there is a trade-off. This plot allows us to select the proper  $L$  of a MOSFET if we know which amount of self gain we need.



The following figure plots the drain current density  $I_D/W$  as a function of  $g_m/I_D$  and  $L$ . With this plot we can find out how to set the  $W$  of a MOSFET once we know the biasing current  $I_D$ , the  $L$  (selected according to self gain,  $f_T$ , and other considerations) and the  $g_m/I_D$  design point we selected. The drain current density  $I_D/W$  is a very useful normalized metric to use, because the physical action in the MOSFET establishes a charge density in the channel below the gate, and the changing of the  $W$  of the device merely transforms this charge density into an absolute parameter (together with  $L$ ).



The following plot shows the minimum drain-source voltage  $V_{ds,sat}$  that we need to establish in order to keep the MOSFET in saturation. As you can see, this value is almost independent of  $L$ , and increases for small  $g_m/I_D$ . So for low-voltage circuits, where headroom is precious, we tend to bias at  $g_m/I_D \geq 10$ , whereas for fast circuits we need to go to small  $g_m/I_D \leq 5$  requiring substantial voltage headroom per MOSFET stage that we stack on top of each other.



For analog circuits the noise performance is usually quite important. Thermal noise of a resistor (the Johnson-Nyquist noise) has a flat power-spectral density (PSD) given by  $\overline{V_n^2}/\Delta f = 4kTR$ , where  $k$  is Boltzmann's constant,  $T$  absolute temperature, and  $R$  the value of the resistor (the unit of  $\overline{V_n^2}/\Delta f$  is  $V^2/\text{Hz}$ ). This PSD is essentially flat until very high frequencies where quantum effects start to kick in.

### 💡 Noise Notation

We usually leave the  $\Delta f$  away for a shorter notation, so we write  $\overline{V_n^2}$  when we actually mean  $\overline{V_n^2}/\Delta f$ . In case of doubt look at the unit of a quantity, whether it shows  $V^2$  or  $V^2/\text{Hz}$  or  $V/\sqrt{\text{Hz}}$  (or  $I^2$  or  $I^2/\text{Hz}$  or  $I/\sqrt{\text{Hz}}$ ).

Please also note that the pair of  $kT$  pretty much always shows up together, so when you do a calculation and you miss the one or the other, that is often a sign for miscalculation. Boltzmann's constant  $k = 1.38 \cdot 10^{-23} \text{ J/K}$  is just a scaling factor from thermal energy expressed as a temperature  $T$  to energy  $E = kT$  expressed in Joule.

Further, when working with PSD there is the usage of a one-sided ( $0 \geq f < \infty$ ) or two-sided power spectral density (PSD) ( $-\infty < f < \infty$ ). The default in this lecture is the usage of the **one-sided PSD**.

In this lecture the only MOSFET noise we consider is the drain noise (as discussed in Section 2.1.2), showing up as a current noise between drain and source. For a realistic MOSFET noise model, also a (correlated) gate noise component and the thermal noise of the gate resistance needs to be considered.

The factor  $\gamma$  (Equation 1) is a function of many things (in classical theory,  $\gamma = 2/3$  in saturation and  $\gamma = 1$  in triode), and it is characterized in the following plot as a function of  $g_m/I_D$  and  $L$ . So when calculating MOSFET noise we can lookup  $\gamma$  in the below plot, and use Equation 1 to calculate the effective drain current noise.

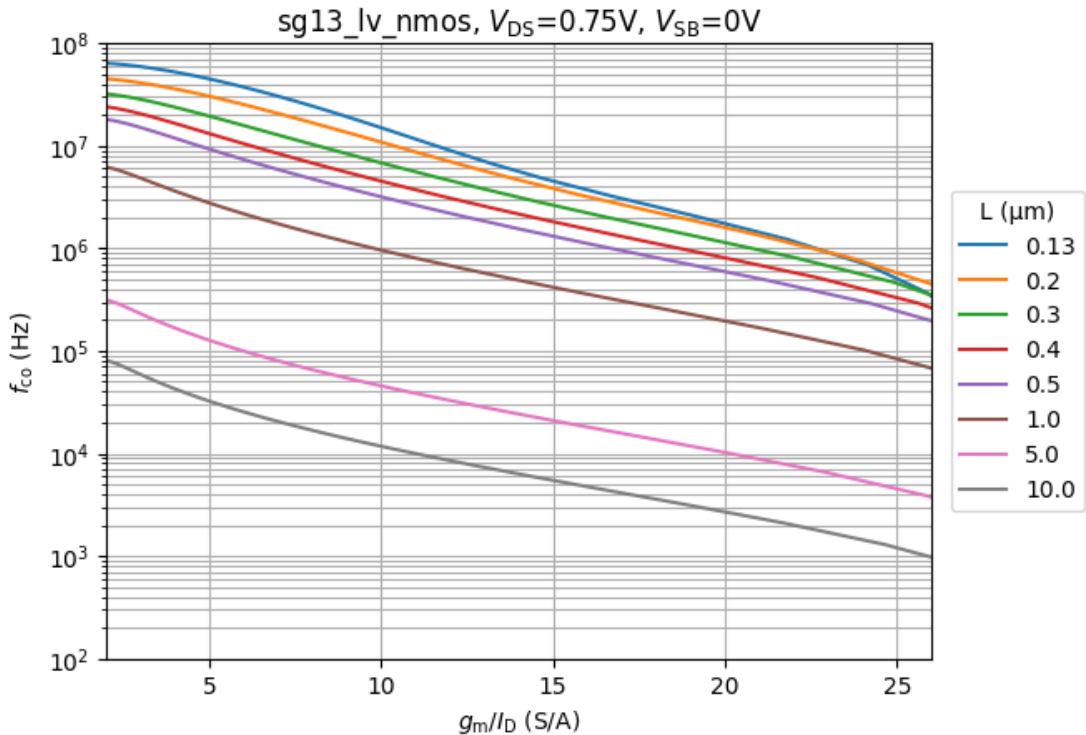


In a MOSFET, unfortunately, besides the thermal noise according to Equation 1, there is also a substantial low-frequency excess noise, called “flicker noise” due to its characteristic  $I_{d,nf}^2 = K_f/f$  behavior (this means that this noise PSD decreases versus frequency). In order to characterize this flicker noise the following plot shows the cross-over frequency  $f_{co}$ , where the flicker noise is as large as the thermal noise. As can be seen in the below plot, this frequency is a strong function of  $L$  and  $g_m/I_D$ . Generally, the flicker noise is proportional to  $(WL)^{-1}$ , so the larger the device is, the lower the flicker noise. The parameter  $g_m/I_D$  largely stays constant when we keep  $W/L$  constant, so for a given  $g_m/I_D$  flicker noise is proportional to  $1/L^2$ . However, increasing  $L$  lowers device speed dramatically, so here we have a trade-off between flicker-noise performance and MOSFET speed, and this can have dramatic consequences for high-speed circuits.

### i MOSFET Flicker Noise

The physical origin of flicker noise is the crystal interface between silicon (Si) and the silicon dioxide ( $\text{SiO}_2$ ). Since these are different materials, there are dangling bonds, which can capture charge carriers traveling in the channel. After a random time, these carriers are released, and flicker noise is the result. The amount of flicker noise is a function of the manufacturing process, and will generally be different between device types and wafer foundries.

As you can see in the following plot,  $f_{\text{co}}$  can reach well into the 10's of MHz for short MOSFETs, significantly degrading the noise performance of a circuit.



During the design phase, it might be convenient to have an overview of the most relevant sizing plots of the NMOS on one page. This overview can be downloaded here.

### 3.3 PMOS Characterization in Saturation

In the following, we have the same plots as discussed in Section 3.2, but now for the PMOS.

#### i PMOS Sign Convention

In all PMOS plots we plot positive values for voltages and currents, to have compatible plots to the NMOS. Of course, in a PMOS, voltages and currents have different polarity compared to the NMOS.

$g_m/I_D$  and  $f_T$  versus the gate-source voltage  $V_{\text{GS}}$ :



$f_T$  against  $g_m/I_D$  for several different  $L$ . One can see a significantly lower top speed for the PMOS compared to the NMOS, which means for high-speed circuits the NMOS should be used. The reason for this is the approximately two to three times higher mobility of electrons compared to the mobility of holes.



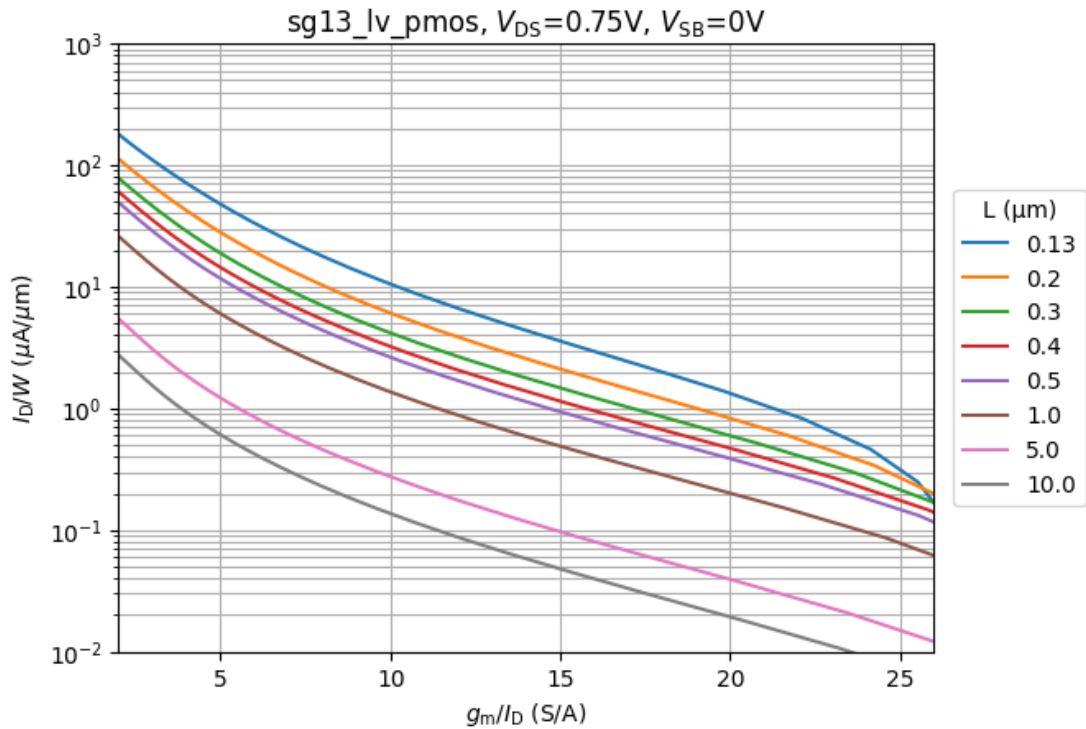
$g_m/g_{ds}$  versus  $g_m/I_D$ . Unfortunately, one can see a modelling error for the PMOS in this plot. The self gain  $g_m/g_{ds}$  reaches non-physical values, which indicates an issue with the  $g_{ds}$  modelling for the PMOS. We can not use these values for our circuit sizing, so we will use the respective NMOS plots also for the PMOS.

**! Beware of Modelling Issues**

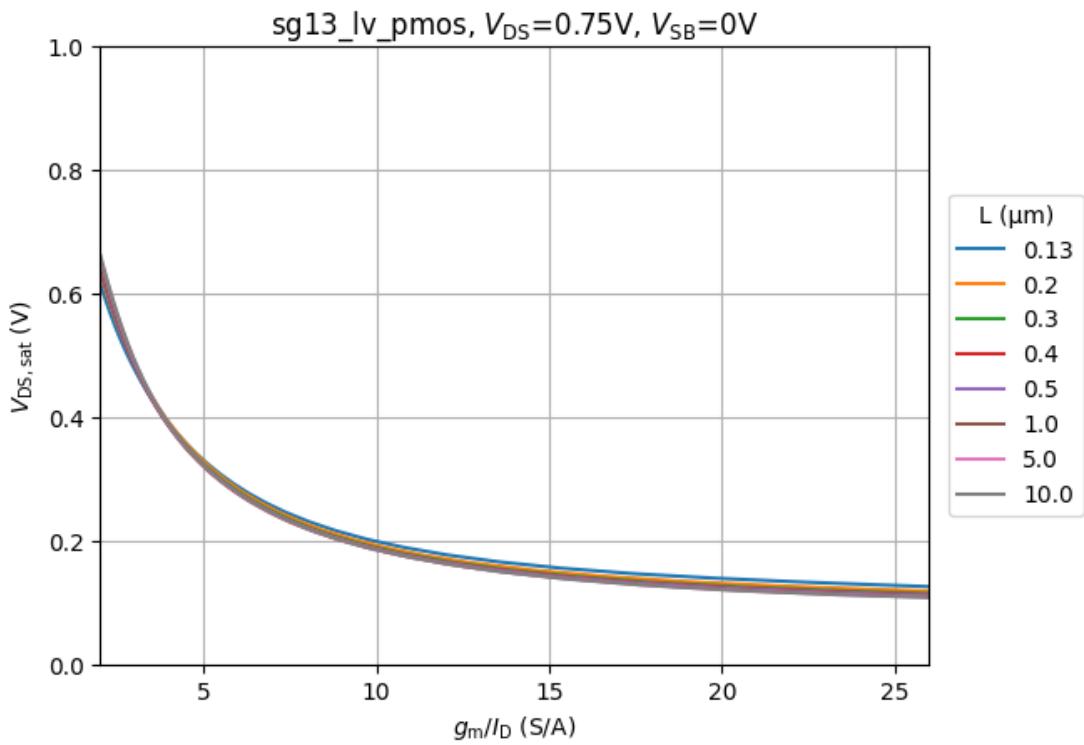
This example shows how important it is to benchmark the device models when starting to use a new technology. Modelling artifacts like the one shown are quite often happening, as setting up the device compact models and parametrize them according to measurement data is a very complex task. In any case, just be aware that modelling issues could exist in whatever PDK you are going to use!



Drain current density  $I_D/W$  as a function of  $g_m/I_D$  and  $L$ :



Minimum drain-source voltage  $V_{ds,sat}$  versus  $g_m/I_D$  and  $L$ :



Noise factor  $\gamma$  versus  $g_m/I_D$  and  $L$ :



Flicker noise corner frequency  $f_{co}$  versus  $g_m/I_D$  and  $L$ . If you compare this figure carefully with the NMOS figure you can see that for some operating points the flicker noise for the PMOS is lower than for the NMOS. This is often true for CMOS technologies, so it can be an

advantage to use a PMOS transistor in places where flicker noise is critical, like an OTA input stage. Using PMOS has the further advantage that the bulk node can be tied to source (which for NMOS is only possible in a triple-well technology, which is often not available), which gets rid of the body effect.



During the design phase, it might be convenient to have an overview of the most relevant sizing plots of the PMOST on one page. This overview can be downloaded [here](#).

### 3.4 Tradeoffs in Saturation

In Figure 13, an overview of the tradeoffs mentioned above is presented. The design parameters are only shown once for their best-case implementation. Their worst-case value is then located at the opposite arrow. In conclusion, strong inversion with short channels is used for high-speed applications, whereas weak inversion with long channels is for low-power and low-noise applications. Moderate inversion with longer channels is used for current sources to maximize their output resistance. Note that the two arrows for strong inversion with long channels and weak inversion with short channels are empty since they make practically no sense. This tradeoff overview simplifies the choice of the starting  $g_m/I_D$  and  $L$  values in the sizing scripts.



Figure 13: Overview of key design tradeoffs depending on the channel length  $L$  and transconductance efficiency  $g_m/I_D$  [10].

### 3.5 NMOS and PMOS Characterization in Triode

Besides using the MOSFET as a transconductor in saturation we often use the MOSFET as a switch in triode mode (to either switch voltages or currents). In this triode/switch mode of operation we are mainly interested in two parameters:

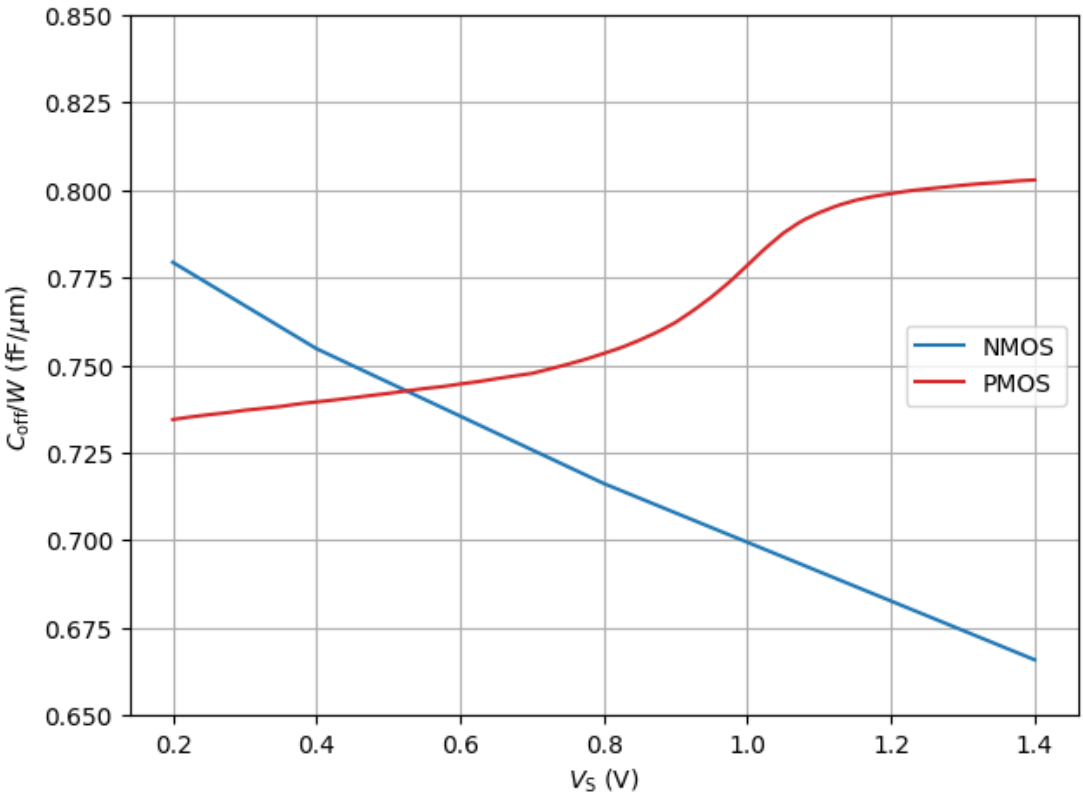
- The resistance of the switch/MOSFET when it is turned on ( $R_{on} = 1/g_{ds}$ ).
- The shunt capacitance of the switch when it is turned off ( $C_{off}$  is defined by the coupling capacitances between drain and source).

In the operation of the NMOS as a switch the gate is usually pulled to  $V_{DD}$  and the bulk is permanently connected to  $V_{SS}$  to achieve the lowest  $R_{on}$  (to turn the switch off the gate is pulled towards  $V_{SS}$ ). Likewise, to turn on a PMOS, the gate is usually pulled to  $V_{SS}$  and the bulk is connected to  $V_{DD}$ . In this situation the drain/source potential is somewhere between  $V_{DD}$  and  $V_{SS}$ , so the MOSFET will experience a  $V_{SB} \neq 0$ , leading to a quite noticeable bulk effect. Once the drain/source potential is sufficiently high for NMOS (low PMOS) the switch resistance will drastically degrade.

In order to get a feeling for the behavior of the MOSFET as a switch the following characterization plots show  $R_{on}$  and  $C_{off}$  for the NMOS and the PMOS, respectively. Both plots are for  $L = L_{min} = 0.13\mu\text{m}$ , as for switches usually minimum length devices are used. Only for special applications (e.g., the drain-source leakage current in off-mode is a concern) MOSFETs with increased  $L$  are used.



As can be seen in the previous plot, an NMOS can be used to switch at potentials close to  $V_{SS}$ , while a PMOS is the better choice when switching at potentials close to  $V_{DD}$ . To construct a switch which can work for all voltage levels between  $V_{DD}$  and  $V_{SS}$  an NMOS is put in parallel to a PMOS, resulting in the well-known **transmission gate**.



As the switch on-resistance gets lower when increasing  $W$ , the off-capacitance gets larger. Thus, a good performance indicator for comparing switches in a given technology is the  $R_{\text{on}}C_{\text{off}}$  product.

### 3.6 Tradeoffs in Triode

Some might think that sizing switches is a straightforward task, but in reality, they also come with several tradeoffs, and depending on the application, they can be incredibly complicated. The essential design parameters in switches are the on-resistance  $R_{\text{on}}$ , the off-capacitance  $C_{\text{off}}$ , the drain-source leakage current  $I_{\text{leak}}$ , and their impact on clock feedthrough and charge injection [11]. In Figure 14, an overview of the tradeoffs of these design parameters depending on the channel width  $W$  and the channel length  $L$  is presented. In conclusion, if  $W/L$  increases,  $R_{\text{on}}$  decreases, and the switching speed increases. If  $W/L$  decreases,  $I_{\text{leak}}$ ,  $C_{\text{off}}$ , and the drain-source overlap capacitance decrease, effectively reducing clock feedthrough and charge injection [1]. Practically, it does not make sense to make the switch both wide and long.

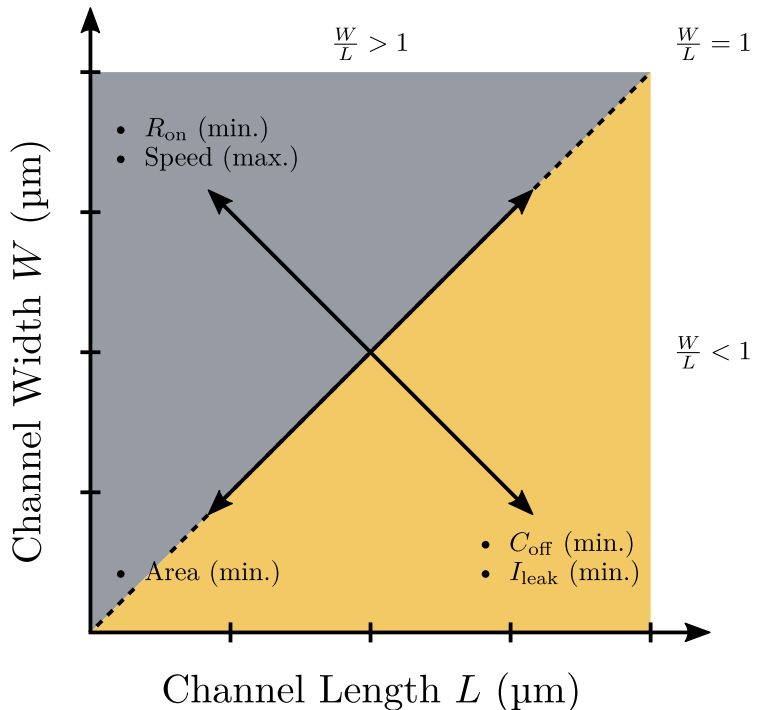


Figure 14: Overview of key design tradeoffs in switches depending on the channel width  $W$  and the channel length  $L$  [10].

#### 4 First Circuit: MOSFET Diode

The first (simple) circuit which we will investigate is a MOSFET, where the gate is shorted with the drain, a so-called MOSFET “diode”, which is shown in Figure 15. This diode is one half of a current mirror, which we will investigate in Section 6.



Figure 15: A MOSFET connected as a diode (drain shorted with gate).

Why looking at a single-transistor circuit at all? By starting with the simplest possible circuit we can develop important skills in circuit analysis (setting up and calculating a small-signal model, calculating open-loop gain, calculate noise, etc.) and Xschem/ngspice simulation test-bench creation. We safely assume that also the Mona Lisa was not Leonardo da Vinci’s first painting, so let’s start slow.

This diode is usually biased by a current source, shown as  $I_{\text{bias}}$  in the figure. Depending on MOSFET sizing with  $W$  and  $L$ , a certain gate-source voltage  $V_{\text{GS}}$  will develop. This voltage can be used as a biasing voltage for other circuit parts, for example. For exemplary sized MOSFET the  $V_{\text{GS}} = f(I_{\text{bias}})$  characteristic is shown in Figure 16. Note that in this MOSFET diode configuration  $V_{\text{DS}} = V_{\text{GS}}$ .

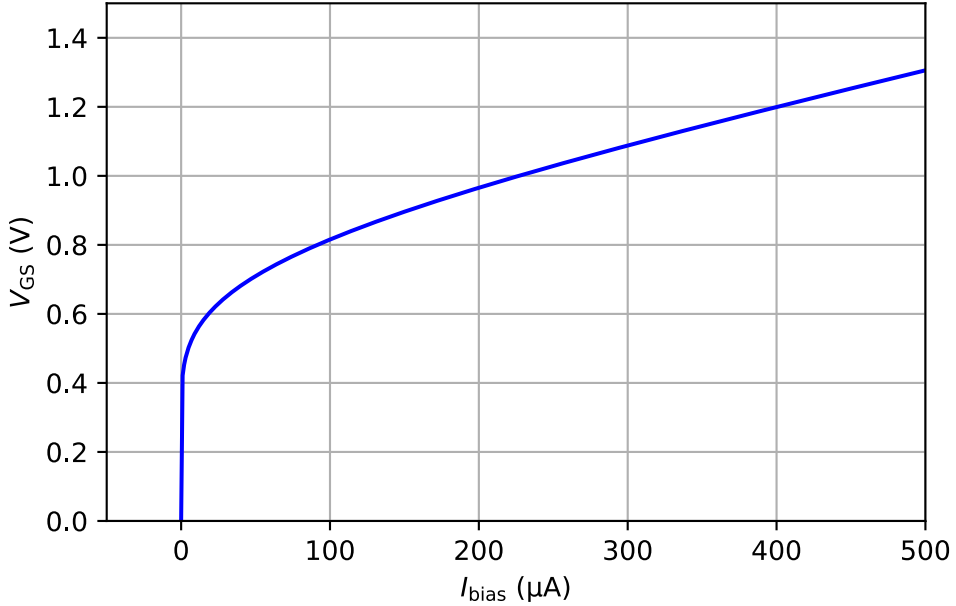


Figure 16: Gate-source voltage of a MOSFET diode with  $W=1\mu\text{m}$  and  $L=0.13\mu\text{m}$  showing the gate-source voltage as a function of the bias current.

If we flip Figure 16 by 90 degrees we can appreciate the name “MOSFET diode” as the characteristic resembles the one of a diode quite well (somewhat steep increase of the current beyond a certain threshold voltage). This is shown in Figure 17. Note that for negative  $V_{\text{GS}}$  the drain current is essentially zero, as the MOSFET is off, confirming the diode-like behavior.

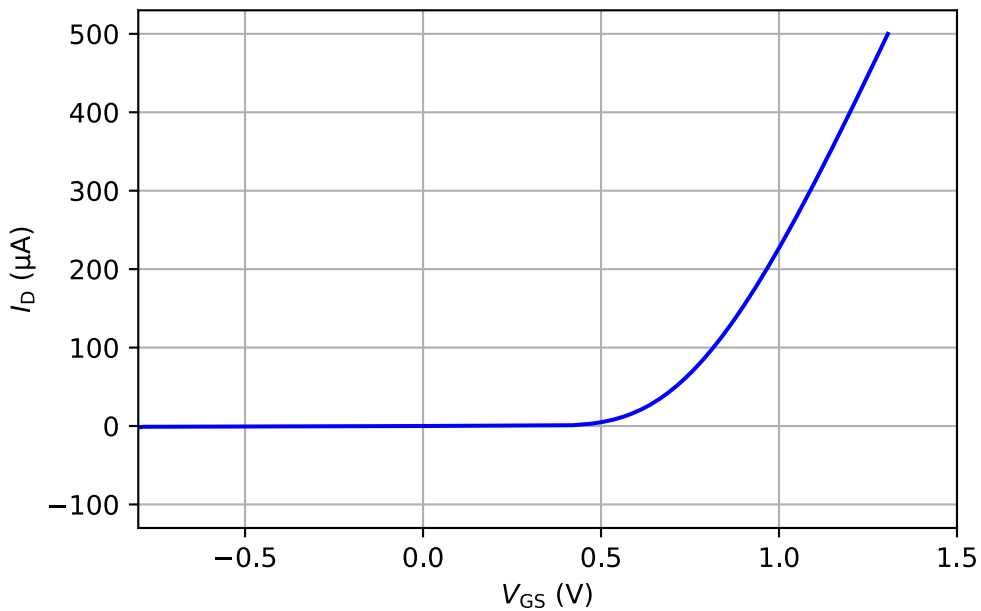


Figure 17: Drain current of a MOSFET diode with  $W=1\mu\text{m}$  and  $L=0.13\mu\text{m}$  showing the drain current as a function of the gate-source voltage.

#### i Feedback in the MOSFET Diode

It is important to realize that this configuration employs a feedback loop for operation. The voltage at the drain of the MOSFET is sensed by the gate, and the gate voltage changes until  $I_D$  is exactly equal to  $I_{\text{bias}}$ . In this sense this is probably the smallest feedback circuit one can build.

### 4.1 MOSFET Diode Sizing

We will now build this circuit in Xschem. For sizing the MOSFET we will use the  $g_m/I_D$  methodology introduced in Section 3.

#### Q Exercise: MOSFET Diode Sizing

Please build a MOSFET diode circuit in Xschem where you use an LV NMOS, set  $I_{\text{bias}} = 20 \mu\text{A}$ ,  $L = 0.13 \mu\text{m}$ , and we want to use  $g_m/I_D = 10$  (often a suitable compromise between transistor speed and  $g_m$  efficiency).

1. Use the figures in Section 3.2 to find out the proper value for  $W$ .
2. What is the  $f_T$  for this MOSFET? What is the value for  $g_m$  and  $g_{ds}$ ?
3. Draw the circuit in Xschem, and simulate the operating point. Do the values match to the values found out before during circuit sizing?

Before continuing, please finish the previous exercise. Once you are done, compare with the below provided solution.

### 💡 Solution: MOSFET Diode Sizing

1. Using the fact that  $I_{\text{bias}} = I_D = 20 \mu\text{A}$  and  $g_m/I_D = 10$  directly provides  $g_m = 0.2 \text{ mS}$ .
2. Using the self-gain plot, we see that  $g_m/g_{\text{ds}} \approx 21$ , so  $g_{\text{ds}} \approx 9.5 \mu\text{S}$ . The  $f_T$  can easily be found in the respective plot to be  $f_T = 23 \text{ GHz}$ .
3. The  $W$  of the MOSFET we find using the drain current density plot and the given bias current. Rounding to half-microns results in  $W = 1 \mu\text{m}$ .
4. Since we are looking at the graphs, we further find  $\gamma = 0.84$ ,  $V_{\text{ds,sat}} = 0.18 \text{ V}$ , and  $f_{\text{co}} \approx 15 \text{ MHz}$ .
5. In addition, we expect  $V_{\text{GS}} \approx 0.6 \text{ V}$ .

An example Jupyter notebook to extract these values accurately you can find [here](#). An Xschem schematic for this exercise is provided as well.

## 4.2 MOSFET Diode Large-Signal Behavior

As discussed above, the MOSFET diode configuration is essentially a feedback loop. Before we will analyze this loop in small-signal, we want to investigate how this loop settles in the time domain, and by doing this we can observe the large-signal settling behavior. To simulate this, we change the dc bias source from the previous example to a transient current source, which we will turn on after some picoseconds. The resulting Xschem testbench is shown in Figure 18.

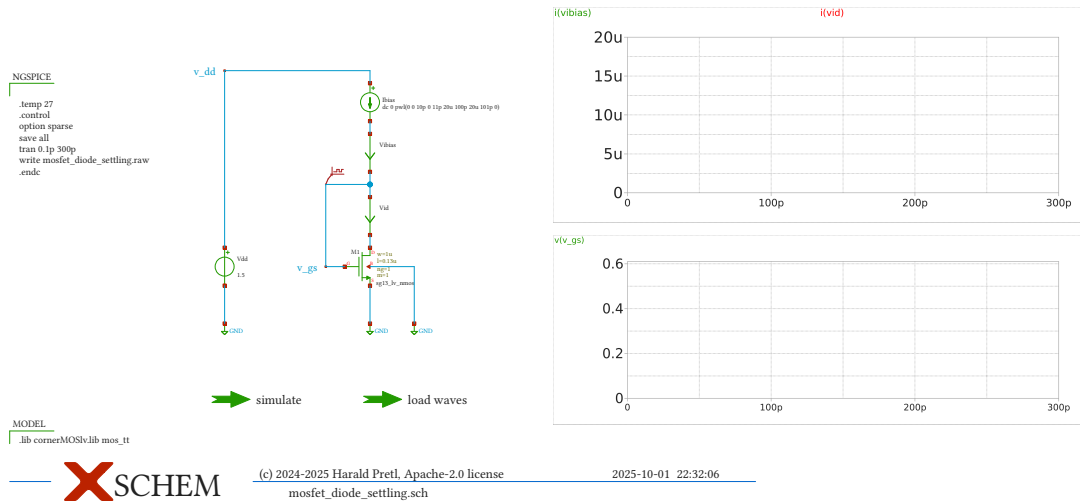


Figure 18: Testbench for MOSFET diode transient settling.

When simulating the circuit in Figure 18 another interesting effect can be observed: While the turn-on happens quite rapidly (essentially the bias current source charges the gate capacitance, until the gate-source voltage is large enough that the drain current counteracts the

bias current), the turn-off shows a very long settling tail. This is due to the fact that as the gate capacitance is discharged by the drain current, the  $V_{GS}$  drops, which in turn reduces the drain current, which will make the discharge even slower. We have an effect similar to a capacitor discharge by a diode [13].

### | Power-Down Switches

It is thus generally a good idea to add power-down switches to the circuits to disable the circuit quickly by pulling floating nodes to a defined potential (usually  $V_{DD}$  or  $V_{SS}$ ) and to avoid long intermediate states during power down. This will also allow a turn-on from a well-defined off-state.

Exemplary implementations of power-down switches are shown in the Xschem implementation of the improved OTA in Figure 76. Which  $W/L$  ratio should these transistors have? Well, in general, switches often have minimum length to be fast and to have low  $R_{on}$ . However, if there are no critical specifications (e.g., like power-down time), then these transistors are often used as dummy transistors for other circuit parts and are sized to fit the layout best.

## 4.3 MOSFET Diode Small-Signal Analysis

We now want to investigate the small-signal behavior of the MOSFET diode. Based on the small-signal model of the MOSFET in Figure 6 we realize that gate and drain are shorted, and we also connect bulk to source. We can thus simplify the circuit to the one shown in Figure 19.

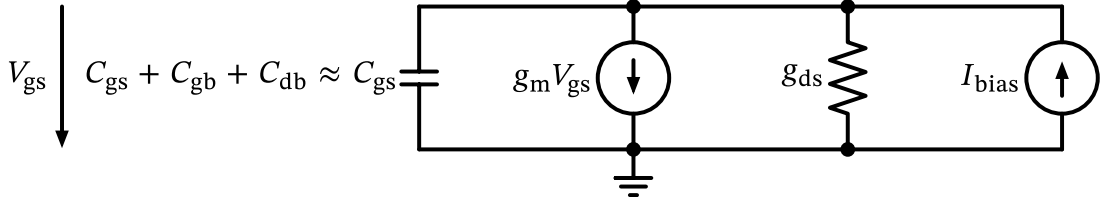


Figure 19: The MOSFET diode small-signal model (drain and gate are shorted, as well as source and bulk).

### | Ground Node Selection

For small-signal analysis we would not need to declare one node as the ground potential. However, when doing so, and selecting the ground node strategically, we can simplify the analysis, as we usually do not formulate KCL for the ground node (as we have only  $N - 1$  independent KCL equations,  $N$  being the number of nodes in the circuit), and the potential difference equations are simpler if one node is at 0 V.

For calculating the small-signal impedance of the MOSFET diode we formulate Kirchhoff's current law (KCL, also Kirchhoff's first law or Kirchhoff's junction rule) at the top node to get

$$I_{bias} - sC_{gs}V_{gs} - g_m V_{gs} - g_{ds} V_{gs} = 0.$$

It follows that

$$Z_{\text{diode}}(s) = \frac{V_{\text{gs}}}{I_{\text{bias}}} = \frac{1}{g_m + g_{\text{ds}} + sC_{\text{gs}}}. \quad (5)$$

When neglecting  $g_{\text{ds}}$ , at dc we get  $Z_{\text{diode}} = 1/g_m$ , which is an important result and should be memorized.

### ! The Admittance is Your Friend

In circuit analysis it is often algebraically easier to work with admittance instead of impedance, so please remember that Ohm's law for a conductance is  $I = G \cdot V$ , and for a capacitance is  $I = sC \cdot V$ . When writing equations, it is also practical to keep  $sC$  together, so we will strive to sort terms accordingly.

Looking at Equation 5 we see that for low frequencies, the diode impedance is resistive, and for high frequencies it becomes capacitive as the gate-source capacitance starts to dominate. The corner frequency of this low-pass can be calculated as

$$\omega_c = \frac{g_m + g_{\text{ds}}}{C_{\text{gs}}} \approx \omega_T$$

which is pretty much the transit frequency of the MOSFET!

## 4.4 MOSFET Diode Stability Analysis

### i Open-Loop Gain, Closed-Loop Gain, and Loop-Gain—A Short Recap

Figure 20 shows a generic negative feedback system with input  $X(s)$  and output  $Y(s)$ , where  $H_{\text{ol}}(s)$  is the transfer function of the feed-forward path (also called **open-loop gain**) and  $G(s)$  is the transfer function of the feedback network. The **loop-gain** is the product of both transfer functions  $T(s) = H_{\text{ol}}(s)G(s)$  and is used for the stability analysis. The **closed-loop** gain is defined as  $H_{\text{cl}}(s) = Y(s)/X(s)$  can be derived with  $Y(s) = H_{\text{ol}}(s)[X(s) - Y(s)G(s)]$  to be

$$H_{\text{cl}}(s) = \frac{Y(s)}{X(s)} = \frac{H_{\text{ol}}(s)}{1 + H_{\text{ol}}(s)G(s)} = \frac{H_{\text{ol}}(s)}{1 + T(s)} \quad (6)$$

If the open-loop gain is sufficiently large  $H_{\text{ol}}(s) \gg 1$ , then the closed-loop gain simplifies to  $H_{\text{cl}}(s) \approx 1/G(s)$ . This result is convenient, since it is independent of  $H_{\text{ol}}(s)$ . Therefore, the overall gain is only set with the feedback gain  $G(s)$  in operational amplifier circuits.

In the case of the MOSFET diode,  $G(s) = 1$  and therefore  $T(s) = H_{\text{ol}}(s)$  and  $H_{\text{cl}}(s) \approx 1$ .

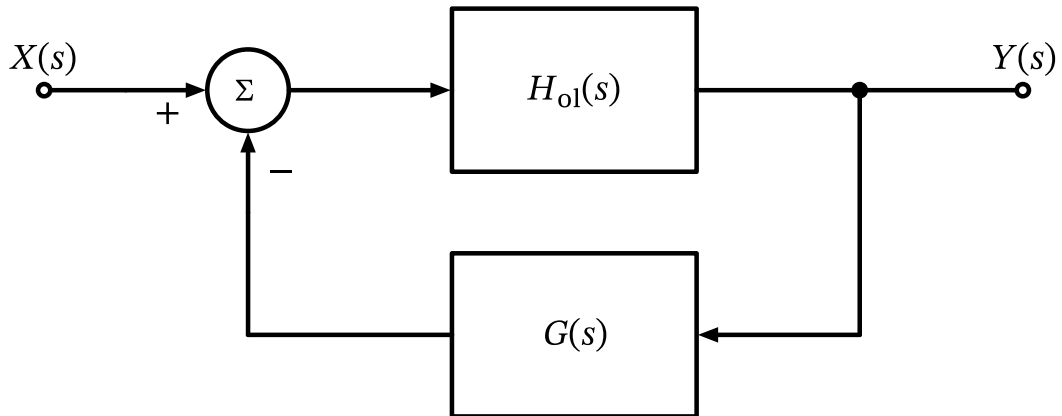


Figure 20: The block diagram of a negative feedback system.

Note that in the feedback system depicted above shows an inversion in the feedback path. Sometimes this inversion is also included in the definition of  $G(s)$ . Please be aware of this when reading literature, as different conventions exist.

## i Gain-Bandwidth Product in Feedback Systems

The gain-bandwidth product (GBP or GBWP) or transit frequency  $f_T$  of a first-order open-loop system is the product of the open-loop dc gain  $H_{\text{ol,dc}} = H_{\text{ol}}(f = 0 \text{ Hz})$  and the open-loop  $-3 \text{ dB}$  cut-off frequency  $f_{c,\text{ol}}$  of  $H_{\text{ol}}(s)$ .

$$\text{GBWP} = f_{T,\text{ol}} = H_{\text{ol,dc}} f_{c,\text{ol}}$$

If a frequency-independent negative feedback  $G$  (e.g., a resistive divider) is applied to this open-loop system, the transit frequency changes to

$$f_{T,\text{cl}} = f_{T,\text{ol}} \sqrt{1 - G^2}$$

Hence, the closed-loop transit frequency is slightly lower than the open-loop transit frequency  $f_{T,\text{cl}} < f_{T,\text{ol}}$ .

The closed-loop  $-3 \text{ dB}$  cut-off frequency  $f_{c,\text{cl}}$  can then be calculated from the open-loop transit frequency and the feedback gain.

$$f_{c,\text{cl}} = H_{\text{ol,DC}} f_{c,\text{ol}} G = f_{T,\text{ol}} G$$

This theory might be interesting when Middlebrook's and Tian's methods for loop gain analysis are later compared in the MOSFET diode testbench (see Figure 22).

The diode-connected MOSFET forms a feedback loop. What is the loop gain? For calculating it, we are breaking the loop, and apply a dummy  $C_{\text{gs}}^*$  at the right side to keep the impedances correct. A circuit diagram is shown in Figure 21, we break the loop at the red crosses. As we can see in this example, it is critically important when breaking up a loop for analysis (also for simulation!) to keep the terminal impedances the same. Only in special cases where the load impedance is very high or the driving impedance is very low is it acceptable to disregard loading effects!

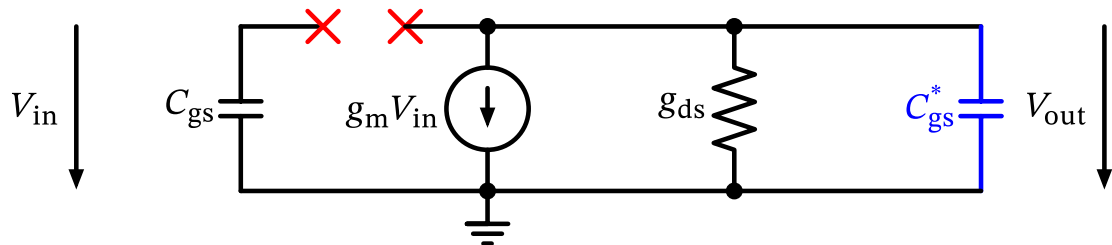


Figure 21: The MOSFET diode small-signal circuit for open-loop analysis.

We are now driving (with a voltage source)  $V_{\text{in}}$  and record the output voltage  $V_{\text{out}}$  to find the loop gain  $T(s)$ . By inspecting Figure 21 we see that

$$V_{\text{out}} = -g_m V_{\text{in}} \frac{1}{g_{\text{ds}} + sC_{\text{gs}}}.$$

The loop gain  $T(s)$  is thus

$$T(s) = (-1) \cdot \frac{V_{\text{out}}}{V_{\text{in}}} = \frac{g_m}{g_{\text{ds}} + sC_{\text{gs}}} = \frac{g_m}{g_{\text{ds}}} \frac{1}{1 + sC_{\text{gs}}g_{\text{ds}}^{-1}}. \quad (7)$$

Inspecting Equation 7 we realize that:

1. The dc gain  $g_m/g_{\text{ds}}$  is the self-gain of the MOSFET, so  $20 \log_{10}(0.2 \cdot 10^{-3}/9.6 \cdot 10^{-6}) = 26.4 \text{ dB}$ .
2. There is a pole at  $\omega_p = -g_{\text{ds}}/C_{\text{gs}}$ , which is at  $9.6 \cdot 10^{-6}/(2\pi \cdot 1.4 \cdot 10^{-15}) = 1.1 \text{ GHz}$ .

With this single pole location in  $T(s)$  this loop is perfectly stable at under all conditions (remember that a single pole results in a maximum phase shift of  $-90^\circ$ ).

The question is now how to simulate this loop gain, i.e., how to break the loop open in simulation? In general there are various methods, as we can use artificially large (ideal) inductors and capacitors to break loops open and still establish the correct dc operating points for the ac loop analysis. This is called **Rosenstark's method** [14]. However, mimicking the correct loading can be an issue, and requires a lot of careful consideration.

There is an alternative method which breaks the loop open only by adding an ac voltage source in series (thus keeps the dc operating point intact), or injects current using an ac current source. Based on both measurements the loop gain can be calculated. This is called **Middlebrook's method** [15] and is based on double injection, and we will use it for our loop simulations. This method is detailed in Section 16.

There are several other methods like Tian's method [16], for example. A comprehensive overview can be found in [17] which describes ten different simulation-based loop gain analysis methods.

We now want to simulate the loop transfer function  $T(s)$  by using Middlebrook's and Tian's method and confirm our analysis above.

## 💡 Exercise: MOSFET Diode Loop Analysis

Please build a simulation testbench in Xschem to simulate the open-loop transfer function of the MOSFET diode. Confirm the dc gain and pole location as given by Equation 7.

If you are getting stuck you can look at this Xschem testbench, shown in Figure 22.

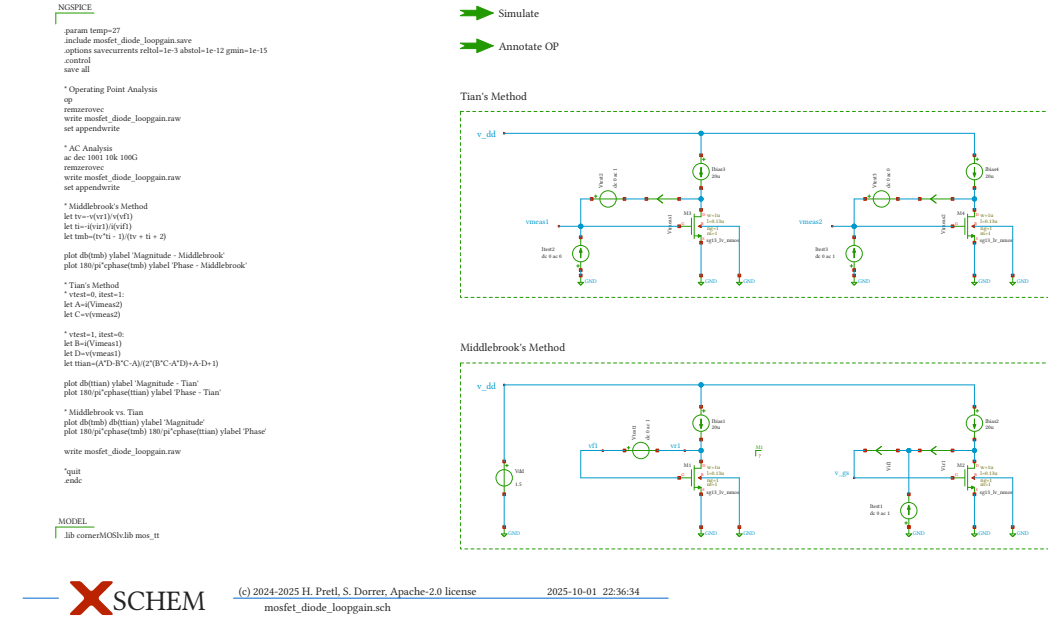


Figure 22: Testbench for MOSFET diode stability analysis.

From simulation we see that the open-loop gain is 24.9 dB at low frequencies, which matches quite well our prediction of 26.4 dB. In the Bode plot we see a low-pass with a  $-3$  dB corner frequency of 1.4 GHz, which again is fairly close to our prediction of 1.1 GHz.

### ❗ What About Large-Signal Stability?

Keep in mind that the above simulation only verifies the small-signal stability in one certain operating point. If we later look at the stability of an OTA it might be a good idea to verify the small-signal stability in different operating points.

Furthermore, one can apply a step response to the closed-loop system input and estimate the phase margin from the overshoot at the output (see “Automatic Control” lecture). One could also use a step-wise step response to simulate different operating points for a certain time (see “Introduction in Integrated Circuit Design” lecture).

## 4.5 MOSFET Diode Noise Calculation

As a final exercise on the MOSFET diode circuit we want to calculate the output noise when we consider  $V_{GS}$  the output reference voltage which is created when passing a bias current through the MOSFET diode. The bias current we will assume noiseless.

We are going to use the small-signal circuit shown in Figure 23.

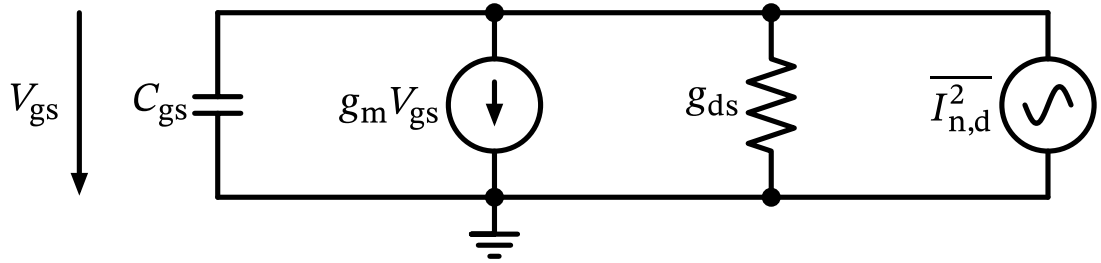


Figure 23: The MOSFET diode small-signal model with drain noise source.

As we have already calculated the small-signal diode impedance in Equation 5 we will use this result, and just note that the drain current noise of the MOSFET flows through this impedance. The noise voltage at  $V_{gs}$  is thus given as

$$\overline{V_n^2} = |Z_{\text{diode}}|^2 \overline{I_{n,d}^2}.$$

The drain current noise of the MOSFET is given as (introduced in Section 2.1.2)

$$\overline{I_{n,d}^2} = 4kT\gamma g_m.$$

For low frequencies (ignoring  $g_{ds}$  and  $C_{gs}$ ) we get

$$\overline{V_n^2} = |Z_{\text{diode}}|^2 \overline{I_{n,d}^2} = \frac{1}{g_m^2} 4kT\gamma g_m = \frac{4kT\gamma}{g_m}$$

which is the thermal noise of a resistor of value  $1/g_m$  enhanced by the factor  $\gamma$ .

We now calculate the full equation, and after a bit of algebra arrive at

$$\overline{V_n^2}(f) = \frac{4kT\gamma g_m}{(g_m + g_{ds})^2 + (2\pi f C_{gs})^2}. \quad (8)$$

If we are interested in the PSD of the noise then Equation 8 gives us the result. If we are interested in the rms value (the total noise) we need to integrate this equation, using the following identity:

**i Useful Integral for Noise Calculations**

$$\int_0^\infty \frac{a}{b^2 + c^2 f^2} df = \frac{\pi}{2} \frac{a}{b \cdot c} \quad (9)$$

Using the integral help in Equation 9, we can easily transform Equation 8 to

$$V_{n,\text{rms}}^2 = \int_0^\infty \overline{V_n^2}(f) df = \frac{kT\gamma g_m}{(g_m + g_{ds})C_{gs}}. \quad (10)$$

The form of Equation 10 is the exact solution, but we gain additional insight if we assume that  $g_m + g_{ds} \approx g_m$  and then

$$V_{n,\text{rms}}^2 = \frac{kT\gamma}{C_{\text{gs}}} \quad (11)$$

Inspecting Equation 11 we see our familiar  $kT/C$  noise multiplied by the factor  $\gamma$ !

### 💡 Exercise: Total Output Noise of RC-Lowpass

If you have never calculated this before then you should work through the following: Calculate the total output noise of an  $RC$ -lowpass filter. Formulate the transfer function in the Laplace domain, and put the equivalent resistor noise voltage source at the input, calculate the transfer to the output, and then integrate the output PSD (like we did for the MOSFET diode noise).

You will find that the output noise is

$$V_{n,\text{rms}}^2 = \frac{kT}{C}$$

which is independent of  $R$ ! This is a surprising result, and is the well-known  $kT/C$  noise. Intuitively, we could argue that the noise increases with larger  $R$ , but at the same time, the bandwidth decreases and therefore  $R$  does not add additional noise. More detailed information and an intuitive explanation of  $kT/C$  noise can be found in [18].

Side note: The shortest derivation of this formula involves the equipartition theorem: Any system in thermal equilibrium with a reservoir of temperature  $T$  has a fluctuation energy of  $kT/2$  per degree of freedom. This  $RC$  system has one degree of freedom in the voltage on the capacitor, and the stored energy in the capacitor is  $CV_{\text{rms}}^2/2$ . Equating both energies we find that  $V_{\text{rms}}^2 = kT/C$  [19].

To calculate the total output noise of a generalized passive network Bode's noise theorem is quite practical (see Section 17.2).

Calculating the rms noise voltage for our MOSFET diode we get

$$\sqrt{V_{n,\text{rms}}^2} = \sqrt{1.38 \cdot 10^{-23} \cdot 300 \cdot 0.84 / 1.4 \cdot 10^{-15}} = 1.58 \text{ mV},$$

which is a sizeable value! Think about it, can this rms noise voltage be measured with an oscilloscope? If not, why? We run circuits in this technology at  $V_{\text{DD}} = 1.5 \text{ V}$ , which leaves us with a signal swing of ca.  $1.1 \text{ V}_{\text{pp}}$  (single-ended), resulting in a dynamic range in this case of  $20 \log_{10}(0.39/1.58 \cdot 10^{-3}) \approx 48 \text{ dB}$  assuming a sinusoidal signal. In order to get a feeling which dynamic range is “good”, we can calculate the required dynamic range of a 16-bit audio ADC to be  $6.02 \cdot 16 + 1.76 \text{ dB} = 98.08 \text{ dB} \approx 100 \text{ dB}$ . This calculation should make clear that, for example, the correct sizing of the sample&hold capacitor is crucial for low rms noise voltage.

### ! Be Careful with Parasitic Capacitances in IC Design

In general, in integrated circuit design, we often have only small parasitic capacitances on many nodes that could sum up to unwanted high noise according to Equation 11. If one wants to lower the noise an increased capacitance could limit the bandwidth (and thus the  $kT/C$  noise).

### ! Large Bandwidth and Noise

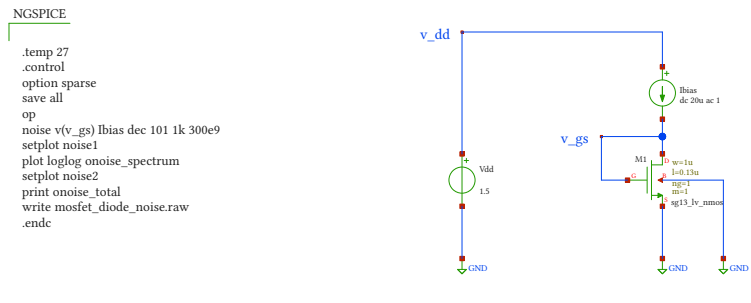
Remember: Large bandwidth circuits integrate noise over a wide bandwidth resulting in (potentially) considerable rms noise. The way to lower the total noise is to lower the PSD of the noise contributions, which usually requires increased power consumption. So in a nutshell:

Large bandwidth plus small noise equals large power consumption.

### 💡 Exercise: MOSFET Diode Noise

Please build a simulation testbench in Xschem to simulate the noise performance of the MOSFET diode, and confirm the rms noise value that we just calculated. Look at the rms value and the PSD of the noise, and play around with the integration limits. What is the effect? Can you see the flicker noise in the PSD? How much is its contribution to the rms noise? What is the value of  $f_{co}$ , and does it correspond to the above calculated one?

If you are getting stuck you can look at this Xschem testbench, shown in Figure 24.



➡ simulate ➡ annotate OP



(c) 2024 H. Pretl, Apache-2.0 license  
mosfet\_diode\_noise.sch

2025-03-16 12:07:57

Figure 24: Testbench for MOSFET diode noise analysis.

## 4.6 Conclusion

In this section we investigated the simple MOSFET-diode circuit. We learned important skills like how to derive a small-signal model and how to calculate important features like noise and open-loop gain for stability analysis. We introduced Middlebrook's method to have a mechanism to open up loops in simulation (and calculation) without disturbing dc operating points or introduce errors by changing loading conditions.

If you feel that you have not yet mastered these topics or are uncertain in the operation of Xschem or ngspice, please go back to the beginning of the section and read through the theory and redo the exercises.

## 5 Common-Source Amplifier

We now want to step up our game, and use more components to design something useful. We will use a basic circuit structure, namely a single-ended common-source amplifier. The structure of this circuit, using a resistor as a load, is shown in Figure 25.

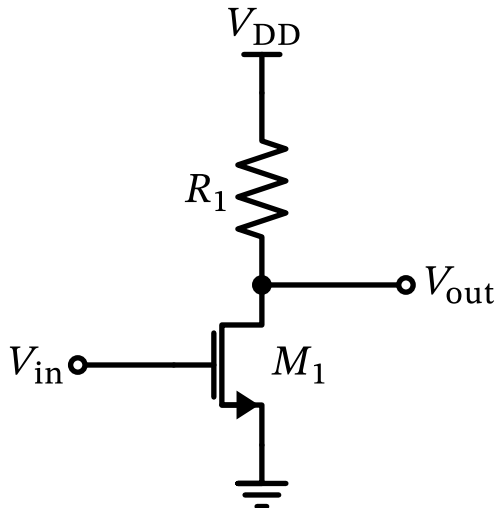


Figure 25: A MOSFET common-source amplifier with resistive load.

The function of this circuit is as follows: Assuming the MOSFET  $M_1$  is kept in saturation, then a small-signal voltage  $V_{in}$  applied at the gate is converted into a drain current  $I_d$  by the MOSFET's transconductance  $g_m$ . Then, this current is converted into a voltage again in the resistor  $R_1$ . Ultimately, we have a dc voltage gain  $A_v$  of

$$A_v = \frac{V_{out}}{V_{in}} \approx -\frac{g_m V_{in} R_1}{V_{in}} = -g_m R_1.$$

As explained above, it is a good approach to see electronic circuit components as

- **voltage-to-current** converter(MOSFET as common-source or common-gate; resistor),
- **current-to-voltage** converter (resistor),
- **current-to-current** converter (MOSFET as common-gate), and
- **voltage-to-voltage** converter (MOSFET as common-drain)

conversions for better understanding.

## 5.1 Sense Amplifier Driving 50 Ohm Matched Load

Let us now size and design an exemplary implementation of this amplifier (of course using the  $g_m/I_D$  method). In order to have useful real-life specifications, we want to build an amplifier which can be used to sense an on-chip voltage and drive off-chip measurement equipment. Often, this equipment has an input impedance of  $50\Omega$ , and we want to have an impedance-matched output. The voltage gain shall be set to 1 (essentially, we want to sense a voltage and drive the measurement equipment).

The resulting circuit is shown in Figure 26. As the load is usually ground-referred, and we want to avoid a dc-block at the output, we use a PMOS amplifier stage (compare with Figure 25).

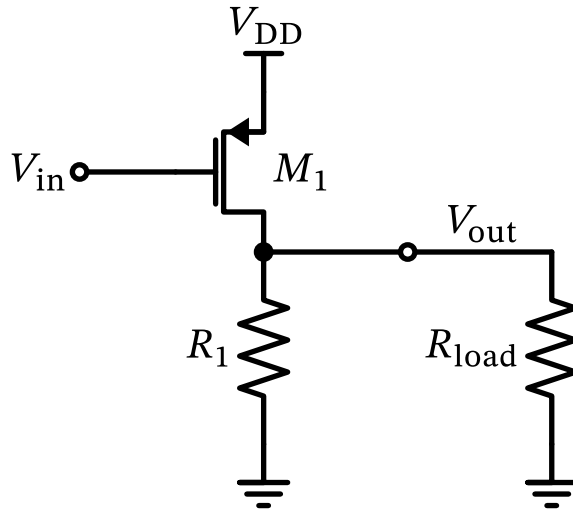


Figure 26: A MOSFET common-source amplifier with 50 Ohm load.

Exercise: PMOS-Based Measurement Amplifier

Please think about why exactly we want this measurement amplifier be based on a PMOS instead of an NMOS.

The power matching requirement at the output mandates that  $R_1 = R_{\text{load}}$ , so  $R'_1 = R_{\text{load}} \parallel R_1 = 25\Omega$ . The voltage gain requirement of  $|A_v| = 1$  results in  $g_m = 1/R'_1 = 40\text{ mS}$ .

We now need to find  $W$  and  $L$  of  $M_1$  and calculate the required bias current  $I_D$ . We also need to find the proper  $V_{GS}$  to set this current. As usual, we use a Jupyter notebook to calculate these values. Since we require modest speed of this buffer we use a  $g_m/I_D = 8$  and set  $L = 0.13\mu\text{m}$ . The notebook is available here. The resulting circuit including all component values is shown at the end of the notebook (the red input capacitor shows the  $C_{gg}$  of the MOSFET).

### ! Important 1: MOSFET Parameters NG and M

When sizing the MOSFET for this example we found that we need a fairly large  $W$ , resulting in a MOSFET aspect ratio of  $W/L \gg 1000$ . When constructing an integrated circuit out of individual MOSFET we strive for an overall IC dimension that is roughly quadratic. For MOSFET with large aspect ratios we need to get them into a comfortable shape.

In order to achieve this, we construct the MOSFET out of smaller pieces, and the size of this pieces (called “gate fingers”) are controlled by the parameter `ng`. These MOSFET gate fingers all have the same  $L$ , but their width is  $W_{\text{finger}} = W / \text{ng}$ . All this individual smaller MOSFET are connected in parallel.

In order to increase the MOSFET model accuracy, often the maximum value of  $W_{\text{finger}}$  is limited. In the case of SG13G2  $W_{\text{finger}} \leq 10 \mu\text{m}$ .

In order to construct even larger MOSFET, we can connect multiple MOSFET in parallel. We can do this in the circuit editor by placing and connecting these MOSFET; but since this is often used there is a more convenient way: By using the parameter `m` (“multiplier” or “multiplicity”) we instantiate  $m$  MOSFET connected in parallel.

When to use `ng` and when to use `m`? The use of `ng` results in a more compact IC layout, and is thus generally preferable. Only in certain instances (e.g., when using a really large  $W$ ) `m` should be used. Further, the thoughtful use of `ng` **allows to construct all the NMOS and PMOS of a circuit out of the same gate finger elements**. This will result in a very compact layout!

## 💡 Exercise: Measurement Amplifier Simulation

Please go through the sizing notebook of the measurement amplifier and double-check the calculations. Do you agree that the calculations are correct?

Once you agree with the circuit sizing please build an Xschem simulation testbench where you simulate the small-signal voltage gain  $A_v$  of this measurement amplifier if it is driven with an ideal voltage source. Keep in mind that the maximum MOSFET finger width is 10µm in this technology, so you need to set the parameter  $ng$  accordingly (see Important 1).

- What is the dc gain of this amplifier when loaded with  $50\Omega$ ?
- The dc gain is likely not exactly 0dB. Why is this so?
- Increase the width  $W$  of the PMOS until the gain is correct. What is the  $W$  that you had to set, and how much is  $I_D$  now?
- What is the bandwidth (i.e., the  $-3\text{dB}$  corner frequency) of the output voltage, when the voltage source has a source resistance of  $1\text{k}\Omega$ ?

If you get stuck, here is the solution to this exercise, and it is also shown in Figure 27.

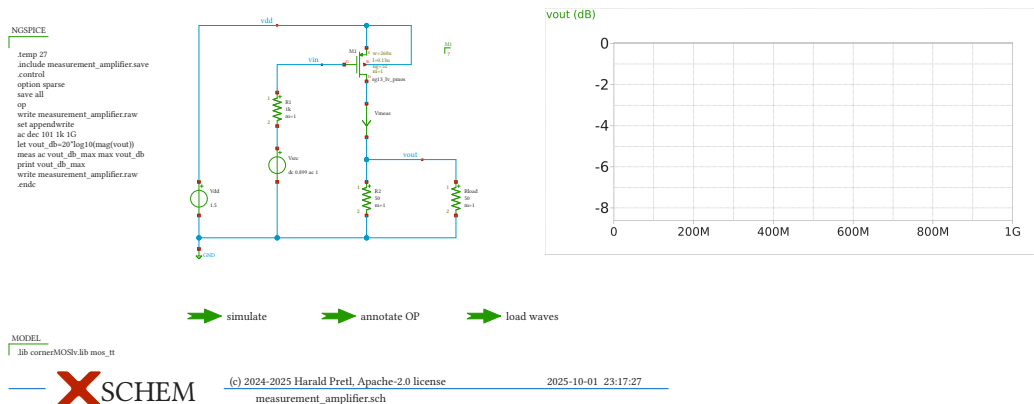


Figure 27: Simulation schematic of the common-source measurement amplifier.

By now we have designed a measurement amplifier based on a common-source stage. One problem with this stage is the relatively large input capacitance  $C_{GG}$  of approx. 0.3pF, which loads the input source. Another issue even more severe is that the fact that the bias point in this circuit is set by the dc voltage level at the input. In general, we want a setup where the bias points of the circuit are largely independent of the dc input voltages. This is why in integrated circuit design we often design **differential circuits** where the input and output signals are given by the differential voltages, and are largely independent from the common-mode voltages. This is usually an advantage.

## 6 Current Mirror

In this section we will look into a fundamental building block which is often used in integrated circuit design, the **current mirror** [20]. A diagram is shown in Figure 28 with one MOSFET diode converting the incoming bias current into a voltage  $V_{GS} = f(I_{D1}) = f(I_{bias})$ , and two output MOSFETs working as current sources, which are biased from the diode. By properly selecting all  $W$  and  $L$  the input current can be scaled, and multiple copies can be created at once. Shown in the figure are two output currents  $I_{out1}$  and  $I_{out2}$ , but any number of parallel branches can be realized (note that this is true for MOSFET as no gate current flows; for the case of BJTs, the base current flowing into the various transistors is subtracted from  $I_{bias}$ , so usually a compensation circuit is added).

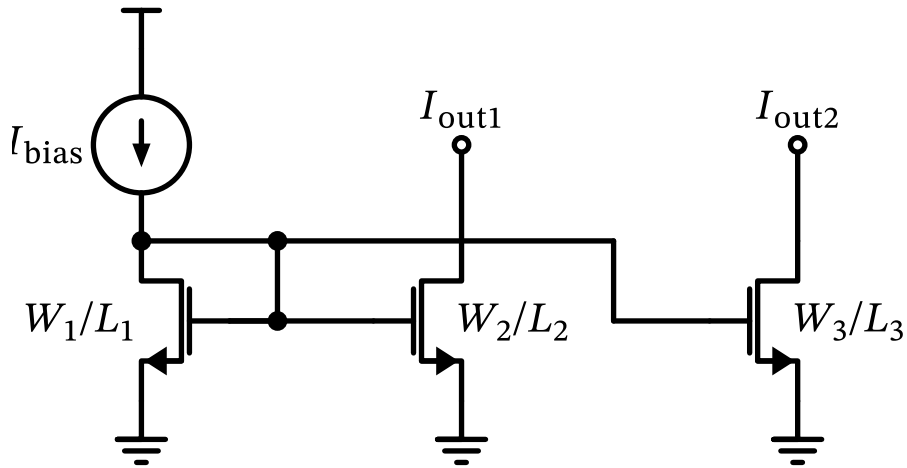


Figure 28: A current mirror with two output branches.

Neglecting the impact of  $g_{ds1}$  and  $g_{ds2}$ , the output current  $I_{out1}$  is then given by

$$I_{out1} \approx I_{bias} \frac{W_2}{L_2} \frac{L_1}{W_1}$$

and the output current  $I_{out2}$  is given by

$$I_{out2} \approx I_{bias} \frac{W_3}{L_3} \frac{L_1}{W_1}.$$

For good matching care has to be taken that the MOSFET widths and lengths are constructed out of **unit elements** of identical size, where an appropriate amount of these single units are then arranged in series or parallel configuration to arrive at the target  $W$  and  $L$  (remember MOSFET parameters  $\text{ng}$  and  $\text{m}$ , see Important 1).

As we know from earlier investigations of the MOSFET performance in Section 3 the drain current of a MOSFET is a function of  $V_{GS}$  and  $V_{DS}$ . As long as the MOSFET stays in saturation (i.e.,  $V_{DS} > V_{ds,\text{sat}}$ ) the drain current is just a mild function of  $V_{DS}$  (essentially the effect of  $g_{ds}$ , which is the output conductance of the MOSFET). A fundamental flaw/limitation of the basic current mirror shown in Figure 28 is the mismatch of the  $V_{DS}$  of the MOSFETs. The input-side diode has  $V_{GS} = V_{DS1}$ , whereas the output current sources have a  $V_{DS2,3}$  depending on the connected circuitry. Improved current mirrors exist (fixing this flaw), however, when

a current mirror is required with mediocre performance requirements this structure can be used for its simplicity.

### 💡 Exercise: Current Mirror

Please construct a current mirror based on the MOSFET-diode which we sized in Section 4.

The input current  $I_{\text{bias}} = 20 \mu\text{A}$ , and we want three output currents of size  $10 \mu\text{A}$ ,  $20 \mu\text{A}$ , and  $40 \mu\text{A}$ .

Sweep the output voltage of all three current branches and see over which voltage range an acceptable current is created. For which output voltage range is the current departing from its ideal value, and why?

You see that the slope of the output current is quite bad, as  $g_{\text{ds}}$  is too large. We can improve this by changing the length to  $L = 5 \mu\text{m}$  (for motivation, please look at the graphs in Section 3). In addition, for a current mirror we are not interested in a high  $g_m/I_D$  value, so we can use  $g_m/I_D = 5$  in this case. Please size the current mirror MOSFETs accordingly (please round the  $W$  to half micron, to keep sizes a bit more practical). Compare this result to the previous one, what changed?

In case you get stuck, here are Xschem schematics for the original and the improved current mirrors.

## 7 Differential Pair

Like the current mirror in Section 6 the **differential pair** is an ubiquitous building block often used in integrated circuit design [21]. The fundamental structure is given in Figure 29.

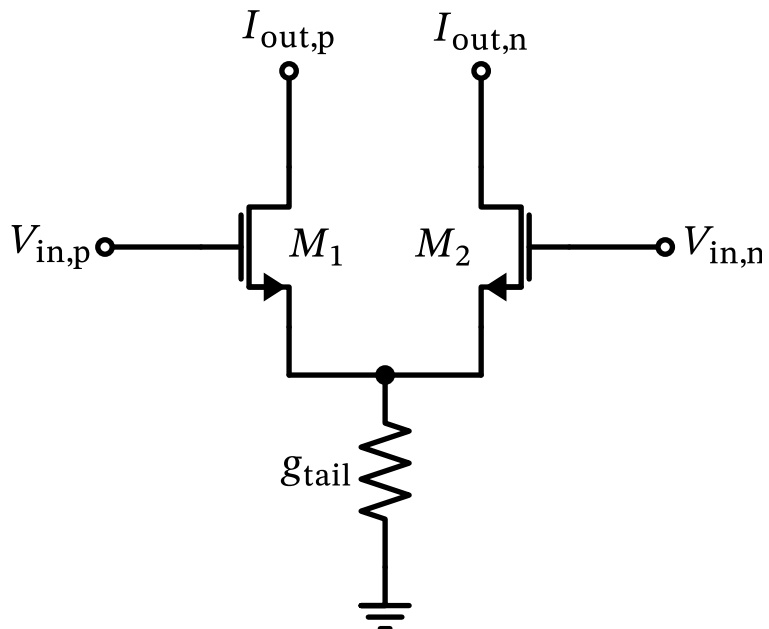


Figure 29: A differential pair.

In order to understand its operation it is instructive to separate the input condition into

1. a purely differential voltage, and
2. a common-mode voltage,

and see what the impact on the output currents is.

### 7.1 Differential Operation of the Diffpair

For a differential mode of operation we assume that the input common mode voltage is constant, i.e.,  $(V_{\text{in},p} + V_{\text{in},n})/2 = V_{\text{CM}}$ . The differential input voltage  $v_{\text{in}} = V_{\text{in},p} - V_{\text{in},n}$ , so that

$$V_{\text{in},p} = V_{\text{CM}} + \frac{v_{\text{in}}}{2}$$

and

$$V_{\text{in},n} = V_{\text{CM}} - \frac{v_{\text{in}}}{2}.$$

For a small-signal differential drive the potential at the tail point stays constant and we can treat it as a virtual ground. The output current on each side is then given by (neglecting  $g_{\text{ds}}$  and  $g_{\text{mb}}$  of  $M_1$  and  $M_2$ )

$$I_{\text{out},p} = g_{m1} \left( \frac{V_{\text{in}}}{2} \right)$$

and

$$I_{\text{out},n} = g_{m2} \left( -\frac{V_{\text{in}}}{2} \right).$$

Usually we assume symmetry in the differential pair, so  $g_{m1} = g_{m2} = g_m$ . The differential output current  $I_{\text{out}}$  is then given by

$$I_{\text{out}} = I_{\text{out},p} - I_{\text{out},n} = g_m V_{\text{in}} \quad (12)$$

We see in Equation 12 that the differential output current is simply the differential input voltage multiplied by the  $g_m$  of the individual transistor. We also note that the bottom conductance  $g_{\text{tail}}$  plays no role for the small-signal differential operation.

### 7.2 Common-Mode Operation of the Diffpair

Usually, the source conductance  $g_{\text{tail}}$  is realized by a current source and ideally should be  $g_{\text{tail}} = 0$ . If this is the case, then the output currents are not a function of the common-mode input voltage ( $I_{\text{tail}}$  is set by the tail current source), and

$$I_{\text{out},p} = I_{\text{out},n} = \frac{I_{\text{tail}}}{2}.$$

However, if we assume a realistic tail current source then  $g_{\text{tail}} > 0$ . For analysis we can simply look at a half circuit since the circuit operation is symmetric. In order to simplify the analysis a bit we remove all capacitors from the MOSFET small-signal model and set  $g_{\text{ds}} = g_{\text{mb}} = 0$ . We then arrive at the small-signal equivalent circuit shown in Figure 30 (note that we set  $V_{\text{in},p} = V_{\text{in},n} = V_{\text{in}}$  and  $I_{\text{out},p} = I_{\text{out},n} = I_{\text{out}}$  under symmetry considerations).

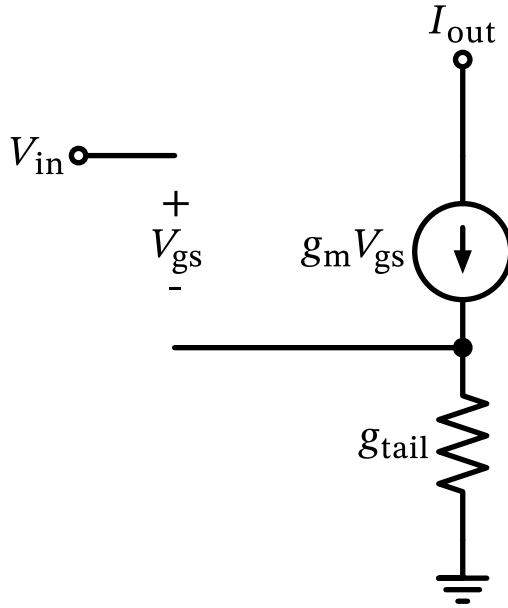


Figure 30: Small-signal model of the differential pair half-circuit in common-mode operation.

Formulating KVL for the input-side loop we get

$$V_{in} = V_{gs} + \frac{I_d}{g_{tail}}.$$

With  $I_{out} = I_d = g_m V_{gs}$  we arrive at

$$I_{out} = \frac{g_m g_{tail}}{g_m + g_{tail}} V_{in} \quad (13)$$

Interpreting Equation 13 we can distinguish the following extreme cases:

1. If  $g_{tail} = 0$  (ideal tail current source) then  $I_{out} = 0$ , the common-mode voltage variation from the input is suppressed and does not show up at the common-mode output current (which is constant due to the ideal tail current source). This is usually the case that we want to achieve.
2. If  $g_{tail} \rightarrow \infty$  then  $I_{out} = g_m V_{in}$ , which means the output current is a function of the MOSFET  $g_m$ . If everything is perfectly matched, then the differential output current is zero, but the common-mode output current changes according to the common-mode input voltage. In special cases this can be a wanted behavior, this configuration is called a “pseudo-differential pair.”
3. For the typical case that  $g_m \gg g_{tail}$  then  $I_{out} \approx g_{tail} V_{in}$ .

Note that the result of Equation 13 is also valid for the general case of a degenerated common-source transistor stage (see Figure 31). The effective transconductance  $g_{(m)'}'$  is given by ( $R_{degen} = g_{tail}^{-1}$ )

$$g_{(m)'}' = \frac{I_{out}}{V_{in}} = \frac{g_m g_{tail}}{g_m + g_{tail}} = \frac{1}{g_m^{-1} + R_{degen}}.$$

When no degeneration resistor is used, then  $g_{(m)'}' = g_m$ . If a degeneration of  $R_{degen} \gg g_m^{-1}$  is used then  $g_{(m)'}' = 1/R_{degen}$ . This result is worth memorizing.

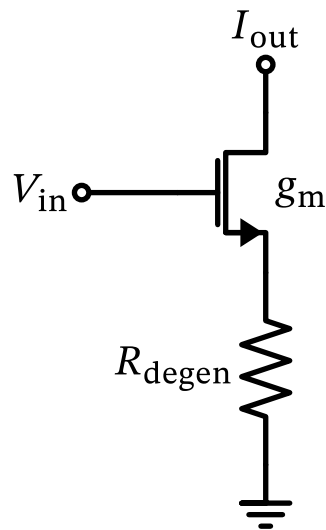


Figure 31: A MOSFET common-source amplifier with resistive degeneration.

## 8 A Basic 5-Transistor OTA

Armed with the insights of basic transistor operation (Section 2 and Section 3) and the working knowledge of the current mirror (Section 4 and Section 6) as well as the differential pair (Section 7) we can now start to design our first real circuit. A fundamental (simple) circuit that is often used for basic tasks is the 5-transistor operational transconductance amplifier (OTA). A circuit diagram of this 5T-OTA is shown in Figure 32.

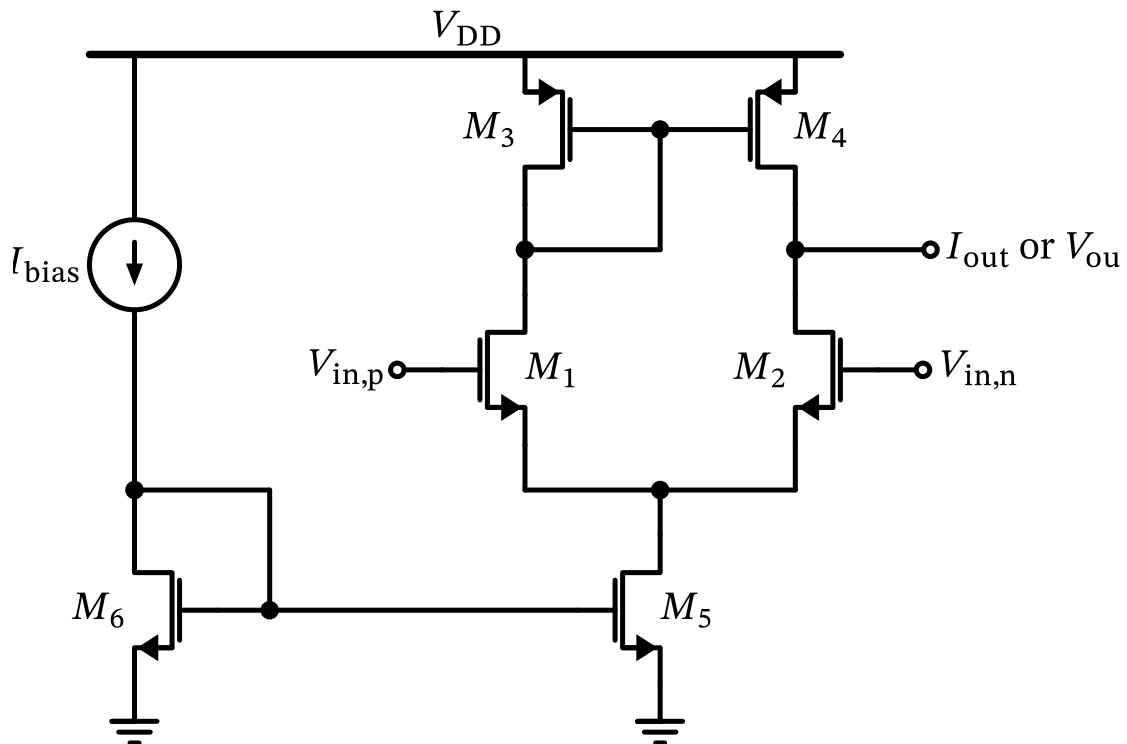


Figure 32: The 5-transistor OTA.

### Refresh MOSFET Basic Circuits

While we repeat the basics of elementary MOSFET amplifier stages (like common-source stage, common-gate stage, and current mirror) in this course material, the following compendium [22] is recommended for review. It is freely available at <https://github.com/bmurmann/Book-on-MOS-stages>.

In addition, we can highly recommend these references [1, B. Razavi [2]] for further study.

The operation is as follows:  $M_{1,2}$  form a differential pair which is biased by the current source  $M_5$ .  $M_{5,6}$  form a current mirror, thus the input bias current  $I_{\text{bias}}$  sets the bias current in the OTA. The differential pair  $M_{1,2}$  is loaded by the current mirror  $M_{3,4}$  which mirrors the drain current of  $M_1$  to the right side. Here, the currents from  $M_4$  and  $M_2$  are summed, and together with the conductance effective at the output node, a voltage builds up.

### Operational Amplifier (op-amp, OPA) vs. Operational Transconductance Amplifier (OTA)

An operational amplifier is a universal electronic building block characterized by (in the ideal case):

- infinite input impedance at the input ports ( $R_{\text{in}} \rightarrow \infty$ )
- zero output resistance, i.e., a voltage output ( $R_{\text{out}} = 0$ )
- infinite voltage gain ( $A_v = V_{\text{out}}/V_{\text{in}} \rightarrow \infty$ )

An operational transconductance amplifier is a building block characterized by (again in the ideal case):

- infinite input impedance at the input ports ( $R_{\text{in}} \rightarrow \infty$ )
- infinite output resistance, i.e., a current output ( $R_{\text{out}} \rightarrow \infty$ )
- infinite transconductance ( $G = I_{\text{out}}/V_{\text{in}} \rightarrow \infty$ )

In integrated circuits, we very often load an OPA/OTA high-ohmic, i.e., with a capacitive load. Hence, an OTA can be used to create a voltage-mode amplifier with high gain, approaching the properties of the OPA. If an OTA is used to drive a low-ohmic load, the voltage gain will be low, and we have to use this block as a transconductance amplifier. Since the output changes behavior depending on high- or low-ohmic loading, we label the output in Figure 32 accordingly.

Why then implement an OTA instead of an OPA? Usually, an OTA is a simpler structure than an OPA. As a general rule, the simplest circuit that can do a job is usually the best choice.

We note that  $M_{1,2}$  and  $M_{3,4}$  need to be symmetric, thus will have the same  $W$  and  $L$  dimensioning.  $M_{5,6}$  we scale accordingly to set the correct bias current in the OTA.

## 8.1 Voltage Buffer with OTA

In order to design an OTA we need an application, and from this we need to derive the circuit specifications. We want to use this OTA to realize a voltage buffer which lightly loads an input

voltage source and can drive a large capacitive load. Such a configuration is often used to, e.g., buffer a reference voltage that is needed (and thus loaded) by another circuit. The block diagram of this configuration is shown in Figure 33.

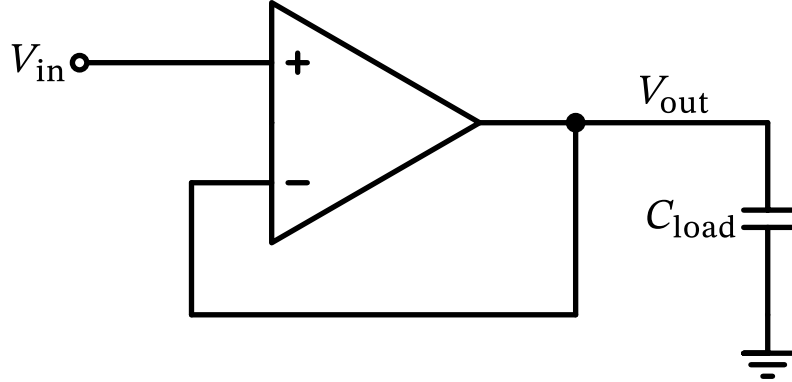


Figure 33: A voltage buffer (based on OTA) driving a capacitive load.

If the voltage gain of the OTA in Figure 33 is high, then  $V_{\text{out}} \approx V_{\text{in}}$ . We now want to design an OTA for this application fitting the following specification values (see Table 2). These values are rather typical of what could be expected for such a buffer design.

Table 2: Voltage buffer specification

Specification	Value	Unit
Supply voltage	$1.45 < \underline{1.5} < 1.55$	V
Temperature range (industrial)	$-40 < \underline{27} < 125$	degC
Load capacitance $C_{\text{load}}$	50	fF
Input voltage range (for buffering 2/3 bandgap voltage)	$0.7 < \underline{0.8} < 0.9$	V
Signal bandwidth (3dB)	> 10	MHz
Output voltage error	< 3	%
Total output noise (rms)	< 1	mV <sub>rms</sub>
Supply current (as low as possible)	< 10	µA
Stability	stable for rated $C_{\text{load}}$	
Turn-on time (settled to with 1%)	< 10	µs
Externally provided bias current (nominal)	20	µA

## 8.2 Large-Signal Analysis of the OTA

The first step when receiving a design task is to look at the specifications, and see whether they make sense. The detailed performance of the design will be the result of the circuit simulation, but before we step into sizing we need to do a few simple calculations to (a) do back-of-the-envelope gauging if the specification makes sense, and (b) use the derived analytical equations as guide for the sizing procedure.

In terms of large-signal operation, we will now check whether the input and output voltage range, as well as the settling time can be roughly met. Since we do not know yet the resulting  $V_{GS}$  of the transistors we use 0.6 V as an initial guess. If we run into issues with that guess we know how to later steer the sizing procedure. The follower configuration showing the transistor-level details including estimated operating points is shown in Figure 34.

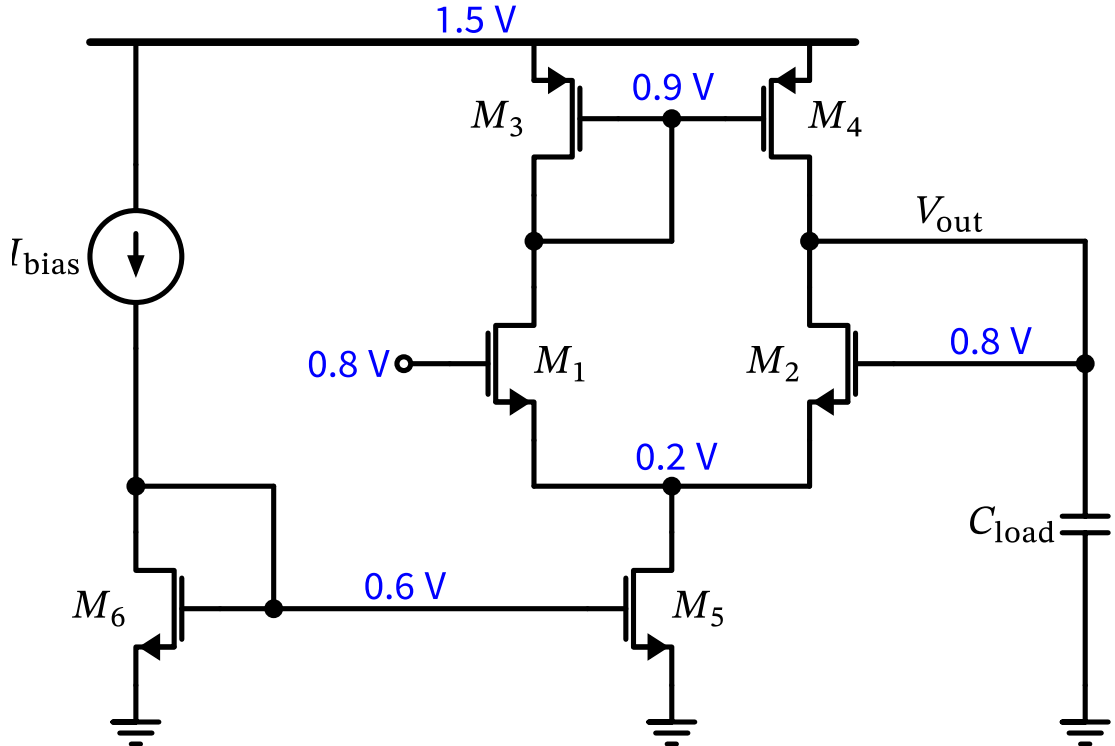


Figure 34: The 5-transistor OTA with external connections and load capacitor. Estimated dc operating points are shown in blue.

- When the input is at its maximum of 0.9 V, we see that we need to keep  $M_1$  in saturation. We can calculate that  $V_{DS1} = V_{DD} - |V_{GS3}| + V_{GS1} - V_{in} = 1.45 - 0.6 + 0.6 - 0.9 = 0.55$  V, which leaves enough margin.
- When the input is at its minimum of 0.7 V, we see that the  $V_{DS5}$  of  $M_5$  is calculated as  $V_{DS5} = V_{in} - V_{GS1} = 0.7 - 0.6 = 0.1$  V, so this leaves little margin, but we can make  $V_{GS1}$  smaller, so it should work out.
- For the output voltage, when the output voltage is on the high side, it leaves  $|V_{DS4}| = V_{DD} - V_{out} = 1.45 - 0.9 = 0.55$  V, which is enough margin.

In summary, we think that we can make an NMOS-input OTA like the one in Figure 32 (and in Figure 34) work for the required supply and input- and output-voltages. If this would not work out, we need to look for further options, like a PMOS-input OTA, or a NMOS/PMOS-input OTA.

Another large-signal specification item that we can quickly check is the settling time. Under slewing conditions, the complete bias current in the OTA is steered towards the output (try to understand why this is the case), so when the output capacitor is fully discharged, and we assume just a linear ramp due to constant-current charging of the output capacitor, the settling time is

$$T_{\text{slew}} \approx \frac{C_{\text{load}} \cdot V_{\text{out,max}}}{I_{\text{tail}}} = \frac{50 \cdot 10^{-15} \cdot 0.9}{10 \cdot 10^{-6}} = 4.5 \text{ ns}$$

so this leaves plenty of margin for additional slow-signal settling due to the limited bandwidth, as well as reducing the supply current.

The small-signal settling (assuming one pole at the bandwidth corner frequency) leads to an approximate settling time (1% error corresponds to  $\approx 5\tau$ ) of

$$T_{\text{settle}} \approx \frac{5}{2\pi f_c} = \frac{5}{2\pi \cdot 10 \times 10^6} = 0.08 \mu\text{s}.$$

which also checks out.

### 8.3 Small-Signal Analysis of the OTA

In order to size the OTA components we need to derive how the MOSFET parameters define the performance. The important small-signal metrics are

- dc voltage gain  $A_0$
- gain-bandwidth product (GBW)
- output noise

The specification for GBW is directly given in Table 2, while the dc gain we have to calculate from the voltage accuracy specification. For a voltage follower in the configuration shown in Figure 33 the voltage gain is given by (see Figure 33)

$$(V_{\text{in}} - V_{\text{out}}) \cdot A_0 = V_{\text{out}} \rightarrow \frac{V_{\text{out}}}{V_{\text{in}}} = \frac{A_0}{1 + A_0}. \quad (14)$$

So in order to reach an output voltage accuracy of at least 3% we need a dc gain of  $A_0 > 30.2 \text{ dB}$ . To allow for process and temperature variation we need to add a bit of extra gain as margin.

#### ! Small-Signal vs. Large-Signal Operation

In order to get the correct dc voltage per the specification we require the large-signal gain calculated with Equation 14. However, calculating the large-signal gain of a circuit is quite involved (usually mandating the use of a large-signal nonlinear model for the used components), so we typically resort to do a simpler small-signal calculation instead, like in Section 8.3. We deliberately introduce this error, but we should not get confused about the difference between large- and small-signal operation!

#### 8.3.1 OTA Small-Signal Transfer Function

In order to derive the governing small-signal equations for the OTA we will make a few simplifications:

- We assume that  $g_{m1,2} = g_{m1} = g_{m2}$ ,  $g_{m3,4} = g_{m3} = g_{m4}$ , and  $C_{gs3,4} = C_{gs3} = C_{gs4}$  for symmetry reasons (as  $M_1$  and  $M_2$  will have to be equally sized, as well as  $M_3$  and  $M_4$ ).
- We will set  $g_{mb} = 0$  for all MOSFETs.

- We will further set  $C_{gd} = 0$  for all MOSFETs except for  $M_4$  where we expect a Miller effect on this capacitor, and we could add its effect by increasing the capacitance at the gate node of  $M_{3,4}$  (for background please see Section 17.1). However, as this does not create a dominant pole in this circuit, we consider this a minor effect (see Equation 17). Thus, only  $2C_{gs3,4}$  is considered at the gate node of the current mirror load.
- We assume  $g_m \gg g_{ds}$ , so we set  $g_{ds1} = g_{ds3} = 0$  as this node is dominated by  $g_{m3}^{-1}$ .
- The drain capacitance of  $M_2$  and  $M_4$ , as well as the gate capacitance of  $M_2$ , we could add to the load capacitance  $C_{load}$  (see Figure 34).

The resulting small-signal equivalent circuit is shown in Figure 35.

**⚠ Refresh MOSFET Small-Signal Model**

Please review the MOSFET small-signal equivalent model in Figure 6 at this point. For the PMOS just flip the model upside-down.

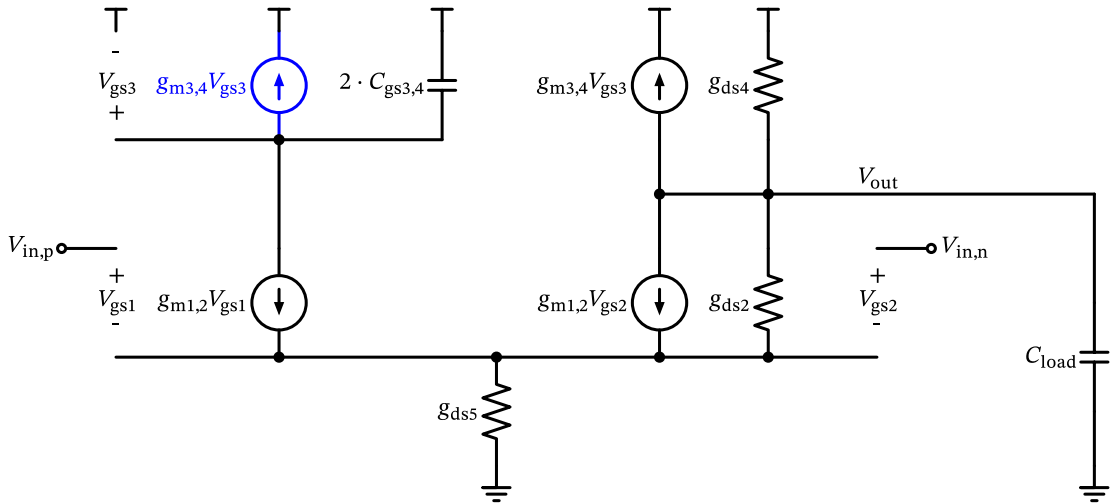


Figure 35: 5-transistor OTA open-loop small-signal model. For the closed-loop model, the input voltage  $V_{in,n}$  is connected to the output voltage  $V_{out}$ . Note that the blue current source can be replaced by a conductance of  $g_{m3,4}$ .

We can further simplify Figure 35 by realizing that we operate the circuit purely differential and thus the tail point of  $M_1$  and  $M_2$  can be treated like a virtual ground, we thus short  $g_{ds5}$ . Therefore, we can move  $g_{ds2} + g_{ds4}$  in parallel to  $C_{load}$ . The current source  $g_{m3,4}V_{gs3}$  is replaced with the equivalent conductance  $g_{m3,4}$ . All the previous steps result in the further simplified equivalent circuit shown in Figure 36.

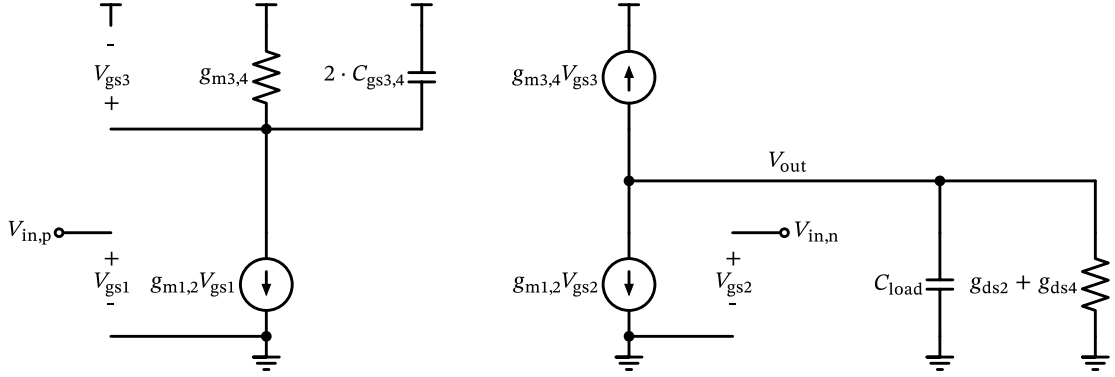


Figure 36: 5-transistor OTA small-signal model with further simplifications.

In the simplified circuit model in Figure 36 we can see that we have two poles in the circuit, one at the gate note of  $M_{3,4}$ , and one at the output. Realizing that  $V_{gs1} = V_{in,p} = V_{in}/2$  and  $V_{gs2} = V_{in,n} = -V_{in}/2$  we can formulate KCL at the output node to

$$-g_{m3,4}V_{gs3} - g_{m1,2}\left(-\frac{V_{in}}{2}\right) - V_{out}(g_{ds2} + g_{ds4} + sC_{load}) = 0. \quad (15)$$

We further realize that

$$V_{gs3} = -g_{m1,2} \frac{V_{in}}{2} \frac{1}{g_{m3,4} + 2 \cdot sC_{gs3,4}}. \quad (16)$$

By combining Equation 15 and Equation 16 and after a bit of algebraic manipulation we arrive at

$$A(s) = \frac{V_{out}(s)}{V_{in}(s)} = \frac{g_{m1,2}}{2} \frac{2 \cdot g_{m34} + 2 \cdot sC_{gs3,4}}{(g_{m3,4} + 2 \cdot sC_{gs3,4})(g_{ds2} + g_{ds4} + sC_{load})}. \quad (17)$$

When we inspect Equation 17 we can see that for low frequencies the (open-loop) gain is

$$A(s \rightarrow 0) = A_0 = \frac{g_{m1,2}}{g_{ds2} + g_{ds4}} \quad (18)$$

which is plausible, and confirms the requirement of a high impedance at the output node. For very large frequencies we get

$$A(s \gg) = \frac{g_{m1,2}}{2 \cdot sC_{load}} \quad (19)$$

which is essentially the behavior of an integrator, and we can use Equation 19 to calculate the frequency where the gain drops to  $|A(s_{ug})| = 1 = g_{m1,2}/|2j\omega_{ug}C_{load}|$ :

$$f_{ug} = \frac{g_{m1,2}}{4\pi C_{load}}$$

Looking at Equation 17, we see that we have a dominant pole at  $s_p$  and a pole-zero doublet with  $s_{pd}/s_{zd}$ :

$$s_p = -\frac{g_{ds2} + g_{ds4}}{C_{load}} \quad (20)$$

$$s_{pd} = -\frac{g_{m3,4}}{2 \cdot C_{gs3,4}} \quad (21)$$

$$s_{zd} = -\frac{g_{m3,4}}{C_{gs3,4}} \quad (22)$$

### i Why a Pole-Zero Doublet?

Looking at Equation 21 and Equation 22 we see that this pair is intimately linked by the same parameters and can only move together. Hence we call it a “doublet”. The effects of pole-zero doublets on the frequency response and settling time of OTAs can be found in [23]. This paper shows that doublets may cause severe degradation of settling time while only causing minor changes in the frequency response of the amplifier.

#### 8.3.2 OTA Noise

For the noise analysis we ignore the pole-zero doublet due to  $C_{gs3,4}$  (we assume minor impact due to this, hence we set  $C_{gs3,4} = 0$ ) and just consider the dominant pole given by Equation 20 due to the load capacitance. For the noise analysis at the output we set the positive input signal to ground and connect the output to the negative input, and thus starting from Figure 36 we arrive at the adapted small-signal circuit shown in Figure 37.

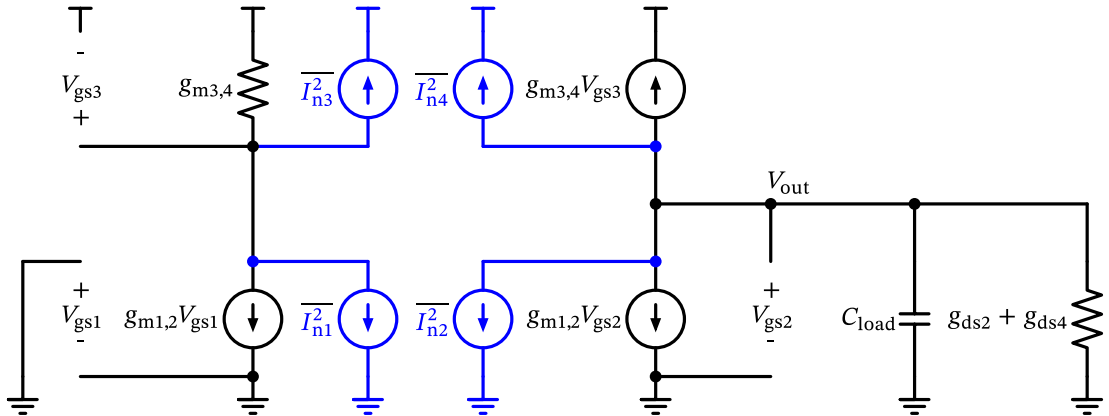


Figure 37: 5-transistor OTA small-signal model for noise calculation (added noise sources shown in blue).

For symmetry reasons we can set  $\overline{I_{n1,2}^2} = \overline{I_{n1}^2} = \overline{I_{n2}^2}$  and  $\overline{I_{n3,4}^2} = \overline{I_{n3}^2} = \overline{I_{n4}^2}$ . We see that we can replace the current source  $g_{m1,2}V_{gs2}$  with its equivalent conductance of  $g_{m1,2}$ , and this conductance is in parallel to  $g_{ds2} + g_{ds4}$ , hence  $g_{m1,2} + g_{ds2} + g_{ds4} \approx g_{m1,2}$ . The resulting simplified small-signal noise equivalent circuit is shown in Figure 38.

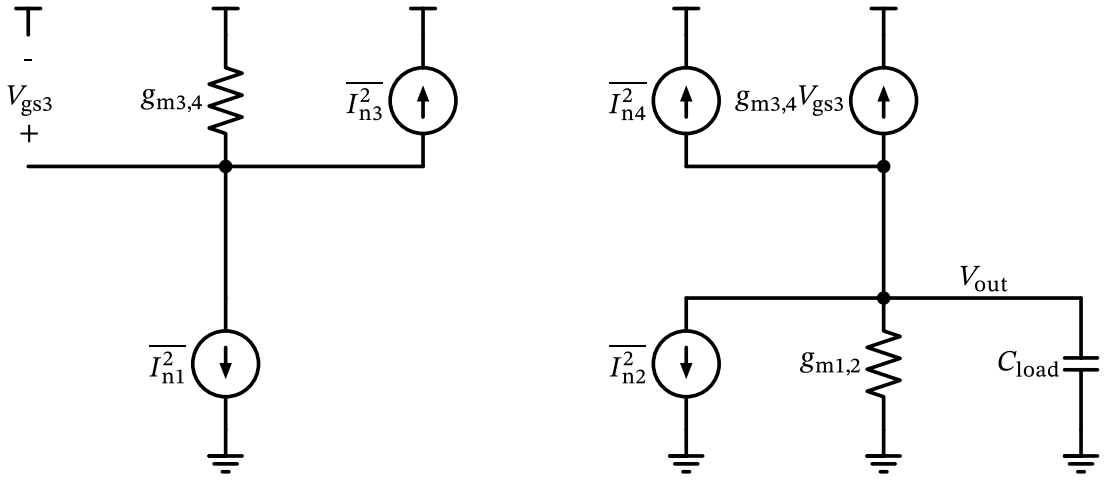


Figure 38: 5-transistor OTA simplified small-signal model for noise calculation.

We see that

$$\overline{V_{gs3}^2} = \frac{1}{g_{m3,4}^2} (\overline{I_{n1}^2} + \overline{I_{n3}^2}).$$

### ! Noise Addition

Remember that **uncorrelated** noise quantities need to be power-summed (i.e.,  $I^2 = I_1^2 + I_2^2$ )!

We can then sum the total output noise current  $\overline{I_n}$  as

$$\overline{I_n^2} = \overline{I_{n2}^2} + \overline{I_{n4}^2} + g_{m3,4}^2 \frac{1}{g_{m3,4}^2} (\overline{I_{n1}^2} + \overline{I_{n3}^2}) = 2(\overline{I_{n1,2}^2} + \overline{I_{n3,4}^2}).$$

The output noise voltage is then (using Equation 1)

$$\begin{aligned} \overline{V_{n,out}^2}(f) &= \frac{\overline{I_n^2}}{|g_{m1,2} + sC_{load}|^2} = \frac{\overline{I_n^2}}{g_{m1,2}^2 + (2\pi f C_{load})^2} \\ &= \frac{8kT(\gamma_{1,2}g_{m1,2} + \gamma_{3,4}g_{m3,4})}{g_{m1,2}^2 + (2\pi f C_{load})^2}. \end{aligned}$$

We can use the identity Equation 9 to calculate the rms output noise to

$$V_{n,out,rms}^2 = \int_0^\infty \overline{V_{n,out}^2}(f) \cdot df = \frac{kT}{C_{load}} \left( 2\gamma_{1,2} + 2\gamma_{3,4} \frac{g_{m3,4}}{g_{m1,2}} \right). \quad (23)$$

Inspecting Equation 23 we can see that the integrated output noise is the  $kT/C$  noise of the output load capacitor, enhanced by the  $\gamma_{12}$  of the input differential pair, plus a (smaller) contribution of the current mirror load  $M_{3,4}$ . Intuitively, this result makes sense. We learn that to reduce the output noise we should set  $g_{m3,4} < g_{m1,2}$ .

### 💡 Exercise: Derivation of 5T-OTA Performance

Please take your time and carefully go through the explanations and derivations for the 5-transistor-OTA in Section 8.2 and Section 8.3. Try to do the calculations yourself; if you get stuck, review the previous chapters. There are additional useful derivations in Section 18.

## 8.4 5T-OTA Sizing

Armed with the governing equations derived in Section 8.3 we can now size the MOSFETs in the OTA, we remember that we have to size  $M_{1,2}$  and  $M_{3,4}$  equally.

First, we need to select a proper  $g_m/I_D$  for the MOSFET. Remembering Section 3 we see that for the input differential pair we should go for a large  $g_m$ , thus we select a  $g_m/I_D = 10$ . As  $g_{ds}$  of  $M_2$  could limit the dc gain (Equation 18) we go with a rather long  $L = 5 \mu\text{m}$ . For current sources a small  $g_m/I_D$  is a good idea, so we start with  $g_m/I_D = 5$  (because we can not go too low because of  $V_{ds,\text{sat}}$ ) and also an  $L = 5 \mu\text{m}$ . The  $g_m/I_D$  is also useful to estimate the required drain-source voltage to keep a MOSFET in saturation (i.e., keep the  $g_{ds}$  small) with this approximate relationship:

$$V_{ds,\text{sat}} = \frac{2}{g_m/I_D} \quad (24)$$

### 💡 Exercise: 5T-OTA Sizing

Please size the 5T-OTA according to the previous  $g_m/I_D$  and  $L$  suggestions. Please calculate the  $W$  of  $M_{1-6}$  and the total supply current. Please check whether gain error, total output noise, and turn-on settling is met with the calculated devices sizes and bias currents.

The sizing procedure and its calculation are best performed in a Jupyter notebook, as we can easily look up the exact data from the pre-computed tables:

## Solution: 5T-OTA Sizing

## Sizing for Basic 5T-OTA

Copyright 2024-2025 Harald Pretl

Licensed under the Apache License, Version 2.0 (the “License”); you may not use this file except in compliance with the License. You may obtain a copy of the License at <http://www.apache.org/licenses/LICENSE-2.0>

```

# read table data
from pygmid import Lookup as lk
import numpy as np
lv_nmos = lk('sg13_lv_nmos.mat')
lv_pmos = lk('sg13_lv_pmos.mat')
# list of parameters: VGS, VDS, VSB, L, W, NFING, ID, VT, GM, GMB, GDS,
CGG, CGB, CGD, CGS, CDD, CSS, STH, SFL
# if not specified, minimum L, VDS=max(vgs)/2=0.9 and VSB=0 are used

```

```

# define the given parameters as taken from the specification table or
initial guesses
c_load = 50e-15
gm_id_m12 = 10
gm_id_m34 = 5
gm_id_m56 = 5
l_12 = 5
l_34 = 5
l_56 = 5
f_bw = 10e6 # -3dB bandwidth of the voltage buffer
i_total_limit = 10e-6
i_bias_in = 20e-6
output_voltage = 1.3
vin_min = 0.7
vin_max = 0.9
vdd_min = 1.45
vdd_max = 1.55

```

```

# we get the required gm of M1/2 from the -3dB bandwidth requirement of
the voltage buffer specification
# note that the -3dB bandwidth of the voltage buffer with gain Av=1 is
equal to the unity gain bandwidth
# of the ota, hence we set them equal here
# we add a factor of 3 to allow for PVT variation plus additional
MOSFET parasitic loading
gm_m12 = f_bw * 3 * 4*np.pi*c_load
print('gm12 = ', round(gm_m12/1e-3, 4), 'mS')

```

$$gm12 = 0.0188 \text{ mS}$$

## 8.5 5T-OTA Simulation

With the initial sizing of the MOSFETs of the 5T-OTA done, we can design the 5T-OTA circuit and setup a simulation testbench to check the performance parameters. Since this is the first time we draw a more complex schematic, and use a hierarchical design, we should note that drawing a schematic is an art, and there exists a set of rules and recommendations how to name pins, how to use annotations, and so on. Please read Section 22 before you start into your design work.

### 💡 Exercise: 5T-OTA Design and Testbench

Please design the circuit of the 5T-OTA. Put the OTA circuit in a separate schematic, create a symbol for it, and use this symbol in a testbench you create in Xschem for this 5T-OTA used as a voltage buffer as shown in Figure 33. Use typical conditions for the simulation, and check how well the specification in Table 2 is met, and how well the derivations in Section 8.2 and Section 8.3 fit to the simulation results.

If you get stuck, you can find the testbench and 5T-OTA schematic here (for the small-signal analysis) and here (for the large-signal settling simulation). For interested students, the loop gain analysis with Middlebrook's and Tian's method of the 5T-OTA can be found here.

## 8.6 Component Mismatch

### 8.6.1 MOSFET Mismatch

So far, we have assumed that implemented MOSFETs show no difference from device to device, which means that two transistors behave completely identical, and the resulting differential circuits are fully symmetric. However, due to manufacturing tolerances, this is not the case in reality. MOSFETs will show **mismatch** due to tiny random fluctuations in manufacturing, and we have to account for this. The mismatch parameters for various components are summarized in Table 3.

For a typical MOSFET, we usually consider two main mismatch effects [24]:

- A variation of the threshold voltage (mainly due to variations in doping levels).
- A variation of the critical dimensions of the MOSFET ( $W$  and  $L$  as well as vertical dimensions).

Both effects influence the drain current of the MOSFET, and they are indirectly proportional to the size of the MOSFET. So, if we want to reduce the mismatch, we have to increase the size of the MOSFET by increasing its gate area  $W \cdot L$ .

If we formulate the drain current mismatch standard deviation  $\sigma\{\Delta I_D/I_D\}$  of two nominally identical MOSFET we get

$$\sigma\left\{\frac{\Delta I_D}{I_D}\right\} = \frac{A_{\text{mosfet}}}{\sqrt{WL}} \quad (25)$$

with  $A_{\text{mosfet}}$  being a mismatch parameter for a given CMOS technology and  $\sigma\{\cdot\}$  being the standard deviation of the parameter in parentheses.

## i MOSFET Mismatch

Usually, the mismatch in MOSFETs is characterized via two mismatch parameters [24]:

- The threshold voltage mismatch standard deviation

$$\sigma\{\Delta V_{\text{th}}\} = \frac{A_{\text{vth}}}{\sqrt{WL}} \quad (26)$$

- and standard deviation of the size mismatch

$$\sigma\left\{\frac{\Delta(W/L)}{(W/L)}\right\} = \frac{A_k}{\sqrt{WL}}. \quad (27)$$

The resulting standard deviation of the input offset voltage  $V_{\text{offs}}$  of a differential pair with small  $g_m/I_D$  is then given by [2]

$$V_{\text{offs}} = \sqrt{\left(\frac{V_{\text{GS}} - V_{\text{th}}}{2}\right)^2 \cdot \sigma^2\left\{\frac{\Delta(W/L)}{(W/L)}\right\} + \sigma^2\{\Delta V_{\text{th}}\}}. \quad (28)$$

The mismatch in the drain current of two current-mirror transistors, characterized as the standard deviation and for small  $g_m/I_D$ , is given by [2]

$$\sigma^2\left\{\frac{\Delta I_D}{I_D}\right\} = \sigma^2\left\{\frac{\Delta(W/L)}{(W/L)}\right\} + 4 \cdot \sigma^2\left\{\frac{\Delta V_{\text{th}}}{V_{\text{GS}} - V_{\text{th}}}\right\}. \quad (29)$$

To minimize the input offset voltage in a differential pair we should strive to minimize  $V_{\text{GS}}$  (i.e., to maximize  $g_m/I_D$ , see Equation 28) and to minimize the mismatch in current mirrors we should target a large  $V_{\text{GS}}$  (i.e., to minimize  $g_m/I_D$ , see Equation 29). In both cases the MOSFET area  $W \cdot L$  needs to be large enough (see Equation 26 and Equation 27).

How can we now cope with mismatch in design and simulation? We can account the transistor mismatch according to Equation 26 and Equation 27 in circuit analysis and quantify its effect. We can then take this into account when performing the circuit sizing procedure.

We can also simulate the effects of MOSFET mismatch on circuit performance by doing a **Monte Carlo** simulation. Here, a random realization of the variations of all circuit components (where mismatch is modelled) is taken and the circuit is simulated. Then, another random realization is simulated, and so on. In summary, we run the same simulation for different realizations  $N$  times and evaluate the resulting variations of the circuit parameters. If  $N$  is large enough then the distributions should approach a Gaussian distribution, and we can then estimate the variances of the circuit parameters. Using statistical analysis we can then assess the **yield** of a circuit, i.e., how many circuit realizations will meet the specification.

### **i** Number of Monte Carlo Simulation Runs

The number of Monte Carlo simulation runs  $N$  has to be large enough to approach Gaussian distributions to allow estimation of the variances. However, this comes at the cost of a large simulation time, so a balance has to be found. Often,  $N = 250$  is a good compromise between simulation time and well-behaved parameter distributions.

As you can see in the previous discussion, running Monte Carlo simulations is a tedious process due to the large number of involved simulations and the required data processing of the heaps of simulation data. Luckily, CACE supports this type of simulation, and we will use it in Section 8.7.

#### **8.6.2 Resistor Mismatch**

Similar to the MOSFET mismatch discussed in Section 8.6.1, resistors will also show mismatch. Equivalently to Equation 25 the standard deviation of the resistor mismatch  $\sigma\{\Delta R/R\}$  can be characterized by

$$\sigma\left\{\frac{\Delta R}{R}\right\} = \frac{A_{\text{res}}}{\sqrt{WL}} \quad (30)$$

with  $A_{\text{res}}$  being a mismatch parameter for a given CMOS technology.

With Equation 30 we now have two criteria for how to select the width  $W$  of a specific resistor (the length  $L$  is then derived from the required resistance value with  $R = R_s \cdot L/W$ ):

1. The current handling capability (the larger the  $W$ , the more dc current a resistor can carry), and
2. the resistor mismatch (the larger the  $W$ , the larger the  $WL$  for a given  $L/W$ ).

If a resistor's dimensions are not limited by the two criteria above then we usually choose the minimum width that is allowed for a given resistor in a specific technology (for SG13G2 it is  $L_{\min} = 0.5 \mu\text{m}$ ) to save area and to minimize the parasitic capacitance of the resistor to substrate.

#### **8.6.3 Capacitor Mismatch**

Similar to the resistor matching discussed in Section 8.6.2, capacitors will also show mismatch. Equivalently to Equation 25 the standard deviation of the capacitor mismatch  $\sigma\{\Delta C/C\}$  can be characterized by

$$\sigma\left\{\frac{\Delta C}{C}\right\} = \frac{A_{\text{cap}}}{\sqrt{WL}} \quad (31)$$

### **8.7 5T-OTA Simulation versus PVT and MC**

As you have seen in Section 8.5 running simulations by hand is tedious. When we want to check the overall performance, we have to run many simulations over various conditions:

1. The supply voltage of the circuit has tolerances, and thus we need to check the performance against this variation.
2. The temperature at which the circuit is operated is likely changing. Also the performance against this has to be verified.

- When manufacturing the wafers random variations in various process parameters lead to changed parameters of the integrated circuit components. In order to check for this effect, wafer foundries provide model files which shall cover these manufacturing excursions. Simplified, this leads to a slower or faster MOSFET, and usually NMOS and PMOS are not correlated, so we have the process corners **SS**, **SF**, **TT**, **FS**, and **FF**. So far, we have only used the **TT** models in our simulations.

The variations listed in the previous list are abbreviated as **PVT** (process, voltage, temperature) variations. In order to finalize a circuit all combinations of these (plus the variations in operating conditions like input voltage) have to be simulated. As you can imagine, this leads to a huge number of simulations, and simulation results which have to be evaluated for pass/fail.

There are two options how to tackle this efficiently:

- As an experienced designer you have a very solid understanding of the circuit, plus based on the analytic equations you can identify which combination of operating conditions will lead to a worst case performance. Thus, you can drastically reduce the number of corners to simulate, and you run them by hand.
- You are using a framework which highly automates this task of running a plethora of different simulations and evaluating the outcome. These frameworks are called simulation runners.

Luckily, there are open-source versions of simulation runners available, and we will use CACE in this lecture. CACE is written in Python and allows to setup a datasheet in YAML which defines the simulation problem and the performance parameters to evaluate against which limits. The resulting simulations are then run in parallel and the simulation data is evaluated and summarized in various forms.

There is a CACE setup available for our 5T-OTA. The datasheet describes the operating conditions and the simulations tasks. For each simulation a testbench template is needed, this one is used for ac simulations, this one is used for noise simulation, and this one is used for transient simulation.

### Running CACE Simulation

The CACE simulation run can be started with

```
cace cace/voltage-buffer-ota.yaml
```

The simulation results are then placed into the `cace/_docs` folder. If in addition to the default Markdown report an HTML output is needed for easier review then using Pandoc it can be easily converted and viewed with

```
cace/cace_view.sh cace/_docs/ota-5t_schematic.md
```

After a successful run, a documentation is automatically generated. The result of a full run of this OTA design is presented here:

**i** Note 2: CACE Summary for 5T-OTA

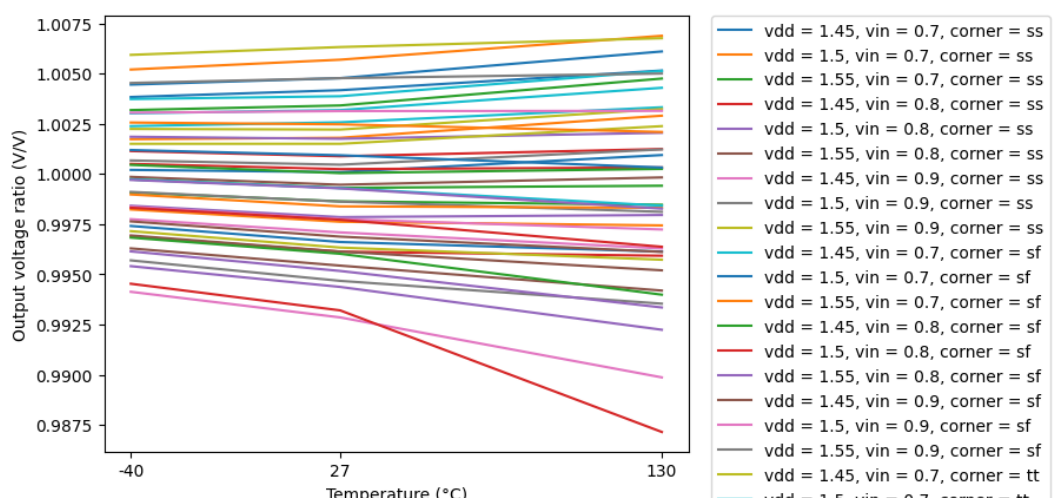
## CACE Summary for ota-5t

netlist source: schematic

Parameter	Tool	Result	Min Lim	Min Value	Type	Ta	Fyp	Value	Max	Max Value	Status
				get					Limit		
Output voltage ratio	ngspice	gain	0.97 V/V	0.987 V/V	any	1.000 V/V	1.03 V/V	1.007 V/V	Pass	✓	
Bandwidth	ngspice	bw	15550400.000 Hz	26912100.000 Hz	26912100.000 Hz	34452200.000 Hz	34452200.000 Hz	34452200.000 Hz	Pass	✓	
Output voltage ratio (MC)	ngspice	gain_mc	any V/V	0.998 V/V	any	0.999 V/V	any	1.001 V/V	Pass	✓	
Bandwidth (MC)	ngspice	bw_mc	24612600.000 Hz	26806900.000 Hz	26806900.000 Hz	28104300.000 Hz	28104300.000 Hz	28104300.000 Hz	Pass	✓	
Output noise	ngspice	noise	any mV	0.308 mV	any	0.371 mV	1 mV	0.454 mV	Pass	✓	
Settling time	ngspice	tsettle	any us	0.137 us	any	0.144 us	10 us	0.156 us	Pass	✓	

## Plots

### gain\_vs\_temp



### 8.7.1 PVT Simulation Analysis

Looking at the CACE report in Note 2 we see that (luckily) the specification is met for all parameters. This is great news! We now have a design that we carefully simulated across PVT and other corners, and which is ready for layout. Once we have the layout ready, we can extract the wiring parasitic ( $R$  and  $C$ ) as well as other layout-dependent effects like well proximity. Using this augmented netlist we can then again use CACE to check performance across conditions and parameter variations, and if we still pass all specification points then our design is finished.

### 8.7.2 Monte Carlo Simulation Analysis

Looking at the CACE report in Note 2 we see that the output voltage specification is not met due to MOSFET mismatch! We have not considered transistor mismatch in the circuit sizing procedure, and as a result the selected MOSFET dimensions prove to be too small. We should now go back and change the transistor sizing (increasing  $L$  significantly while keeping the  $g_m/I_D$  values). Likely we will find that some performance parameters are now deteriorating due to the increased MOSFET dimensions, and we need to iterate until all performance metrics are met in the presence of transistor mismatch.

It is not unusual that the power consumption now increases, as we have to increase the size of the MOSFETs for matching, and these larger MOSFETs increase the parasitic capacitances which in turn lead to larger power consumption to keep the required bandwidth by increasing the  $g_m$ .

#### 💡 Exercise: Re-Sizing of 5T-OTA for Mismatch

Go back to Section 8.4 and repeat the sizing procedure of the 5T-OTA by increasing the  $L$  of the MOSFETs significantly. Focus first on the differential pair as it will likely have the biggest impact (see Equation 28). Then, tune the size of the output current mirror if necessary (see Equation 29).

Once you are happy with the sizing result repeat the PVT simulations in CACE to confirm the performance of the voltage buffer including mismatch.

## 8.8 OTA Variants

Following, we are going to discuss two popular variants of the simple 5T-OTA. The first version provides an almost rail-to-rail single-ended output, and can thus be used for a variety of applications requiring this range. The arrangement is shown in Figure 57. It is a single-stage amplifier, as the only high-impedance point is at the output where significant voltage-gain is produced. The current mirrors can be used to scale up the current generated in the input differential pair to some extent in the output stage (or can be used to lower the current compared to the bias current in the diffpair); i.e., the bias currents of the input stage and the output stage can be set independently.

Being a single-stage amplifier stability is usually not an issue, as only the output node is high-ohmic; all other nodes feature a MOSFET diode so the node impedance is  $\approx g_m^{-1}$  and thus the according poles are located at high frequencies.

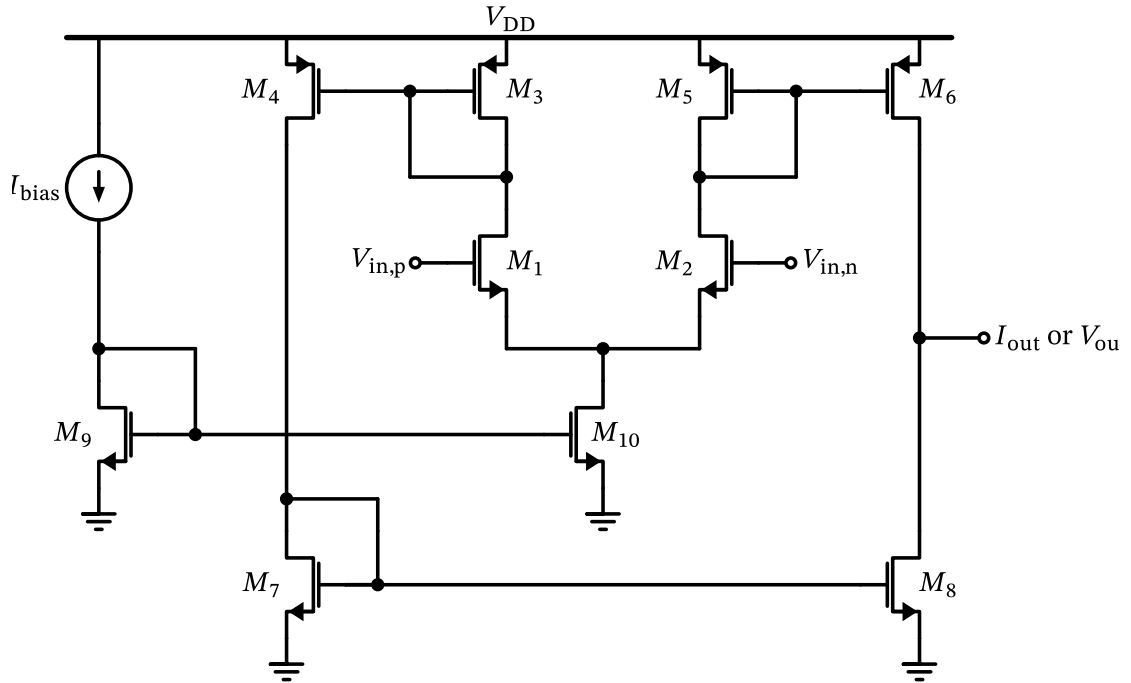


Figure 57: Single-ended OTA with rail-to-rail output stage.

Another popular version is shown in Figure 58. Here, we have a two-stage amplifier able to provide higher voltage gain. The first stage (the diffpair loaded by a current mirror) is followed by a single-stage common-source amplifier with current-source load. Being a two-stage amplifier with two high-ohmic nodes, stability is a concern, so usually we need some form of compensation. Figure 58 shows a very simplistic Miller-compensation using  $C_M$ . Often, we would want to implement a more advanced scheme. Some examples can be found in [25]. An interesting technique is the indirect compensation with cascaded input differential pairs (see Figure 75) for higher power supply rejection. An advantage of this two-stage amplifier (compared with the simple 5T-OTA) is the dc-balanced load on top of the differential pair, as each side sees a voltage drop from  $V_{DD}$  of one  $V_{GS}$  ( $V_{GS3}$  on the left side,  $V_{GS5}$  on the right side).

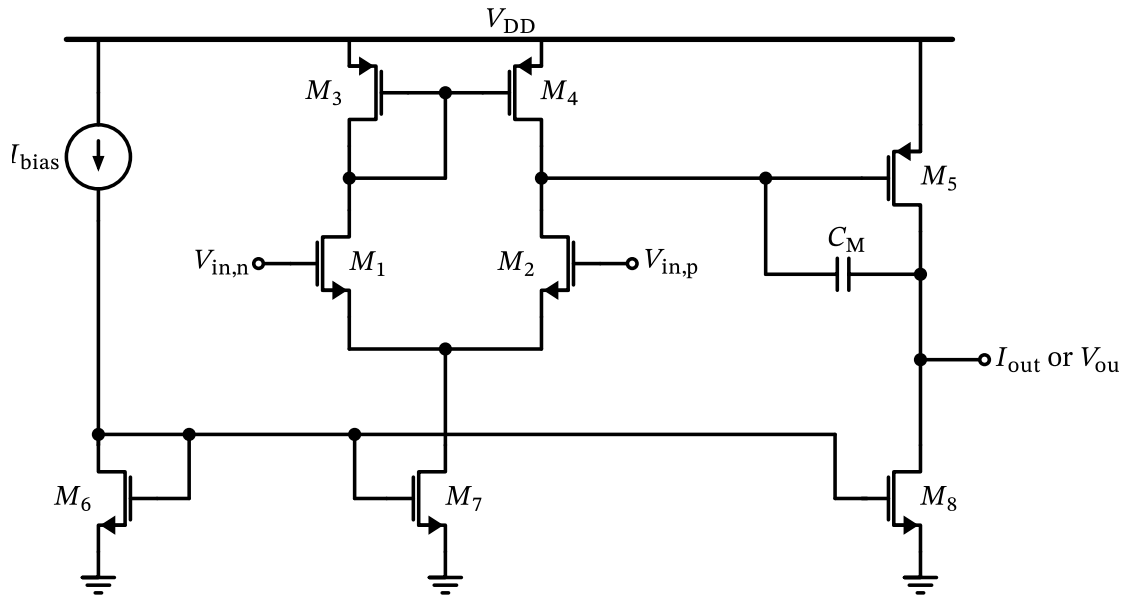


Figure 58: Single-ended two-stage OTA with rail-to-rail output.

Note that the circuit of Figure 58 can be easily modified into a low-dropout voltage regulator (LDO). This simple yet often effective circuit is shown in Figure 59. The pass transistor  $M_{pass}$  has to be sized according to the load current and the dropout voltage.

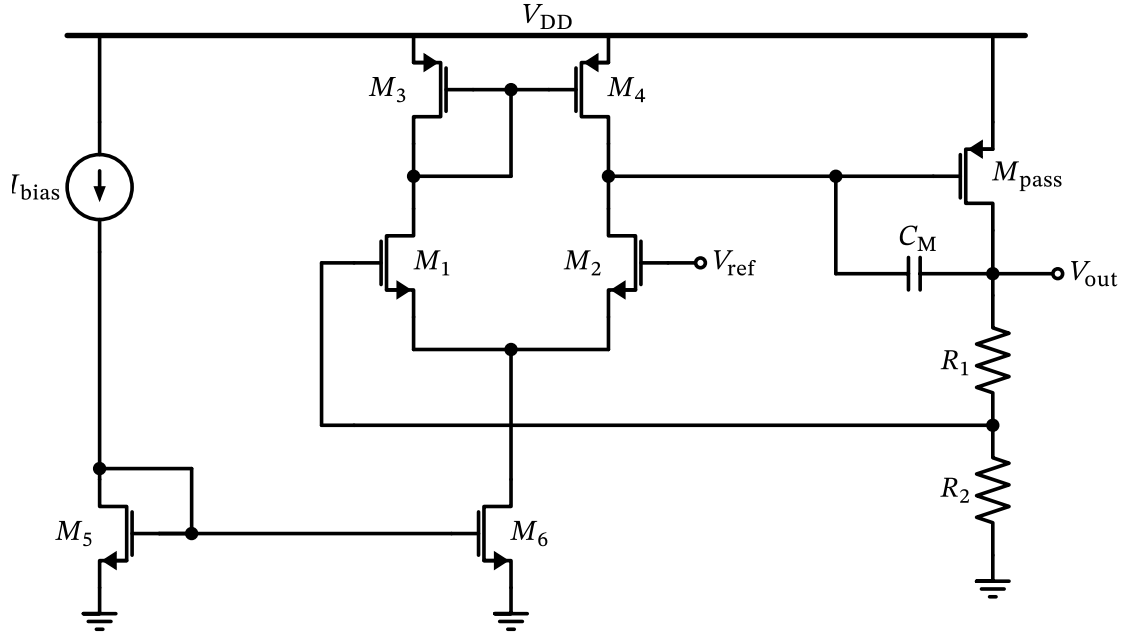


Figure 59: A basic low-dropout voltage regulator (LDO) with Miller compensation.

The reference voltage  $V_{ref}$  is scaled by  $R_1$  and  $R_2$ , so that the output voltage  $V_{out}$  is given by

$$V_{out} \approx V_{ref} \left( 1 + \frac{R_1}{R_2} \right)$$

if the gain of the OTA is sufficiently high. The quiescent current through  $R_{1,2}$  establishes a minimum load current for the LDO, which is often good for stability. More information on LDOs can be found in [26].

## 9 Cascode Stage

As we have seen in Section 8 the performance of the OTA is generally quite acceptable (see Table 2), but we might want to aim for better output voltage accuracy. As our analysis has shown the output voltage tolerance is limited by the open-loop dc gain  $A_0$  of the OTA (see Equation 14), which in turn is limited by the output conductance of  $M_2$  and  $M_4$  in Figure 32, which is also confirmed by the analytical result in Equation 18.

During the sizing procedure we have seen that the achievable  $g_m/g_{ds}$  ratio of a single MOSFET is limited, even if we increase  $L$ . We are thus searching for a better option, and here (local) feedback in form of a **cascode** comes to help.

For analysis of a cascode, we use the following single-transistor stage shown in Figure 60.

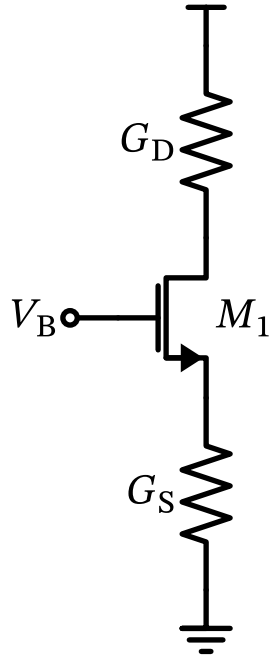


Figure 60: A MOSFET cascode circuit.

In order to derive the operation of the cascode analytically, we draw the small-signal equivalent circuit in Figure 61. We assume that  $V_B$  is a low-ohmic bias voltage, thus we replace it by ac ground. We further set  $g_{mb} = 0$ .

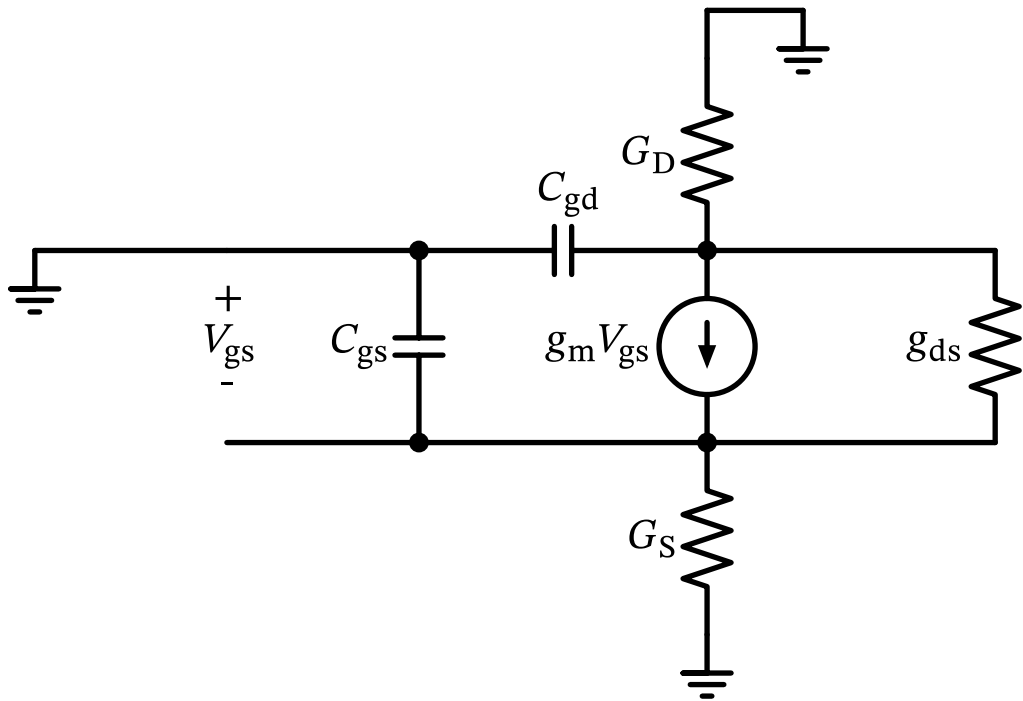


Figure 61: The MOSFET cascode small-signal model.

Since the gate is assumed at a fixed potential, we can put  $C_{gs}$  in parallel to  $G_S$  as  $G_S^* = G_S + sC_{gs}$ , and we can put  $C_{gd}$  in parallel to  $G_D$  as  $G_D^* = G_D + sC_{gd}$ . As a result we will disregard these capacitors for now, and just consider  $G_S$  and  $G_D$ .

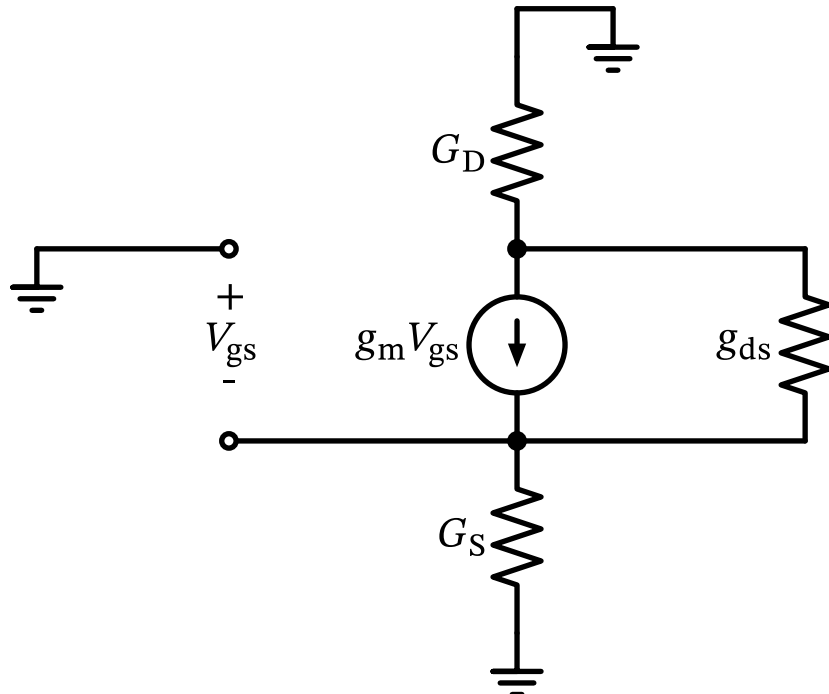


Figure 62: The simplified MOSFET cascode small-signal model.

## 9.1 Cascode Output Impedance

As a first step, we want to calculate the output impedance at the drain of the MOSFET (i.e., looking into the drain). For this, we replace  $G_D$  with a current source. The resulting small-signal equivalent circuit is shown in Figure 63.

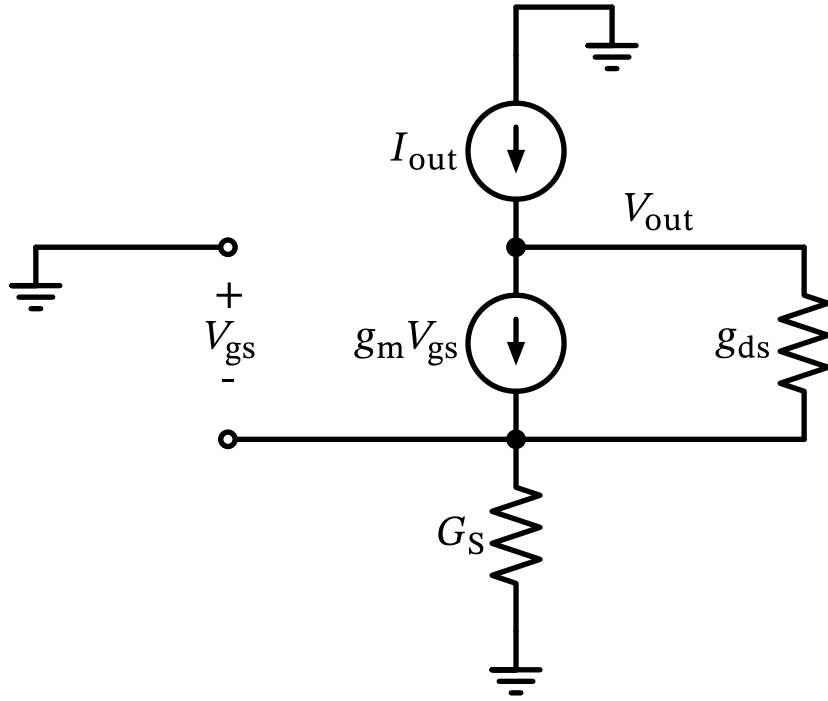


Figure 63: The simplified MOSFET cascode small-signal model for calculation of the output impedance.

We realize that  $I_{\text{out}}$  flows through  $G_S$  and drops  $V_{\text{gs}}$  (note the sign):

$$V_{\text{gs}} = -\frac{I_{\text{out}}}{G_S}$$

Further,  $V_{\text{out}} = -V_{\text{gs}} + V_{\text{ds}}$ . Calculating KCL at the output node results in

$$I_{\text{out}} - g_m V_{\text{gs}} - g_{\text{ds}} V_{\text{ds}} = 0.$$

Using the previously found identities, and after a bit of algebraic manipulations we arrive at

$$g_{\text{out}} = \frac{I_{\text{out}}}{V_{\text{out}}} = \frac{g_{\text{ds}}}{1 + \frac{g_m + g_{\text{ds}}}{G_S}} = \frac{g_{\text{ds}} \cdot G_S}{G_S + g_m + g_{\text{ds}}} \quad (32)$$

We find that if  $G_S = 0$  (an open) then  $g_{\text{out}} = 0$ , and if  $G_S = \infty$  (a short) then  $g_{\text{out}} = g_{\text{ds}}$ . We can calculate the benefits of a cascode if we assume we put a cascode on top of a common-source transistor stage (thus  $G_S = g_{(\text{ds})'}$ ) and get

$$g_{\text{out}} = \frac{g_{\text{ds}} \cdot g_{(\text{ds})'}}{g_{(\text{ds})'} + g_m + g_{\text{ds}}} \approx g_{(\text{ds})'} \frac{g_{\text{ds}}}{g_m}. \quad (33)$$

### ! Benefit of Cascode (Output)

The output impedance of the lower MOSFET ( $r_{ds} = 1/g_{(ds)'}^*$ ) is **increased** by the self-gain of the cascode transistor! This is a powerful technique to increase the output impedance of a transistor stage by cascoding, much better than increasing  $L$ .

## 9.2 Cascode Input Impedance

To calculate the input impedance of a cascode (i.e., looking into the source) we replace  $G_S$  with a current source. The resulting small-signal equivalent circuit is shown in Figure 64.

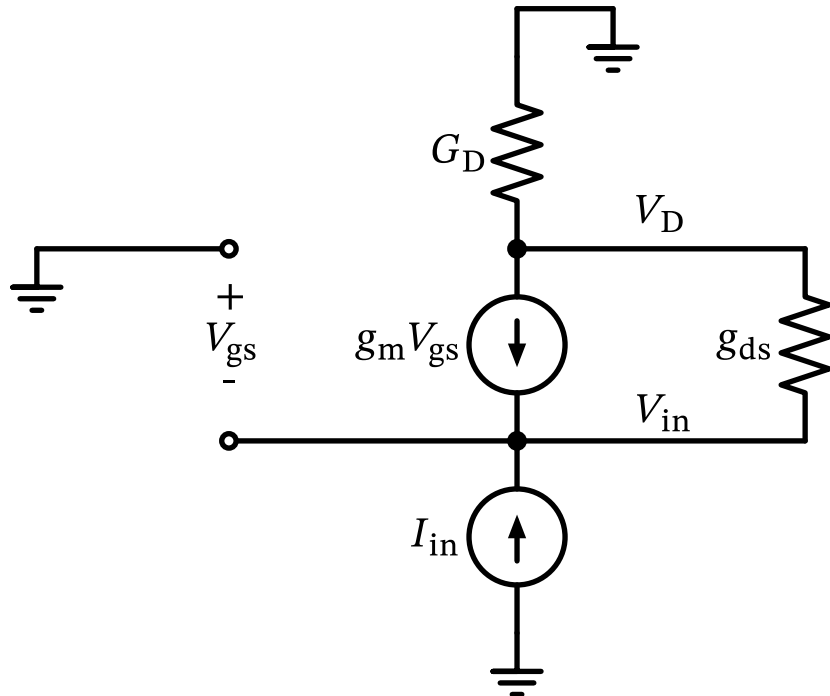


Figure 64: The simplified MOSFET cascode small-signal model for calculation of the input impedance.

We note that  $V_{gs} = -V_{in}$  and that  $I_{in}$  flows through  $G_D$ , resulting in  $V_D = I_{in}/G_D$ . Note that  $V_{ds} = V_D - V_{in}$ . Formulating KCL at the input node results in

$$I_{in} + g_{ds} V_{ds} + g_m V_{gs} = 0.$$

After some manipulation we find that

$$g_{in} = \frac{I_{in}}{V_{in}} = \frac{(g_m + g_{ds}) \cdot G_D}{g_{ds} + G_D}. \quad (34)$$

Setting  $G_D = 0$  (an open) results in  $g_{in} = 0$  as well, so the input impedance of the cascode is very large when the drain impedance is large.

However, setting  $G_D = \infty$  (a short or low-ohmic impedance) results in the well-known result of  $g_{in} = g_m + g_{ds} \approx g_m$ , which means that the input impedance looking into a cascode is approximately  $1/g_m$ .

### ! Benefit of Cascode (Input)

This has the practical benefit that a capacitance connected at this node results in a high-frequency pole, which is often not critical in terms of stability. Further, the voltage swing at a cascode input node is small due to the often small impedance, and this minimizes the Miller effect at connected inter-node capacitors (see Section 17.1).

## 10 Improved Current Mirrors

In Section 6, we looked into the operation of the basic current mirror. While it is a useful structure and easy to implement, its output resistance is limited by the MOSFET's output conductance  $g_{ds}$ , and its current mirroring accuracy is also limited by channel-length modulation effects since the  $V_{DS}$  of the output transistor varies with load conditions, and is thus different from the  $V_{DS}$  of the reference transistor.

Using the cascode principle introduced in Section 9, we can improve both the output resistance and the current mirroring accuracy of the current mirror. The improved current mirror structure is shown in Figure 65. We use the so-called “high-swing” cascode structure here.

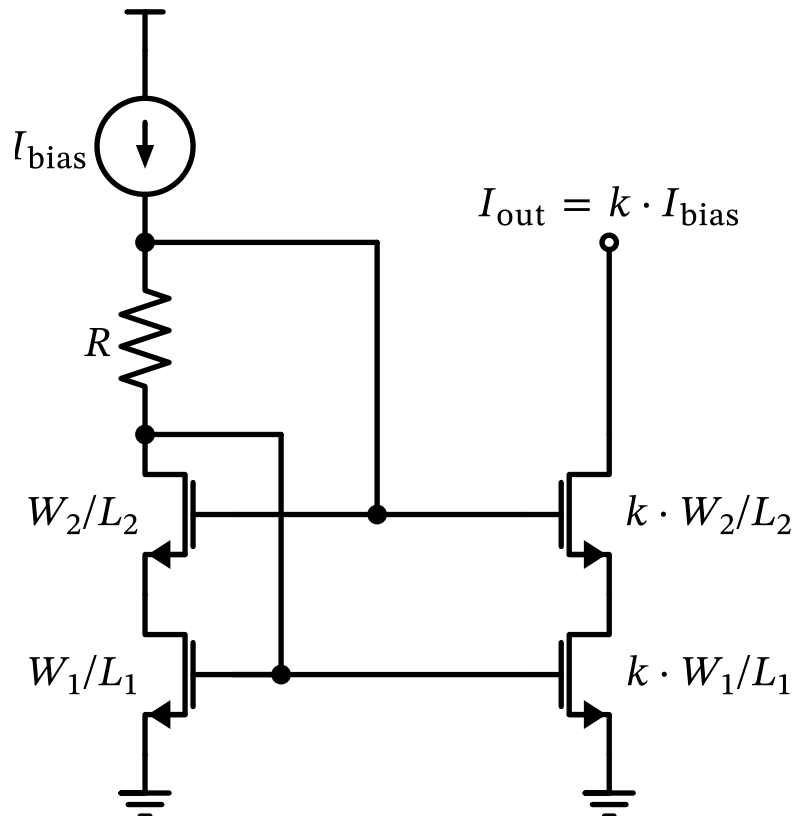


Figure 65: A high-swing cascoded current mirror. The voltage drop across the resistor  $R$  sets the drain-source voltage of the lower transistors (together with the sizing of the MOSFETs).

The output impedance according to Equation 33 of the improved current mirror is approximately given by ( $r_{ds} = g_{ds}^{-1}$  and  $g_{mcasc}$  are the parameters of the cascode transistor, and  $r_{ds} = g_{ds}^{-1}$  are the parameters of the bottom transistor):

$$r_{\text{out}} = r_{\text{ds,casc}} + r_{\text{ds}} \cdot (1 + g_{\text{m,casc}} \cdot r_{\text{ds,casc}}). \quad (35)$$

We can bias the gate voltages of the cascode transistors with any suitable bias circuit, but a simple way is to use a resistor  $R$  as shown in the figure. The voltage drop across this resistor sets the drain-source voltage of the lower transistors (together with the sizing of the MOSFETs). By choosing a sufficiently large value for  $R$ , we can ensure that both transistors remain in saturation for the desired range of output currents. The cascode transistors make sure that the drain-source voltage of the output transistor remains nearly constant and equal to the drain-source voltage of the reference transistor, thus improving the current mirroring accuracy.

Another option is to use source degeneration with a resistor. This configuration is shown in Figure 66. Here, the source degeneration resistors  $R$  help to stabilize the operating point of the current mirror using series feedback.

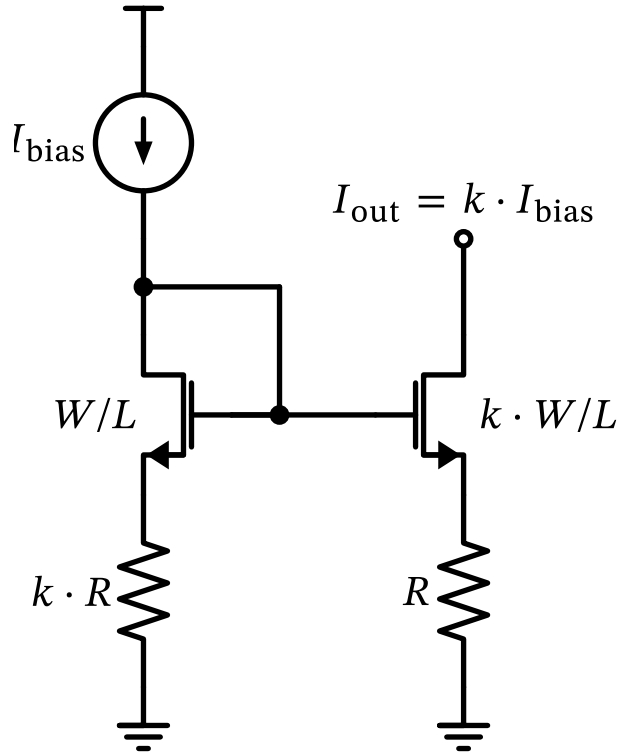


Figure 66: A current mirror with resistive degeneration.

Here, similar to Equation 35, the output resistance can be approximated by

$$r_{\text{out}} = r_{\text{ds}} + R \cdot (1 + g_{\text{m}} \cdot r_{\text{ds}}). \quad (36)$$

A third popular option is to use the so-called regulated current mirror, which uses an additional amplifier to sense the drain potential of the bottom transistor and keep it constant [27]. Note that the output current will not change if the  $V_{\text{DS}}$  of the bottom transistor is kept constant. We can use any suitable amplifier for this purpose, e.g., a simple OTA as introduced in Section 8. In the most basic form, we use a common-source stage with a current mirror load as shown in Figure 67.

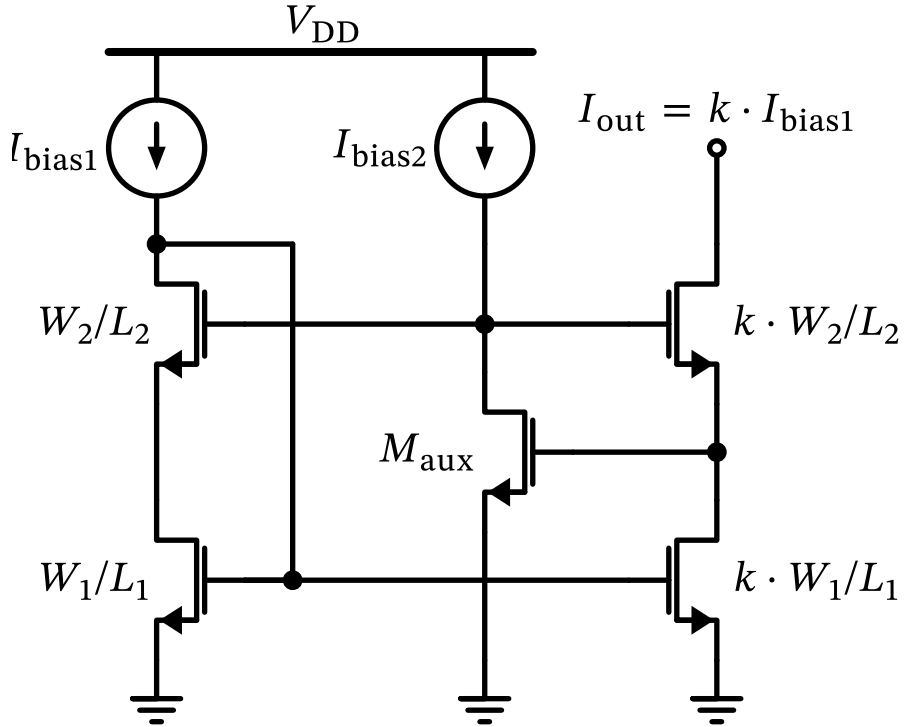


Figure 67: A regulated-cascode current mirror. The simple common-source amplifier is used to keep the drain voltage of the bottom transistor constant, thus improving the current mirroring accuracy and output resistance.

We assume the voltage gain of the auxiliary amplifier to be  $A_v = g_{maux}/g_{dsaux}$ , where  $g_{maux}$  and  $g_{dsaux}$  are the transconductance and output conductance of the auxiliary amplifier, respectively. The output resistance of the regulated cascode current mirror can then be approximated by

$$\begin{aligned} r_{out} &= r_{ds,casc} + r_{ds} \cdot [1 + g_{mcasc} \cdot r_{ds,casc} \cdot (1 + g_{maux}/g_{dsaux})] \\ &\approx r_{ds} \cdot g_{mcasc} \cdot r_{ds,casc} \cdot g_{maux} \cdot r_{ds,aux} \end{aligned} \quad (37)$$

which, compared to Equation 35, is further improved by the gain of the auxiliary amplifier.

We now want to size all these current mirror structures and simulate their performance. We try to size them for similar chip area in order to get a fair comparison. We assume a reference current of  $I_{bias} = 50 \mu\text{A}$  and a mirror ratio of 1:1. We size for a minimum voltage headroom for the current sources of  $V_{DS,min} = 0.4 \text{ V}$ . The calculations are summarized in this sizing notebook.

The resulting circuits are drawn in Figure 68. The testbench simulates the dc output characteristics of all four current mirror variations (the three improved ones and the basic one for reference). The testbench also runs a Monte-Carlo simulation to evaluate the current mirroring accuracy under device mismatch (see Section 8.6.1).

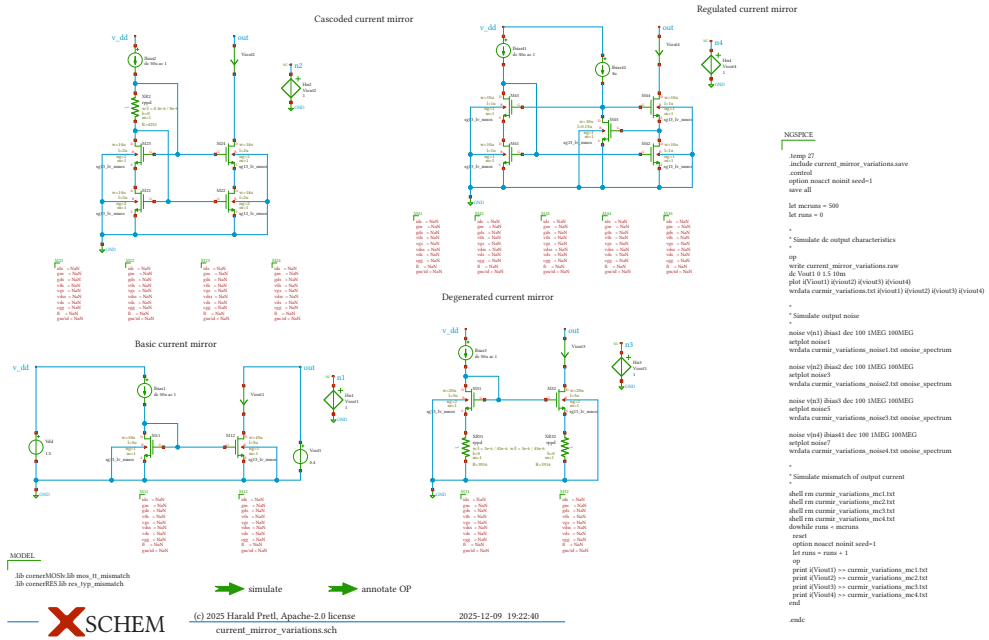


Figure 68: Simulation schematic of the improved current mirrors.

The output characteristics from the dc sweep simulation are shown in Figure 69, and a zoom-in in Figure 70. We can see that all improved current mirror structures achieve a significantly higher output resistance compared to the basic current mirror. The regulated cascode structure achieves the highest output resistance, as expected.

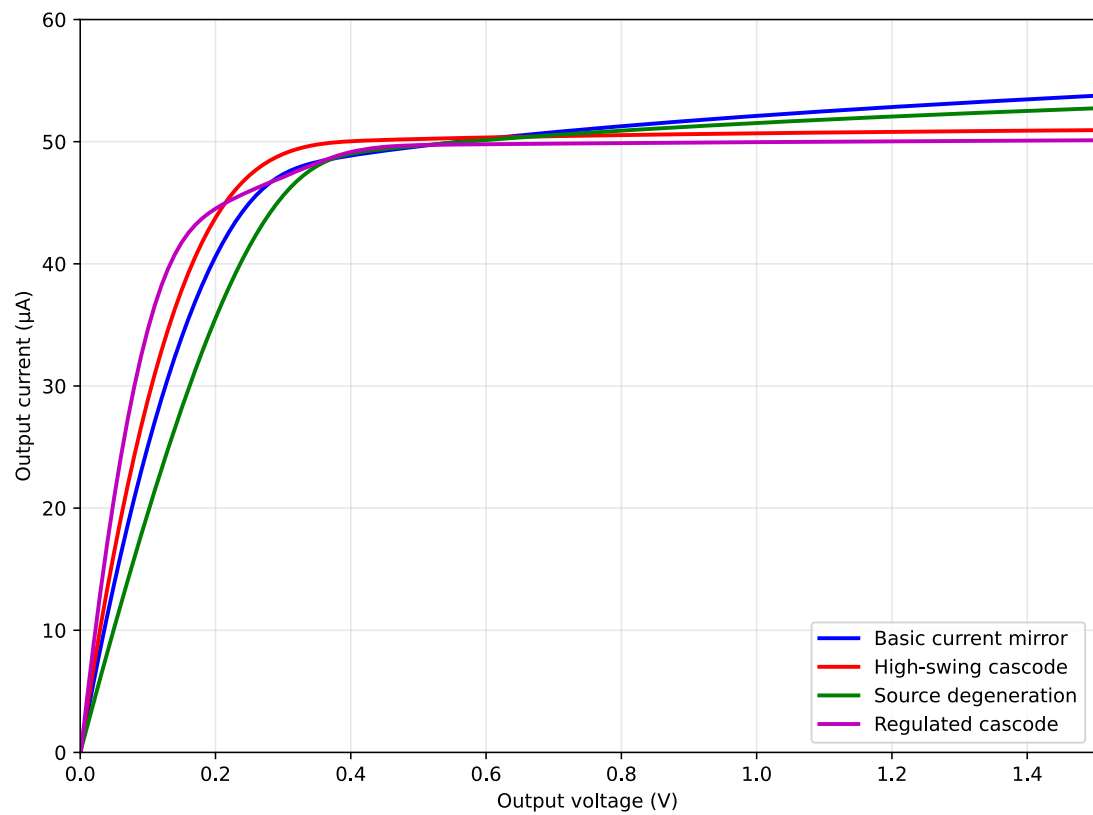


Figure 69: Output characteristics of the four current mirror structures.

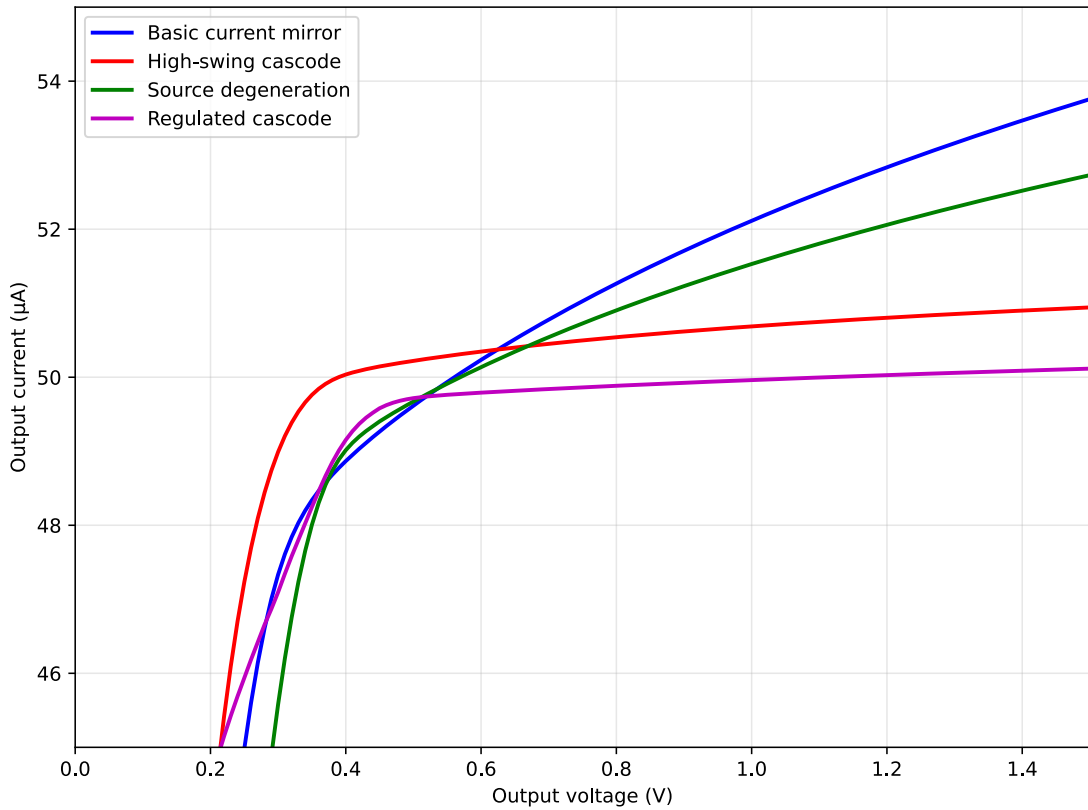


Figure 70: Output characteristics of the four current mirror structures (zoom in). The high-swing cascode and the regulated cascode achieve significantly higher output resistance compared to the basic and degenerated current mirror.

We now look into the results of the Monte-Carlo simulation to evaluate the current mirroring accuracy under device mismatch using 500 runs and a compliance voltage of 0.4 V. The results are summarized in Figure 71. We can see that the high-swing cascode and the regulated cascode achieve a very precise nominal current accuracy of almost 50  $\mu\text{A}$ . However, the source-degenerated current mirror shows a significantly reduced spread of the output current, indicating a reduced mismatch of the poly-silicon resistors compared to the MOSFETs.

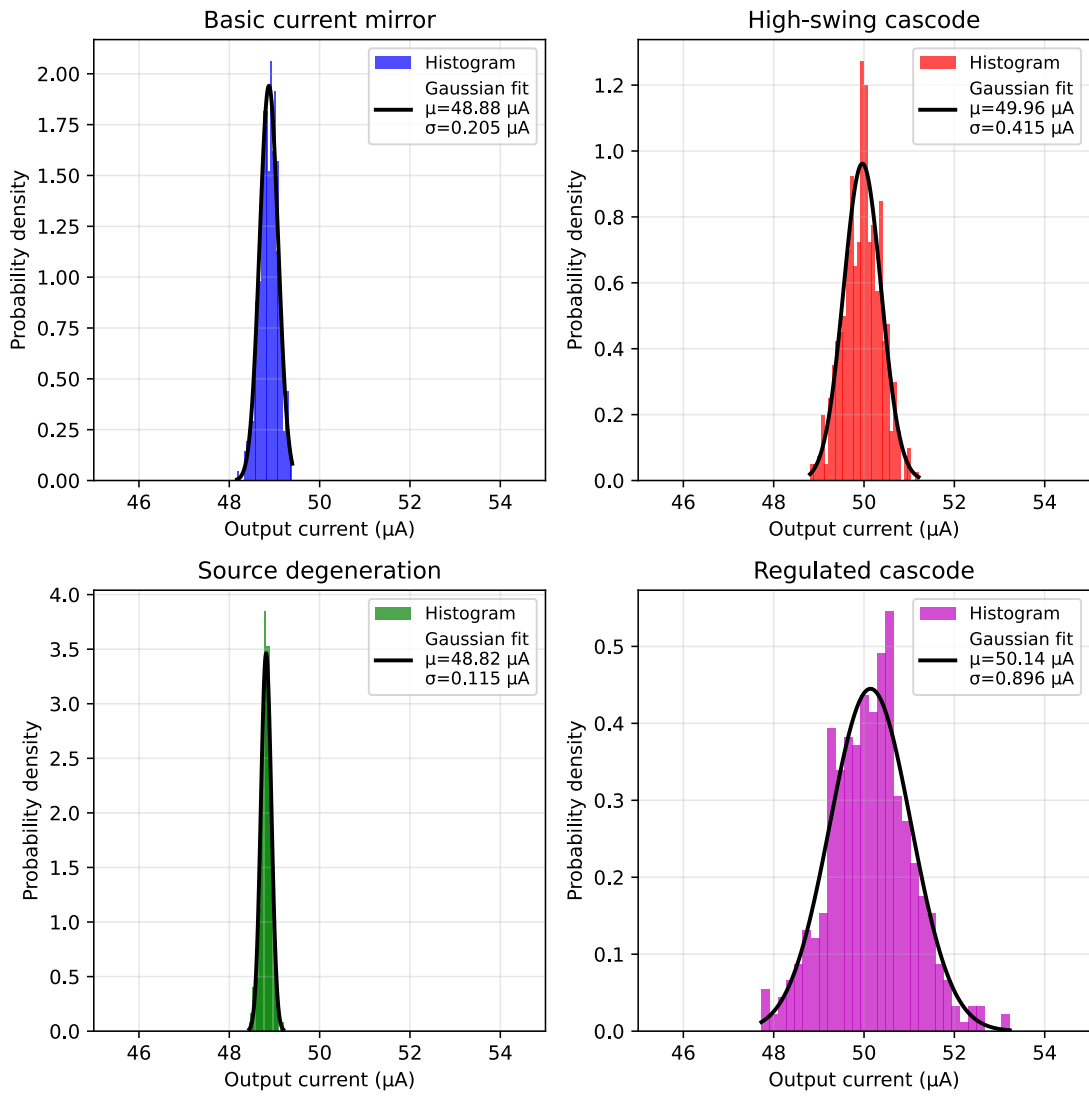


Figure 71: Monte Carlo analysis of the four current mirror structures showing current distribution and fitted Gaussian curves.

Finally, we compare the output noise of the four different current mirror structures in Figure 72. We can see that the regulated cascode has the highest output noise due to the additional auxiliary amplifier, while the source-degenerated mirror has the lowest output noise.

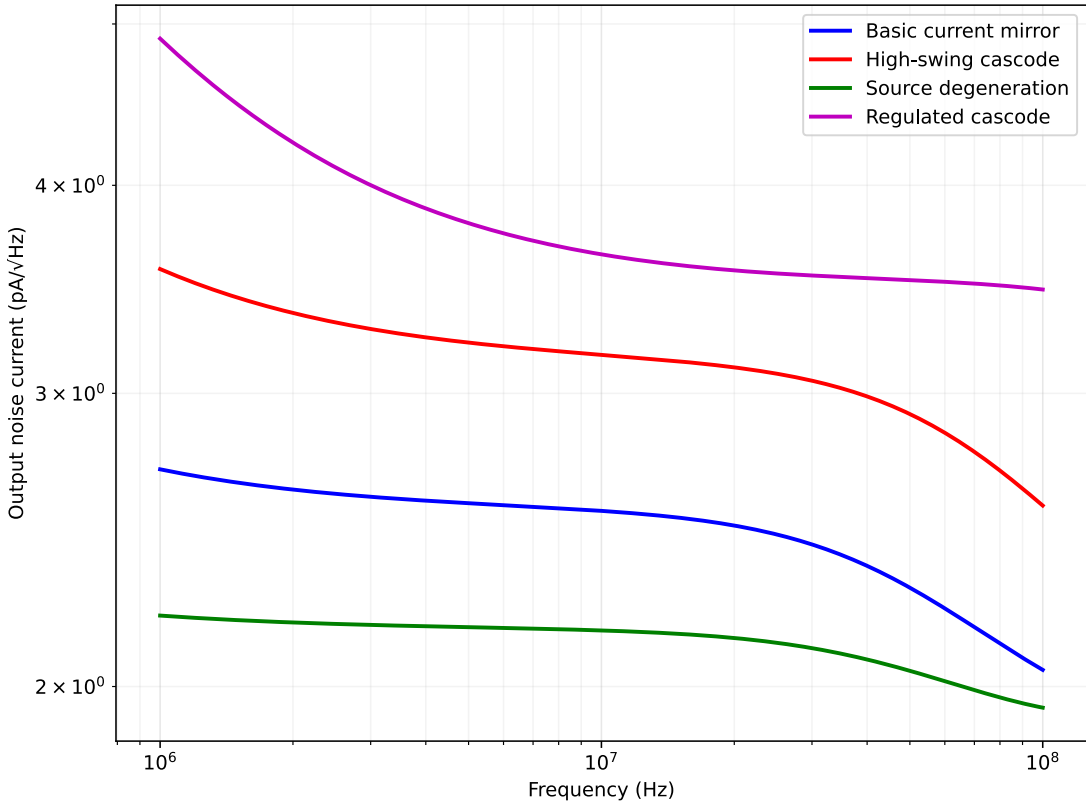


Figure 72: Output noise current vs. frequency for the four current mirror structures.

### 10.1 Low-Voltage Regulated Current Mirror

The one drawback of the regulated cascode current mirror shown in Figure 67 is its relatively high compliance voltage, which is due to the fact that  $V_{DS1} = V_{GSaux}$ . One alternative implementation that reduces the compliance voltage is shown in Figure 73. Here, we use a differential common-gate stage (essentially a current mirror with inputs at the sources of the transistors) as an auxiliary amplifier, which significantly reduces the required voltage headroom, at the expense of a slightly increased circuit complexity [28]. However, the bias current sources  $I_{bias2,3}$  of the auxiliary amplifier introduce some additional noise and mismatch.

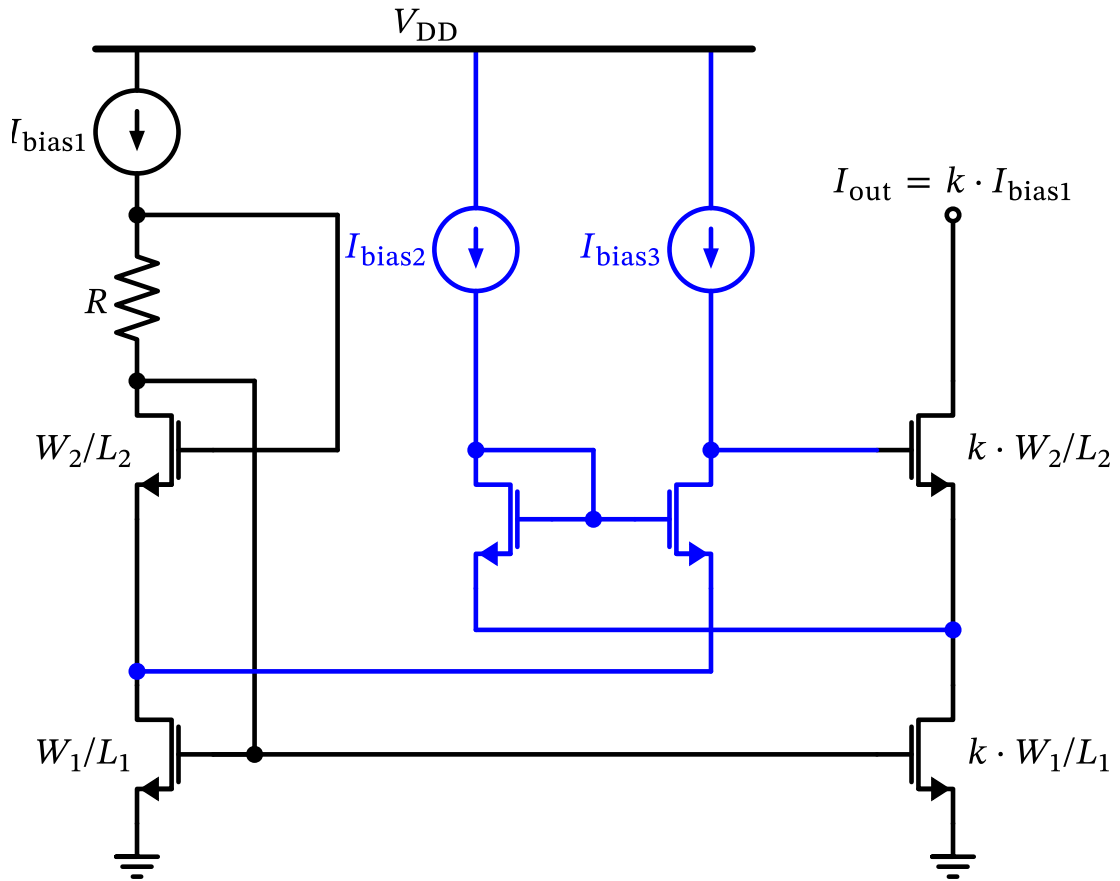


Figure 73: A low-voltage regulated-cascode current mirror. The differential common-gate error amplifier is used to keep the drain voltage of the bottom transistors constant, thus improving the current mirroring accuracy and output resistance.

## 10.2 Current Source Variations Summary

In summary, we can classify the usage of the different current mirror structures as follows:

- For general applications where output resistance and current accuracy are not critical, the **basic current mirror** can be used. It also has the lowest compliance voltage since only one transistor is stacked.
- The **high-swing cascode current mirror** is a good choice when higher output resistance is needed, while still keeping the circuit relatively simple.
- The **source-degenerated current mirror** is a good choice when the best current matching and low output noise are required. The additional voltage headroom that is dropped across the source degeneration can be adapted (higher is better), but a minimum value of 0.1 V should be used.
- The **regulated cascode current mirror** is the best choice when the highest output resistance is required, and the additional complexity and output noise are acceptable.
- The **low-voltage regulated cascode current mirror** is a good alternative to the regulated cascode when a low compliance voltage is required.

Please note that the absolute performance can be tweaked by proper sizing. The examples shown here are sized for similar chip area and a fair comparison.

### 10.3 Current Mirror Matching

Looking at the different current mirror architectures in Section 10, we can see that the current mirror matching is dominated by the bottom transistor pair (assuming equal  $V_{DS}$ ), with the exception of the resistively degenerated current mirror. We asserted that the matching of the resistively-degenerated current mirror is improved due to the lower impact of MOSFET mismatch compared to resistor mismatch. We will now substantiate this claim.

We will derive the current mirror matching of a pair of resistively-degenerated current mirror transistors shown in Figure 66.

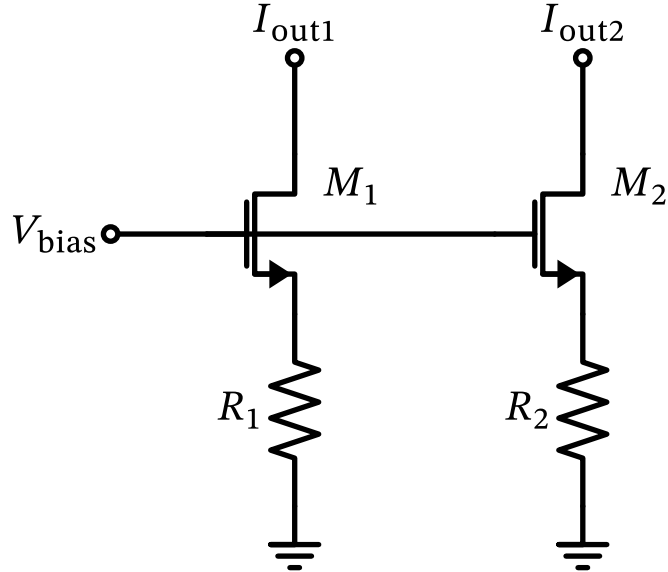


Figure 74: A current mirror pair with resistive degeneration.

The standard deviation  $\sigma$  of the output current difference, normalized to the current, is given by [1]

$$\begin{aligned} \sigma^2 \left\{ \frac{\Delta I_D}{I_D} \right\} &= \frac{\sigma^2 \{ \Delta V_{th} \}}{(V_{drv} + V_{deg})^2} + \left( \frac{V_{drv}}{V_{drv} + V_{deg}} \right)^2 \cdot \sigma^2 \left\{ \frac{\Delta K}{K} \right\} \\ &\quad + \left( \frac{V_{deg}}{V_{drv} + V_{deg}} \right)^2 \cdot \sigma^2 \left\{ \frac{\Delta R}{R} \right\}. \end{aligned} \quad (38)$$

The definition of  $V_{drv}$  is adapted here and understood as half of the  $V_{DS}$  saturation voltage, i.e.,  $V_{drv} = V_{DS,sat}/2 \approx I_D/g_m$ . The degeneration voltage is the voltage drop across the degeneration resistors and given by  $V_{deg} = I_D \cdot R$ .

The standard deviation of the resistor  $\sigma \{ \Delta R / R \}$  can be calculated using Equation 30. Further, the threshold voltage mismatch  $\sigma \{ \Delta V_{th} \}$  can be calculated using Equation 26.

By using the approximation of Equation 4, we can express Equation 38 in terms of our preferred sizing parameter  $g_m/I_D$ :

$$\begin{aligned} \sigma^2 \left\{ \frac{\Delta I_D}{I_D} \right\} &= \frac{\sigma^2 \{\Delta V_{th}\}}{\left[ (g_m/I_D)^{-1} + V_{deg} \right]^2} + \left( \frac{1}{1 + V_{deg} \cdot g_m/I_D} \right)^2 \cdot \sigma^2 \left\{ \frac{\Delta K}{K} \right\} \\ &\quad + \left( \frac{V_{deg} \cdot g_m/I_D}{1 + V_{deg} \cdot g_m/I_D} \right)^2 \cdot \sigma^2 \left\{ \frac{\Delta R}{R} \right\}. \end{aligned} \quad (39)$$

The standard deviation of the transconductance parameter mismatch  $\sigma\{\Delta K/K\}$  can be calculated similarly as (which is an alternative form to Equation 27)

$$\sigma^2 \left\{ \frac{\Delta K}{K} \right\} = \sigma^2 \{\Delta W\} \cdot \frac{1}{W^2} + \sigma^2 \{\Delta L\} \cdot \frac{1}{L^2} + \sigma^2 \left\{ \frac{\Delta \mu}{\mu} \right\} \cdot \frac{1}{WL}, \quad (40)$$

where  $\sigma\{\Delta W\}$  and  $\sigma\{\Delta L\}$  are the process-dependent mismatch parameters for the width  $W$  and length  $L$ , respectively, and  $\sigma\{\Delta \mu/\mu\}$  is the mobility mismatch parameter.

The standard deviations of the components of the SG13G2 process are summarized in Table 3. For mismatch calculations we can assume them as uncorrelated.

Table 3: IHP SG13G2 device mismatch

Component	Matching Parameter	Value
Resistor <code>r<sub>sil</sub></code>	$\sigma\{\Delta R/R\} \cdot \sqrt{WL}$	1.2 % $\mu\text{m}$
Resistor <code>r<sub>ppd</sub></code>	$\sigma\{\Delta R/R\} \cdot \sqrt{WL}$	1.5 % $\mu\text{m}$
Resistor <code>r<sub>high</sub></code>	$\sigma\{\Delta R/R\} \cdot \sqrt{WL}$	5 % $\mu\text{m}$
MIM <code>cap_cmim</code>	$\sigma\{\Delta C/C\} \cdot \sqrt{WL}$	1 % $\mu\text{m}$ (estimated)
MOSFET <code>sg13_lv_nmos</code>	$\sigma\{\Delta V_{th}\} \cdot \sqrt{WL}$	3.9 mV $\mu\text{m}$
MOSFET <code>sg13_lv_nmos</code>	$\sigma\{\Delta W\}$	4 nm
MOSFET <code>sg13_lv_nmos</code>	$\sigma\{\Delta L\}$	2 nm
MOSFET <code>sg13_lv_nmos</code>	$\sigma\{\Delta \mu/\mu\} \cdot \sqrt{WL}$	0.5 % $\mu\text{m}$
MOSFET <code>sg13_lv_pmos</code>	$\sigma\{\Delta V_{th}\} \cdot \sqrt{WL}$	2.2 mV $\mu\text{m}$
MOSFET <code>sg13_lv_pmos</code>	$\sigma\{\Delta W\}$	4 nm
MOSFET <code>sg13_lv_pmos</code>	$\sigma\{\Delta L\}$	2 nm
MOSFET <code>sg13_lv_pmos</code>	$\sigma\{\Delta \mu/\mu\} \cdot \sqrt{WL}$	0.33 % $\mu\text{m}$

Inspecting Equation 38 we can see that by implementing a common-source transistor without source degeneration (i.e.,  $V_{\text{deg}} = 0$ ), the current mirror matching is dominated by the threshold voltage mismatch and the transconductance parameter mismatch of the MOSFETs:

$$\sigma^2 \left\{ \frac{\Delta I_D}{I_D} \right\} = \sigma^2 \{ \Delta V_{\text{th}} \} \left( \frac{g_m}{I_D} \right)^2 + \sigma^2 \left\{ \frac{\Delta K}{K} \right\} \quad (41)$$

The first term in Equation 41 can be minimized by choosing a low  $g_m/I_D$  ratio, while the latter term is minimized by increasing the device area (i.e., increasing  $W$  and  $L$ ).

Looking at the resistively-degenerated current mirror, and using a large degeneration voltage  $V_{\text{deg}}$ , we can simplify Equation 39 to

$$\sigma^2 \left\{ \frac{\Delta I_D}{I_D} \right\} = \sigma^2 \left\{ \frac{\Delta R}{R} \right\} \quad (42)$$

indicating that now the current matching of the degenerated current mirror is defined by the resistor matching only. Since resistors typically have a significantly better matching than MOSFETs, this can lead to a significant improvement in current mirror accuracy.

## i Current Mirror Matching Calculation

Let us now calculate the current mirror matching of the simple current mirror. Using Equation 41, and using the sizing values of  $g_m/I_D = 5 \text{ V}^{-1}$ ,  $W = 10 \mu\text{m}$ , and  $L = 5 \mu\text{m}$ , we can calculate the standard deviation of the transconductance parameter mismatch using Equation 40 and Table 3:

$$\sigma\left\{\frac{\Delta K}{K}\right\} = \sqrt{\left(\frac{4 \text{ nm}}{10 \mu\text{m}}\right)^2 + \left(\frac{2 \text{ nm}}{5 \mu\text{m}}\right)^2 + \left(\frac{0.5 \% \mu\text{m}}{\sqrt{10 \mu\text{m} \cdot 5 \mu\text{m}}}\right)^2} = 0.08 \text{ \%}.$$

The standard deviation of the threshold voltage mismatch can be calculated using Equation 26 and Table 3:

$$\sigma\{\Delta V_{\text{th}}\} = \frac{2 \text{ mV } \mu\text{m}}{\sqrt{10 \mu\text{m} \cdot 5 \mu\text{m}}} = 0.28 \text{ mV}.$$

Bringing both results into Equation 41, we get

$$\sigma\left\{\frac{\Delta I_D}{I_D}\right\} = \sqrt{(0.28 \text{ mV} \cdot 5 \text{ V}^{-1})^2 + (0.08 \text{ \%})^2} \approx 0.16 \text{ \%}.$$

Comparing with the simulation results in Figure 71 for the basic current mirror, we can see that this matches quite ok with the standard deviation of about  $0.21 \mu\text{A}/48.9 \mu\text{A} = 0.43 \text{ \%}$  obtained from the Monte-Carlo simulation.

Let us now calculate the current mirror matching of the resistively-degenerated current mirror. Using Equation 39, we can analyze this configuration. We use the sizing values of  $g_m/I_D = 10 \text{ V}^{-1}$ ,  $W = 20 \mu\text{m}$ , and  $L = 3 \mu\text{m}$ , for the MOSFET, and  $V_{\text{deg}} = 0.2 \text{ V}$ ,  $L = 15 \mu\text{m} / W = 1 \mu\text{m}$  for the used  $\text{rppd}$  resistor.

The standard deviation of the transconductance parameter mismatch can be calculated as

$$\sigma\left\{\frac{\Delta K}{K}\right\} = \sqrt{\left(\frac{4 \text{ nm}}{20 \mu\text{m}}\right)^2 + \left(\frac{2 \text{ nm}}{3 \mu\text{m}}\right)^2 + \left(\frac{0.5 \% \mu\text{m}}{\sqrt{20 \mu\text{m} \cdot 3 \mu\text{m}}}\right)^2} = 0.07 \text{ \%}.$$

The standard deviation of the threshold voltage mismatch can be calculated

$$\sigma\{\Delta V_{\text{th}}\} = \frac{2 \text{ mV } \mu\text{m}}{\sqrt{20 \mu\text{m} \cdot 3 \mu\text{m}}} = 0.26 \text{ mV}.$$

The standard deviation of the resistor mismatch can be calculated using Equation 30 and Table 3:

$$\sigma\left\{\frac{\Delta R}{R}\right\} = \frac{1.5 \% \mu\text{m}}{\sqrt{15 \mu\text{m} \cdot 1 \mu\text{m}}} = 0.39 \text{ \%}.$$

Plugging these results into Equation 39, we get

$$\begin{aligned} \sigma^2\left\{\frac{\Delta I_D}{I_D}\right\} &= \left(\frac{0.26 \text{ mV}}{0.1 \text{ V} + 0.2 \text{ V}}\right)^2 + \left(\frac{1}{1 + 0.2 \text{ V} \cdot 10 \text{ V}^{-1}} \cdot 0.07 \%\right)^2 \\ &\quad + \left(\frac{0.2 \text{ V} \cdot 10 \text{ V}^{-1}}{1 + 0.2 \text{ V} \cdot 10 \text{ V}^{-1}} \cdot 0.39 \%\right)^2 \\ &= (0.26 \%)^2. \end{aligned}$$

We see that compared to the basic current mirror, the resistively-degenerated current mirror achieves a significantly improved current matching. This matches quite well with the simulation results in Figure 71 for the resistively-degenerated current mirror, where

## 11 Improved (Telescopic) OTA

With the new learned know-how of the cascode stage we can set out to improve our original basic 5T-OTA design. Essentially this means to add cascodes to  $M_2$  and  $M_4$  in Figure 32. For symmetry reasons we will add cascodes to both sides, and the resulting schematic is shown in Figure 75. This configuration is also referred to as “**telescopic OTA**” (likely because of the stacked structure, where all the transistors are stacked in current path like the tubes of a telescope).

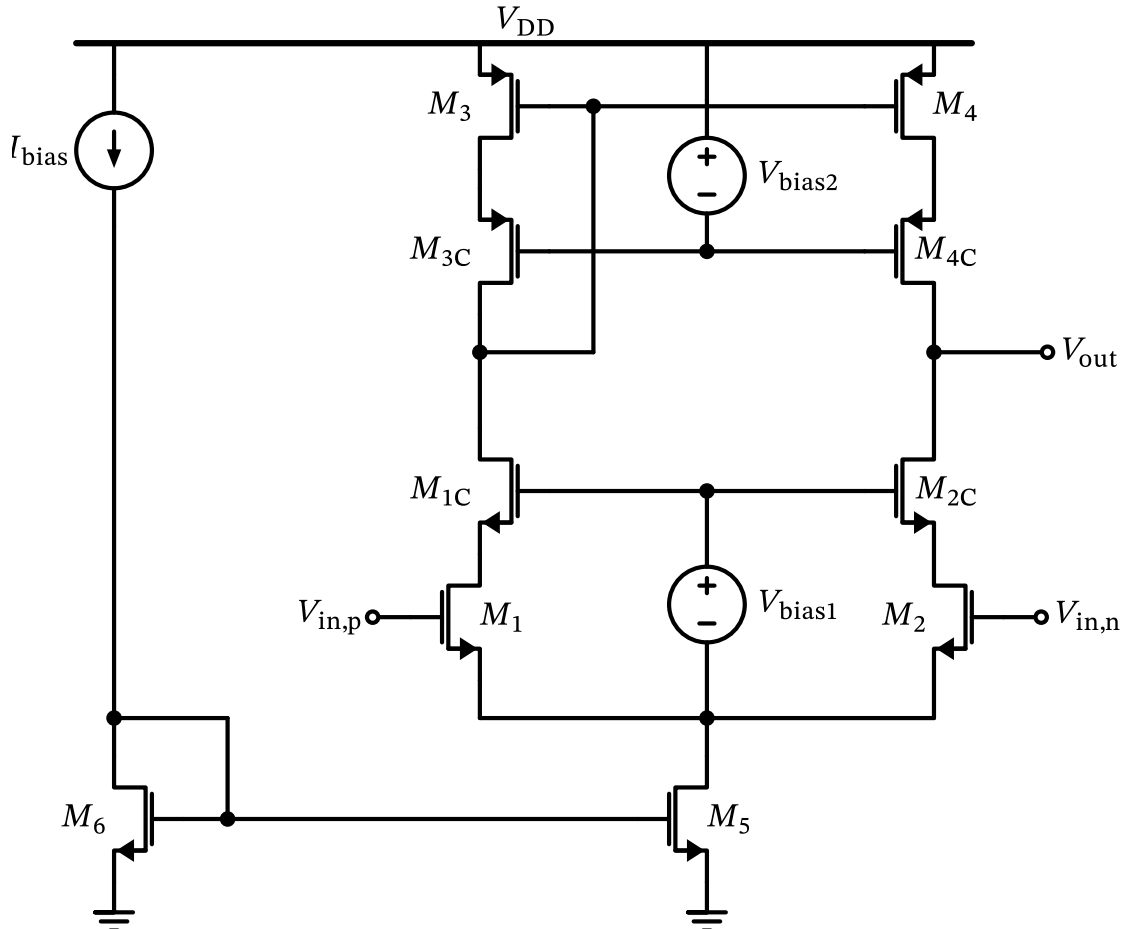


Figure 75: The improved OTA based on the 5T-OTA design.

The transistor name appendix “C” indicates a cascode device sitting atop its base transistor. The bias voltage  $V_{\text{bias}2}$  is referenced to  $V_{\text{DD}}$  (it is shown differently in Figure 75 to simplify the schematic), and the floating bias voltage  $V_{\text{bias}1}$  creates a voltage bias for  $M_{1C}$  and  $M_{2C}$  relative to the tail point, so that the  $V_{\text{DS}}$  of  $M_{1,2}$  stays constant with a changing common-mode input voltage.

### ! Cascode Bias Voltage Generation

It is critically important for a stable performance across PVT that the bias voltages for the cascode gates are created in a manner that tracks variations with process, temperature, and supply voltage!

The current mirror constructed out of  $M_{3,3C}$  and  $M_{4,4C}$  is a special kind of **cascode current mirror for low-voltage operation**, also referred to as high-swing cascode current mirror [9]. This type is very often used, as it forces the  $V_{GS}$  and  $V_{DS}$  of  $M_{3,4}$  to be equal, so the current mirror ratio is independent of  $g_{ds}$ .

#### 💡 Exercise: Cascode Current Mirror vs. High-Swing Cascode Current Mirror

Try to verify the above statement of equal drain-source voltages by deriving both, an equation for  $V_{DS4}$  assuming a high-swing cascode current mirror (Figure 75) and  $V_{DS4}$  in case of a simple cascode current mirror, where the reference branch ( $M_{3,3C}$ ) is comprised of two MOSFET diodes.

Further, by properly selecting the bias voltages of the cascode a low-voltage operation is achieved as  $V_{DS}$  can be minimized, allowing even triode operation of the current-mirror MOSFETs (as, noted above, a large  $g_{ds}$  is not a big issue).

A simplified small-signal gain calculation of this improved OTA uses the result of Equation 18 and Equation 33 to arrive at the approximate dc gain of

$$A_0 \approx \frac{g_{m12}}{g_{ds2} \frac{g_{ds2C}}{g_{m2C}} + g_{ds4} \frac{g_{ds4C}}{g_{m4C}}} \quad (43)$$

leading to a significant boost in dc gain due to cascading. We will use this increased gain to reduce the  $L$  of all MOSFET to

1. save area (a smaller  $L$  will lead to a smaller  $W$  for a given  $W/L$  ratio) and
2. push the additional poles and zeros at the inner nodes of the cascode transistors (e.g., the connection of the drain of  $M_4$  to the source of  $M_{4C}$ ) to higher frequencies to result in stable behavior and a reasonable gain transfer function (too many poles and zeros in the pass band of the amplifier create many issues with stability margin).

### 11.1 Sizing the Improved OTA

Like the sizing of the 5T-OTA in Section 8.4 we will again use the  $g_m/I_D$  method using a Python notebook. Instead of using  $L = 5 \mu\text{m}$  we will this time use a reduced  $L = 0.5 \mu\text{m}$  for  $M_{1/1C,2/2C,3/3C,4/4C}$  (for speed reasons) and  $L = 5 \mu\text{m}$  for  $M_{5,6}$  for better common-mode rejection (the tail current mirror is less critical in terms of speed and stability).

We set  $g_m/I_D = 13$  across the board for a good trade-off between speed, current efficiency, and voltage headroom for the MOSFETs (this is now way more critical than in the basic 5T-OTA as we stack now double as many MOSFET at the same supply voltage). Please look at Section 3 to confirm this choice.

## i Improved OTA Sizing

### Sizing for Basic (Improved) OTA

Copyright 2024-2025 Harald Pretl

Licensed under the Apache License, Version 2.0 (the “License”); you may not use this file except in compliance with the License. You may obtain a copy of the License at <http://www.apache.org/licenses/LICENSE-2.0>

```
# read table data
from pygmid import Lookup as lk
import numpy as np
lv_nmos = lk('sg13_lv_nmos.mat')
lv_pmos = lk('sg13_lv_pmos.mat')
# list of parameters: VGS, VDS, VSB, L, W, NFING, ID, VT, GM, GMB, GDS,
CGG, CGB, CGD, CGS, CDD, CSS, STH, SFL
# if not specified, minimum L, VDS=max(vgs)/2=0.9 and VSB=0 are used
```

```
# define the given parameters as taken from the specification table or
initial guesses
c_load = 50e-15
gm_id_m12 = 13
gm_id_m12c = 13
gm_id_m34 = 13
gm_id_m34c = 13
gm_id_m56 = 13
l_12 = 0.5
l_12c = 0.5
l_34 = 0.5
l_34c = 0.5
l_56 = 5
f_bw = 10e6 # -3dB bandwidth of the voltage buffer
i_total_limit = 10e-6 # we plan 2x5uA in addition for additional bias
voltage generation
i_bias_in = 5e-6
output_voltage = 1.3
vin_min = 0.7
vin_max = 0.9
vdd_min = 1.45
vdd_max = 1.55
vds_headroom = 0.2
```

```
# we get the required gm of M1/2 from the -3dB bandwidth requirement of
the voltage buffer specification
# note that the -3dB bandwidth of the voltage buffer with gain Av=1 is
equal to the unity gain bandwidth
# of the ota, hence we set them equal here
# we add a factor of 3 to allow for PVT variation plus additional
MOSFET parasitic loading
```

```
is power still in the budget)
# calculate gm of M1/2
gm12 = round(gm_id_m12*1e-3*(f_bw**2/(2*vdd_max))) # gm of M1/2
gm12c = round(gm_id_m12c*1e-3*(f_bw**2/(2*vdd_max))) # gm of M1/2c
# calculate gm of M3/4
gm34 = round(gm_id_m34*1e-3*(f_bw**2/(2*vdd_max))) # gm of M3/4
gm34c = round(gm_id_m34c*1e-3*(f_bw**2/(2*vdd_max))) # gm of M3/4c
# calculate gm of M5/6
gm56 = round(gm_id_m56*1e-3*(f_bw**2/(2*vdd_max))) # gm of M5/6
gm56c = round(gm_id_m56*1e-3*(f_bw**2/(2*vdd_max))) # gm of M5/6c
```

Looking at this sizing result we see that we achieve an improved  $A_0 > 43$  dB while meeting also the other performance requirements of Table 2 with margin. In addition, we check the voltage headroom of the critical MOSFET to see if we can squeeze it into the available supply voltage range, and see that this is possible with our above choice selection of parameters.

## Exercise: Improved OTA Sizing

Please take a detailed look at the above sizing notebook and play with the numbers and calculations. Do you find a better trade-off for the input parameters? Can you understand the thinking process behind the choices and calculations?

## 11.2 Designing the Improved OTA

Based on the collected experience in this lecture and the result of the sizing procedure in Section 11.1 you should be able to design this OTA. If you want, please go ahead and try an implementation and check its performance with CACE.

As an alternative there is a prepared OTA design shown in Figure 76 which we will discuss in detail next.

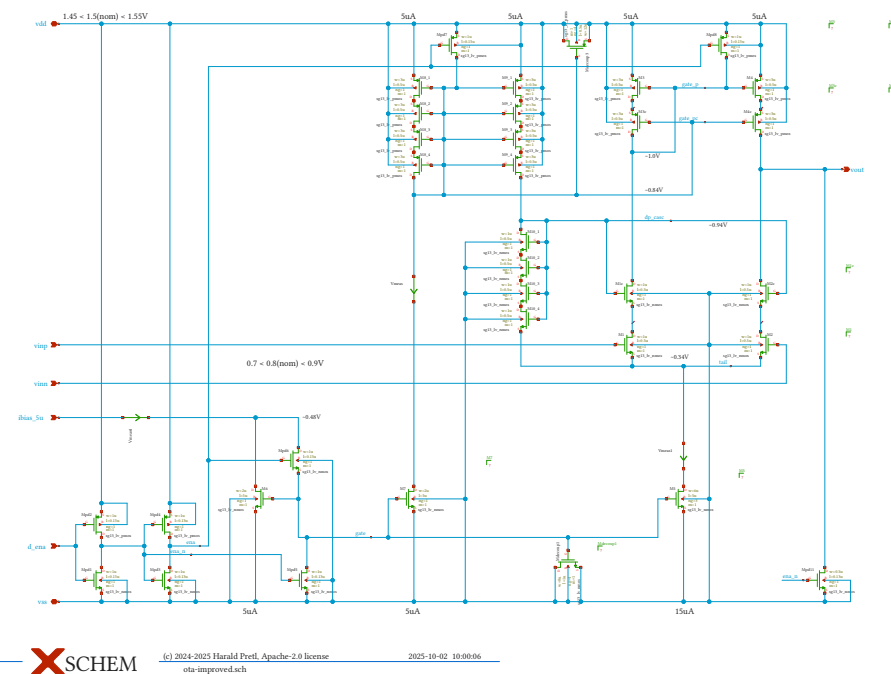


Figure 76: Improved OTA design in Xschem.

### **11.2.1 Discussion of the OTA Design**

We will now do an analysis of the circuit design of the OTA including all the complications which make this design practical.

1. For easier navigation, the device identifier are consistent with the circuit sketch in Figure 75.
  2. Some MOSFET dimensions are rounded to make a better fit in the IC layout. Please also look carefully at  $W$ ,  $L$ , and  $ng$ . The parameter  $ng$  defines how the total  $W$  of a MOSFET

should be split into individual MOSFET fingers with  $W_f = W/ng$ . This is done to arrive at a suitably sized MOSFET physical implementation. As we will not deal with IC layout in this lecture we will leave it at that.

3. In order to allow good matching in the IC layout, MOSFETs (and other components) have to be constructed from equal pieces. To that end,  $W/L$  scaling is done using unit elements (see finger width  $W_f$ ). Sometimes, besides  $W$  the length  $L$  has to be scaled, and this leads to the oddly-looking series stacking of some MOSFET (easily recognizable by the connected gates). In order to increase circuit readability, a subcircuit could be constructed hiding this series stacking of MOSFET, but it is sometimes easier to avoid subcircuits. There is a fine line in this trade-off, sometime a depth of 4 is the decision point between subcircuit use/no-use.
4. As you can (hopefully) see the circuit is carefully drawn to ease readability. Important nets are named, text comments state certain properties like nominal voltage levels, bias currents, etc. Current sensing elements are added to directly see the dc currents in the circuit simulation.
5. The bias voltage generation for the cascodes is included as well. The voltage drop for the bottom transistors is developed by properly scaling the MOSFETs in the reference branch. We reduce the  $W/L$  ratio to increase the  $V_{GS}$  to create a voltage headroom for the bottom MOSFET. We are using a dummy branch for bias generation (constructed with  $M_{7-10}$ ).
6. The floating bias voltage  $V_{bias1}$  is created by implementing a current source from  $V_{DD}$  ( $M_9$ ), then a MOSFET diode  $M_{10}$ , and an increased current towards  $V_{SS}$  through  $M_5$ .
7. Power-down transistors  $M_{pd,x}$  are added to allow a proper shutdown of the circuit with a digital enable input. It is generally a good idea to clamp floating nodes in off-mode so that no issues during power-down (like increased leakage currents) or delayed startup or shutdown are occurring. It is further a good design principle to buffer all incoming digital signals with inverters ( $M_{pd,1-4}$ ) connected to the local supply. This lowers the risk of unwanted noise coupling or excessive slew rates on the incoming digital signals.
8. Sensitive bias nodes are buffered with decoupling capacitors. We are using MOSFETs as nonlinear capacitors, which is not an issue in this application, but we value the increased capacitive density. Please note how the MOSFET are connected (some are tied to  $V_{DD}$  while others are tied to  $V_{SS}$ ).

### Parallel Connection

Note that a parallel connection of devices is effectively possible using the multiplier notation of Xschem.

## 11.3 Simulation of Improved OTA

Now that the circuit design of the improved OTA is done, we can use the same simulation testbenches as for the basic OTA. The testbenches are shown in Figure 77, Figure 78, and Figure 79.

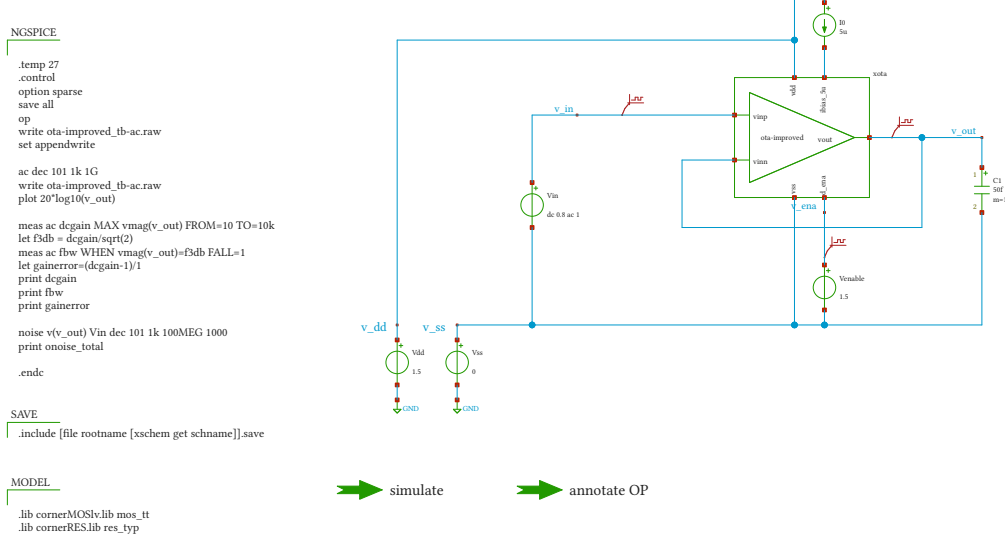


Figure 77: Simulation testbench of the improved OTA design (small-signal).

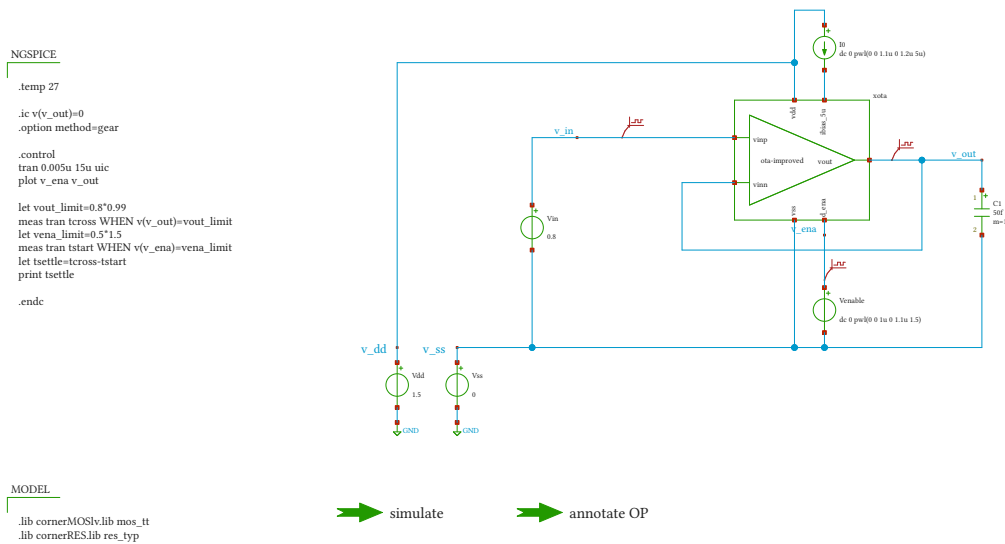


Figure 78: Simulation testbench of the improved OTA design (large-signal).

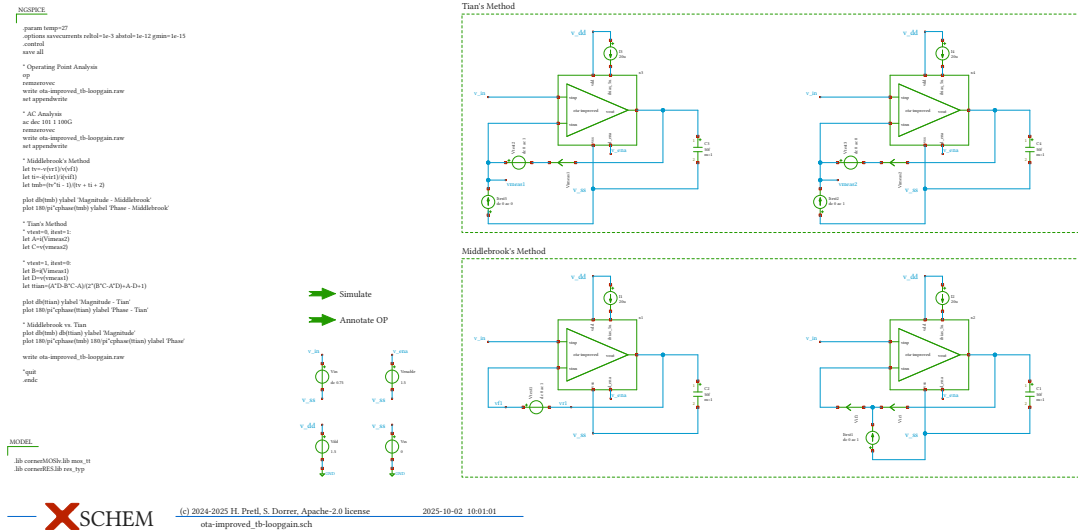


Figure 79: Simulation testbench of the improved OTA design (loop gain analysis).

### 💡 Exercise: Improved OTA Initial Simulation

Please use the above testbenches to simulate the improved OTA:

1. Check the dc bias points. Are they good? How stable are they across PVT variations?
2. What are the small-signal parameters like gain, noise and bandwidth? Are they fitting the specification?
3. What is large-signal performance? Is the settling fast enough? Is the settling well behaved, i.e., are there overshoots or other strange ringing indicating potential stability issues?
4. Try to improve the design. Change various device parameters and see what happens. Whenever you change something, check the dc operating point first. If the dc operating point is not good no further simulations make sense.

## 11.4 Corner Simulation of Improved OTA

Just like for the basic OTA we use the CACE system to check the performance of the improved OTA design holistically across variations like PVT and input signal variations. The results of the CACE run are shown below in Note 3.

**i Note 3: CACE Summary for Improved OTA**

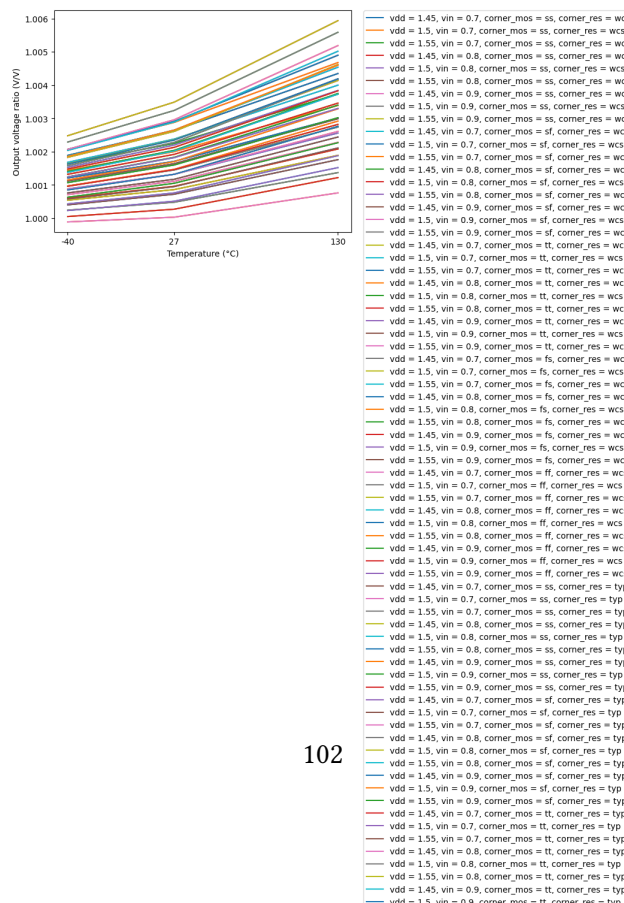
## CACE Summary for ota-improved

**netlist source:** schematic

Parameter	Tool	Result	Min Value	Max Value	Type	Typical Value	Min Value	Max Value	Status
			get				Limit		
Output voltage ratio	ngspice	gain	0.99 V/V	1.000 V/V	any	1.002 V/V	1.01 V/V	1.006 V/V	Pass ✓
Bandwidth	ngspice	bw	140000000.000 Hz	204153000.000 Hz	254164000.000 Hz	204169000.000 Hz	210169000.000 Hz	214169000.000 Hz	Pass ✓
Output voltage ratio (MC)	ngspice	gain_mc	any V/V	1.002 V/V	any	1.002 V/V	any	1.002 V/V	Pass ✓
Bandwidth (MC)	ngspice	bw_mc	204156000.000 Hz	205170500.000 Hz	210169000.000 Hz	205170500.000 Hz	210169000.000 Hz	214169000.000 Hz	Pass ✓
Output noise	ngspice	noise	any mV	0.309 mV	any	0.391 mV	0.6 mV	0.530 mV	Pass ✓
Settling time	ngspice	tsettle	any us	0.134 us	any	0.141 us	1 us	0.151 us	Pass ✓

### Plots

#### gain\_vs\_temp



The improved performance allows to improve the specifications in a few important points, notably the output voltage tolerance which is an important metric for a reference voltage buffer. We have intentionally increased the power consumption a little bit, but we negotiated with the chip lead designer a changed bias current level, so overall the situation is even slightly improved. The new situation with the improved design is summarized in Table 4 (unchanged entries are not shown).

Table 4: Voltage buffer specification

Specification	Basic OTA	5T- OTA	Improved OTA	Unit
Output voltage error	< 3	< 1	< 1	%
Total output noise (rms)	< 1	< 0.6	< 0.6	mV <sub>rms</sub>
Supply current (as low as possible)	< 10	< 20	< 20	µA
Turn-on time (settled to with 1%)	< 10	< 1	< 1	µs
Externally provided bias current (nominal)	20	5	5	µA

## 12 Biasing

So far, we have pushed one unresolved issue in front of us. We have studied ways to multiply and scale bias currents using current mirrors (see Section 6) and we have also found ways to buffer (and scale) bias voltages (see Section 8.1, scaling can be readily achieved by using a resistive divider in the feedback path). We can generate bias voltages by running a current through a resistor. However, what has not been discussed so far is **how to generate one stable bias current in the first place**.

If we would have a stable reference voltage, then we can use the arrangement shown in Figure 98 to generate a bias current that is given by (note the use of feedback using an error amplifier which could be a simple OTA)

$$I_{\text{bias}} = \frac{V_{\text{ref}}}{R_1}.$$

Using  $A_1$  and  $M_1$  the voltage  $V_{\text{ref}}$  is regulated across  $R_1$  and available at the drain of  $M_1$ .

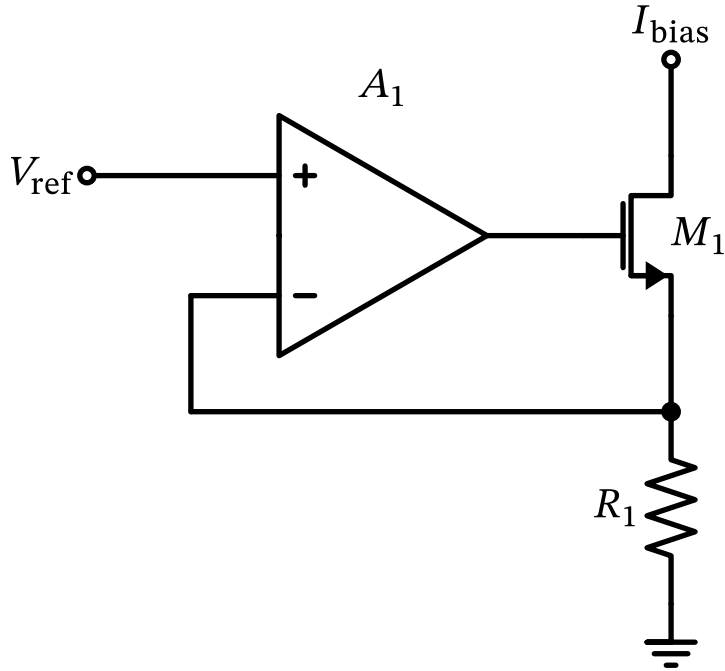


Figure 98: A constant-current generator based on OTA.

The resistor  $R_1$  will show variation with the process tolerance, but we can either (a) use an external resistor for a precise current generation, or (b) use some sort of trimming to correct this resistor value. Depending on the further use of the bias currents a variation of the resistor might no be a bad thing. Assuming we use the resulting bias current to generate somewhere a bias voltage  $V_{\text{bias}}$  by running the current through resistor  $R_2$ , then this voltage is given by

$$V_{\text{bias}} = R_2 I_{\text{bias}} = \frac{R_2}{R_1} V_{\text{ref}}.$$

We can see in the above equation that the absolute values of  $R_1$  and  $R_2$  do not play a role, only the *ratio* is important. Luckily, components in integrated circuits match very well, so we can multiply and scale one reference voltage  $V_{\text{ref}}$  across our IC.

Since all components on chip will experience manufacturing tolerances of at least  $\pm 10\%$  we strive for something more accurate. We can resort to an off-chip property like an externally provided reference current or voltage, or use the power supply as a voltage reference (often, power supply rails are specified to  $\pm 5\ldots 10\%$ ).

The only option left is to use a material property of the silicon itself for stable reference voltage generation.

## 12.1 Bandgap Reference

It has been realized that a bipolar junction transistor (BJT) has the wonderful property, that the base-emitter voltage  $V_{\text{BE}}$  has the following approximate relationship vs. temperature [29]

$$V_{\text{BE}} \approx V_{\text{g0}} \left( 1 - \frac{T}{T_0} \right) + V_{\text{BE0}} \left( \frac{T}{T_0} \right) \quad (44)$$

where  $V_{g0} = 1.205$  V is the bandgap voltage of silicon at 0 K and  $V_{BE0}$  is the base-emitter voltage of a BJT as reference temperature  $T_0$ . Further, the difference in  $V_{BE}$  of two BJT operated at different emitter current densities  $J_1$  and  $J_2$  is given as

$$\Delta V_{BE} = \frac{kT}{q} \ln\left(\frac{J_1}{J_2}\right) \quad (45)$$

with  $k$  the Boltzmann constant, and  $q$  the elementary charge.

Adding Equation 44 and Equation 45 results in a reference voltage of value

$$V_{ref} = V_{g0} \left(1 - \frac{T}{T_0}\right) + V_{BE0} \left(\frac{T}{T_0}\right) + \frac{kT}{q} \ln\left(\frac{J_1}{J_2}\right) \quad (46)$$

which can be made temperature-insensitive when the terms, which are a function of  $T$ , cancel each other, and only

$$V_{ref} = V_{g0} \quad (47)$$

remains. We thus have created an on-chip reference (called the *bandgap voltage reference*) which is almost independent of manufacturing tolerances with a very small temperature coefficient. Of course, this is only true neglecting second-order effects, but nevertheless, reference accuracies of  $\pm 1\ldots 3\%$  without trimming are perfectly possible.

The original implementation in [29] uses NPN transistors. The question is, where do we find BJT in a CMOS process? Luckily, when looking at the typical implementations, we find that there is a layer sandwich of P-N-P available. While the PNPs constructed parasitically out of this available layers are available for free without extra processing cost, they are very slow, show unusually small  $\beta < 10$ , and the collector is tied to  $V_{SS}$  as it is the substrate. Still, for bandgap references, they are very useful.

A simple implementation of a bandgap reference circuit is shown in Figure 99. If we scale  $R_1$  and  $R_2$  correctly then we can achieve Equation 47. Note that the output voltage is ca. 1.2 V, so operating this circuit on low supply voltages will be problematic.

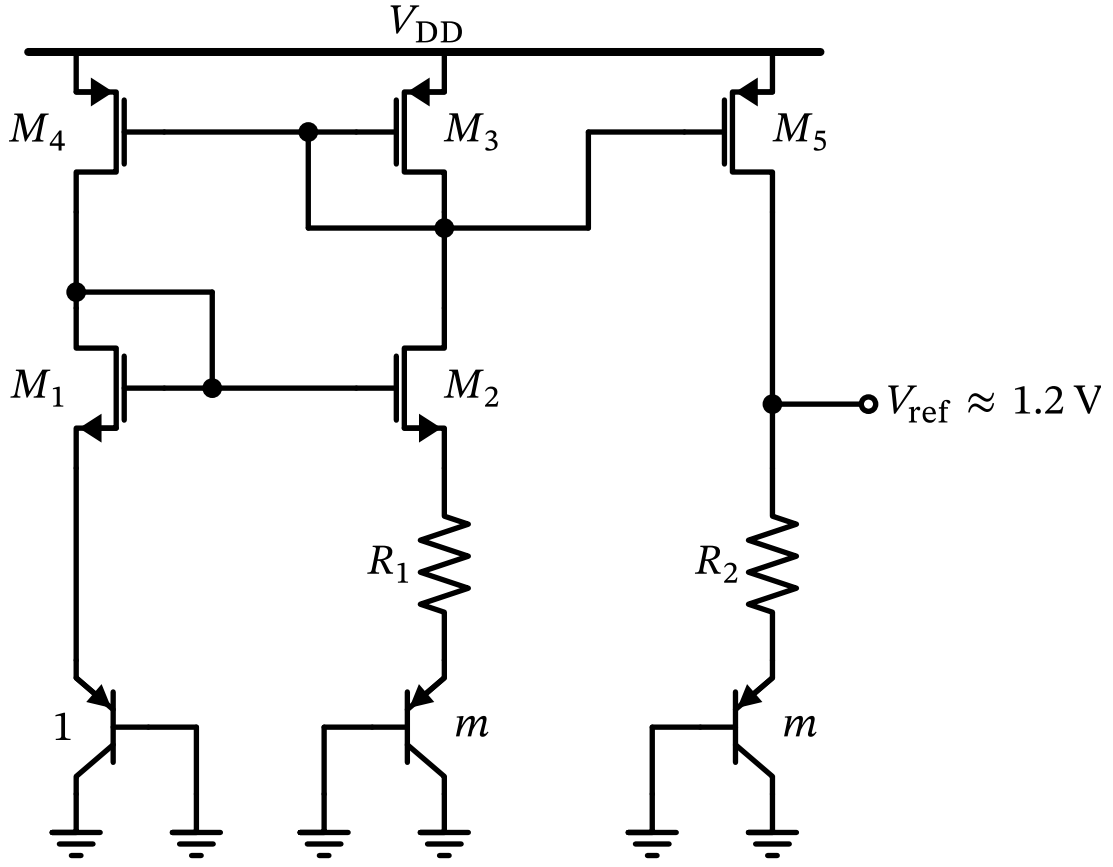


Figure 99: A simple bandgap reference.

$M_1$  to  $M_4$  are scaled in a way that in both branches the same bias current is flowing. Further,  $M_1$  and  $M_2$  ensure that there is the same potential at their sources. Since the PNP are scaled by the factor  $n$  (thus the current density is different) so that the following voltage develops across  $R_1$ :

$$\Delta V_{\text{BE}} = \frac{kT}{q} \ln m$$

Hence, the bias current in all the branches is given by

$$I_{\text{bias}} = \frac{\Delta V_{\text{BE}}}{R_1} = \frac{1}{R_1} \frac{kT}{q} \ln m. \quad (48)$$

Inspecting Equation 48 we see that  $I_{\text{bias}} = k_1 T$  is a linear function of temperature  $T$ , a property that is very useful and called **PTAT** (proportional to absolute temperature). With  $M_5$  we mirror this bias current into the output branch, and the output voltage  $V_{\text{ref}}$  is then given by

$$V_{\text{ref}} = V_{\text{BE}} + \frac{R_2}{R_1} \frac{kT}{q} \ln m.$$

By proper selection of  $R_1$ ,  $R_2$  and  $m$  we can satisfy Equation 46 to result in Equation 47.

### Improved Bandgap Reference

For an improved implementation of Figure 99, the current mirrors should be cascoded, and a startup circuit should be included to guarantee proper operation after enabling it. Further, Equation 44 and Equation 45 build on the relationship  $I_C = f(V_{BE})$ , while we control  $I_E$  in this circuit. If  $\beta$  is large then  $I_C \approx I_E$ , but this is not the case for the used PNPs.

Many more different bandgap architectures exist, with the Kuijk [30] or the Brokaw [31] types being popular choices.

The circuit of Figure 99 has been implemented in Xschem and is shown in Figure 100. The current sources have been improved by using cascodes. We are using the low-voltage current mirror type already introduced in Section 11. The bias voltages for the cascodes are generated via the voltage drops of  $R_3$  and  $R_4$ , respectively.

No base current compensation for the BJTs is implemented, as it is assumed that the  $\beta$  of the PNP are similar although they are operated at different emitter current densities.

Note the addition of a startup branch with  $M_{\text{startup}}$  which is inactive during normal operation but will inject a startup current if no proper bias point has yet been found.

There is no circuitry added for enabling/disabling the circuit, which would also be needed for a practical implementation. As usual, the MOSFET sizing has been done in this notebook.

The resistors  $R_{1-4}$  have been implemented out of unit elements of ca.  $5\text{ k}\Omega$  for optimum matching. Building a bandgap for the first time on silicon likely will show a slightly deviating temperature coefficient, which is why we keep a few dummy resistors around in  $R_2$  to compensate the TC in a redesign.

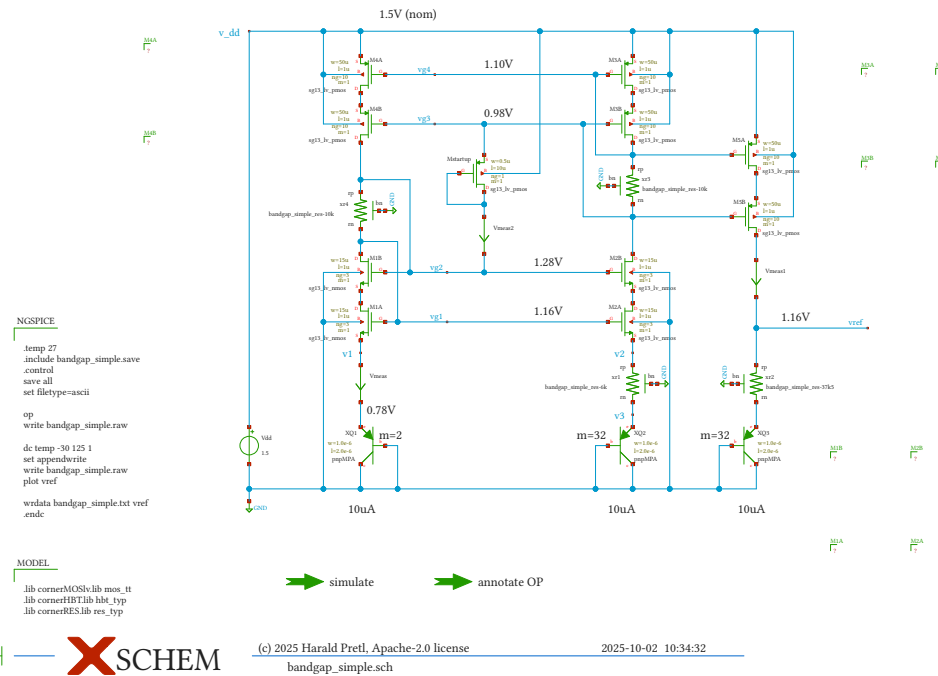


Figure 100: Simple bandgap reference circuit in Xschem.

The Xschem schematic is available [here](#) and the simulated reference voltage vs. temperature is shown in Figure 101. For a typical process we achieve a TC of  $\pm 0.2\%$ .

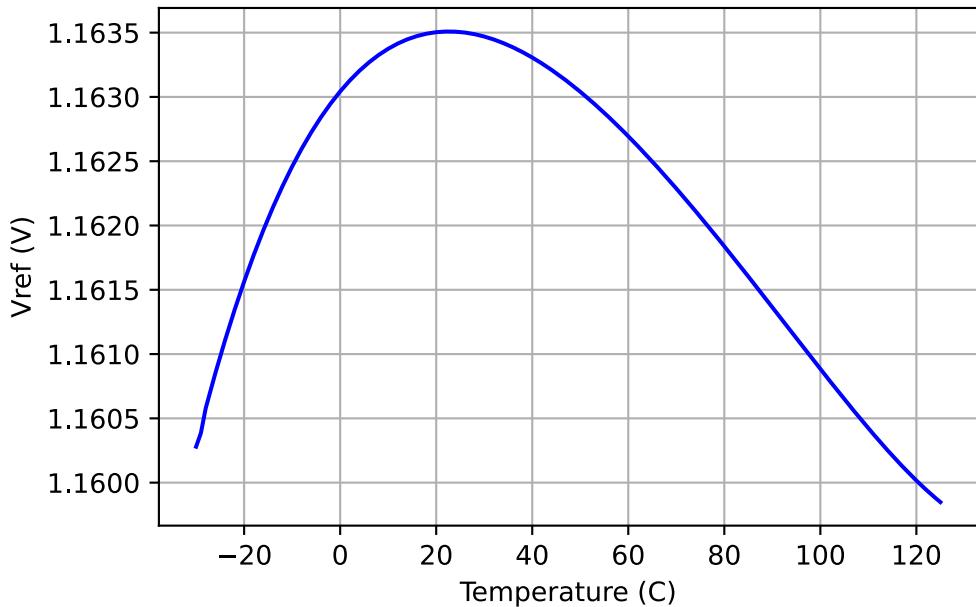


Figure 101: Reference voltage from simulated bandgap circuit.

Please note how tight the dc operating point is in this design to keep all MOSFET saturated. We only use 100 mV nominally as headroom. The circuit in Figure 100 works only marginally at  $V_{DD} = 1.5$  V, but would not work at 1.2 V or lower. Improved circuit architectures for < 1 V operation exist; see [32] or [33].

## 12.2 Banba Bandgap Reference

The Banba reference [32] is quite a bit trickier to design than the classical bandgap shown in Figure 99. It requires the use of an error amplifier; luckily, we can use the 5T-OTA which we designed in Section 8. Since a loop is involved the startup of this circuit is not easy and requires the use of a transient simulation and a proper pre-charge of critical nodes. We can use the ngspice scripting language to (a) set the temperature for a sweep, (b) run a transient simulation, and (c) capture the final reference voltage and save it.

A first design has been implemented and is shown in Figure 102, and the testbench is shown in Figure 103. The supply voltage (which could be lower than 1.5 V) is limited by our OTA design; however, it works well at  $V_{DD} = 1.5$  V. The simulated reference voltage (which is scaled to roughly  $V_{bandgap}/2$ ) is shown in Figure 104.

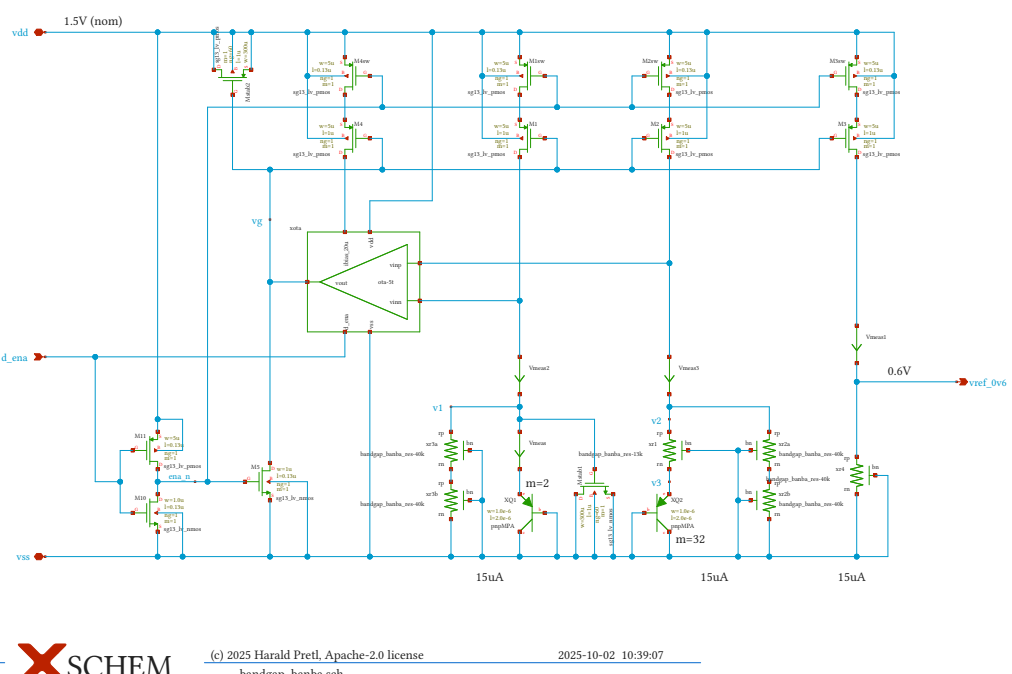


Figure 102: Banba bandgap reference circuit in Xschem.

Note the self-biasing of the OTA with the current generated in the reference branches. The feedback loop needs capacitors for stabilization, and we use area-efficient MOSFET for this task. For a detailed explanation of this circuit please refer to [32], but in brief, the operation is as follows:

The CTAT and PTAT currents required for compensating each others TC's are built using a  $\Delta V_{BE}$  cell (given the PTAT current) with parallel resistors (providing the CTAT current). Voltages are sensed using an error amplifier and current sources are controlled to achieve matching currents in both branches. This current can then also be mirrored to flow through another resistor which can be scaled to produce the output voltage.

In comparison to the classical bandgap reference shown in Figure 99 (where the developed currents in all branches are PTAT) the currents developed in the Banba reference are constant vs. temperature.

The minimum supply voltage for the Banba reference is the  $V_{BE}$  of the PNP plus the saturation voltage of one MOSFET current source, so ca.  $V_{DD\min} \geq 0.8\text{ V} + 0.2\text{ V} \approx 1\text{ V}$ . Of course we also need to design an OTA which can work at this low supply.

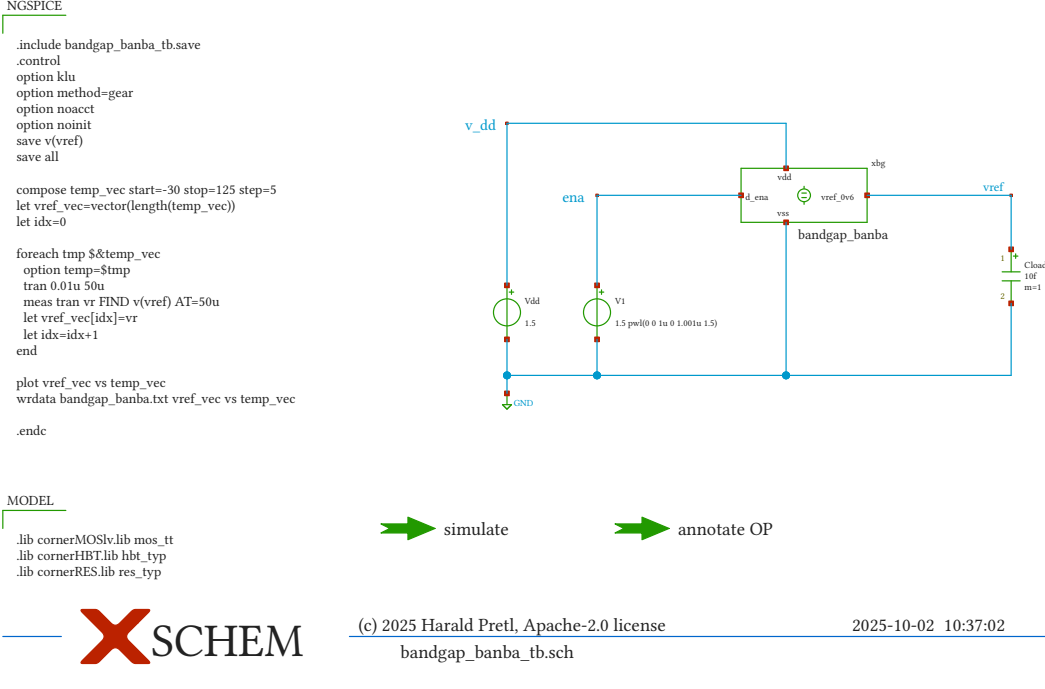


Figure 103: Banba bandgap testbench Xschem.

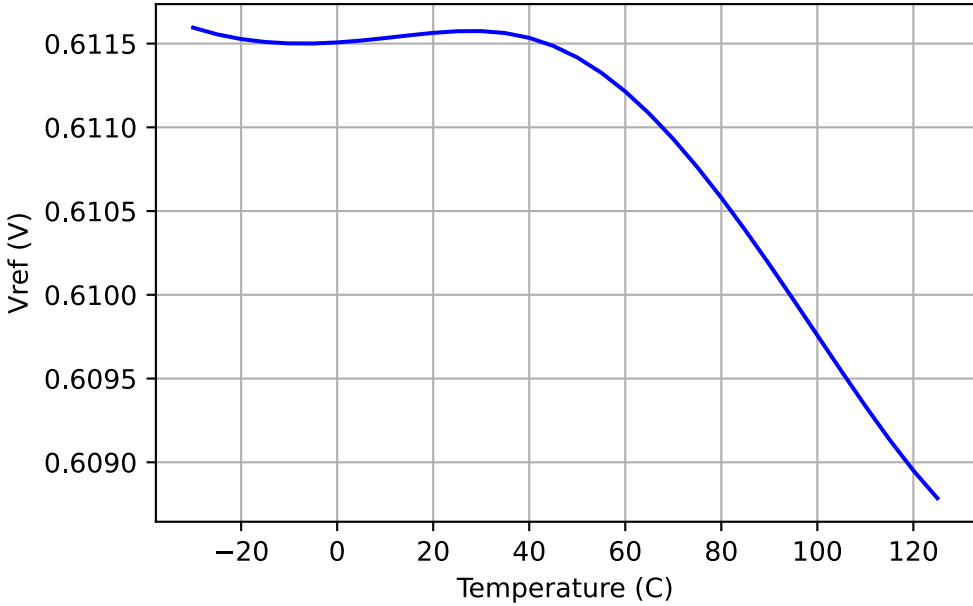


Figure 104: Reference voltage from simulated Banba bandgap circuit.

A well described design of a Banba bandgap reference (including a two-stage OTA and a regulated cascode for the output current mirror), covering much more details than discussed here, can be found in [34].

 Exercise: Improved Low-Voltage Bandgap

As an *optional* exercise for advanced users: Design a bandgap circuit following [Razavi\_2021\_bandgap]. Implement the shown two-stage OTA and the regulated cascode.

As a starting point, the design of Section 12.2 can be used. As this design will contain more blocks, please build up a hierarchical design, with the OTAs designed in separate subcircuits.

## 13 Differential OTAs

So far, we have discussed the implementation of OTAs with a differential input and a single-ended output. Often, in integrated circuits, we want to implement fully differential signal chains, as this allows an almost-rail-to-rail swing around a common-mode voltage. Further, noise pickup due to limited power-supply rejection ratio (PSRR) or coupling into the differential signal routing can be suppressed by designing amplifiers with high common-mode rejection ratio (CMRR).

The OTA presented in Section 8.8 can be readily adapted for differential output. Striving for maximum utility, we are discussing a popular two-stage differential-output OTA with a special kind of load, shown in Figure 105.

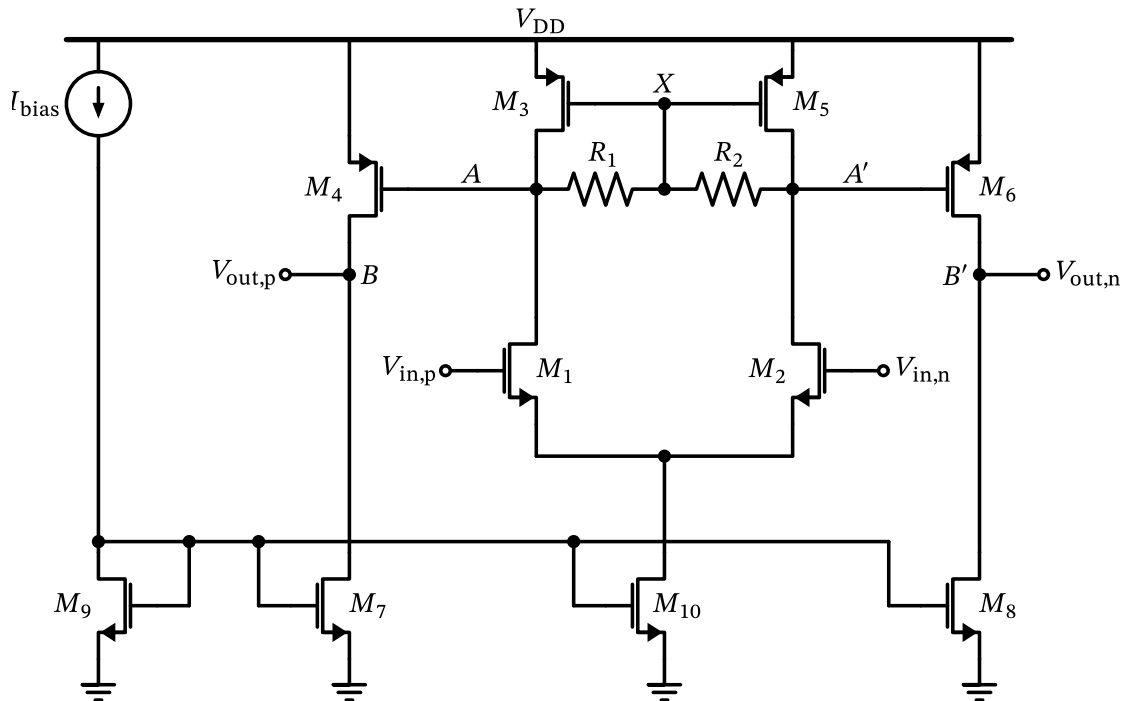


Figure 105: Differential two-stage OTA with resistive load.

This OTA shows a load on top of the differential pair that we have not yet studied. It is instructive to analyze this structure in terms of differential and common-mode operation.

For common-mode operation (i.e., injecting the same current into the drain of  $M_3$  and  $M_4$ ) we have the same voltage at the drains of  $M_{3,5}$ , thus  $V_{DS3} = V_{DS5}$ . We have thus no current flowing through  $R_{1,2}$  and as a result  $V_{DS3} = V_{DS5} = V_X = V_{GS3} = V_{GS5} = V_{GS3,5}$ . We realize

that  $M_3$  and  $M_5$  are diode-connected for common-mode operation. We thus have well-defined dc operating points, and also low common-mode gain, since the common-mode load is  $g_{m3}^{-1} \parallel g_{m5}^{-1}$ .

For pure differential operation, the mid-point  $X$  of  $R_{1,2}$  acts as a virtual ground. The bias voltage  $V_{GS3,5}$  is thus not changed (it is set only by the common-mode operation) and thus  $M_3$  and  $M_5$  operate as current sources. The differential load impedance is high and is given by  $R_{load} = (R_1 + R_2) \parallel (g_{ds3}^{-1} + g_{ds5}^{-1})$ .

In addition, we realize that  $V_{GS4} = V_{GS3} = V_{GS5} = V_{GS6}$  for common-mode operation, hence the quiescent current of  $M_{4,6}$  is set in a current-mirror-like fashion by the diode-connected  $M_{3,5}$ .

For differential operation, the differential pair of  $M_{1,2}$  is loaded by  $R_{load}$  and provides fairly high gain. The second gain stage is formed by current-source-loaded common-source stages  $M_{4,6}$  and provides additional gain (of course, this is a function of the load impedance).

As soon as we implement a two-stage amplifier we need to look into stability. We likely have more than two poles, and in the case of the amplifier in Figure 105 we have a low-frequency pole at the drains of  $M_{1,3}$  and  $M_{2,5}$  and a further low-frequency pole at the output. Any additional pole will add further phase shift making stability critical. We now need a method to stabilize this amplifier and thus we will look into *Miller compensation*.

Of course, loop gain analysis of differential OTAs can and should be carried out. An exemplary testbench where the loop gain is simulated with Rosenstark's, Middlebrook's, and Tian's method can be found [here](#). Note that there is no underlying circuit right now and it should only show how it could be done.

### 13.1 Miller Compensation

A popular way to stabilize a multi-pole feedback-system is to make one pole dominant, and try to shift the other poles to sufficiently high frequencies, that we have enough phase margin in the closed-loop system. We may strive for  $60^\circ$  as this will only cause a minor peaking in the frequency response [1].

The question now is where to implement this dominant pole. In order to create a low-frequency pole we need a high-impedance point and a large capacitance. Placing just a large capacitor is unwelcome, as this causes large area consumption on chip.

Luckily, we know from the analysis in Section 17.1 that we can use voltage gain to increase the apparent value of a capacitor by feedback. Inspecting our circuit in Figure 105 we see that we have voltage gain from node  $A$  to node  $B$  and node  $A'$  and  $B'$ , respectively. This means we have an opportunity to strap a capacitor between those nodes, and create a dominant pole at node  $A$  (and  $A'$ ).

We can now add these so-called “Miller capacitors” to our circuit. The result is shown in Figure 106. (We have also added resistors in series with the capacitors; we ignore these resistors for the time being).

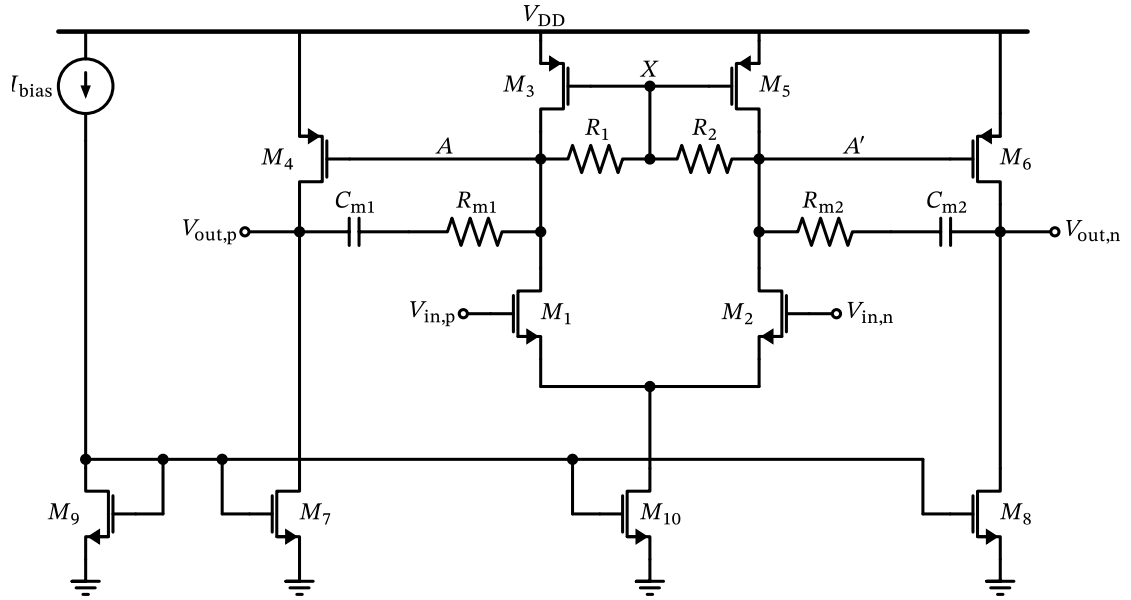


Figure 106: Differential two-stage OTA with resistive load and Miller compensation.

It is instructive to look at the small-signal equivalent circuit of the common-source stage  $M_4$  loaded by current-source  $M_7$ . The resulting model is shown in Figure 107 (we are ignoring the bulk effect of  $M_4$ , and lump components of  $M_{4,7}$  into the input and the output impedances formed by  $C_L$ ,  $C_{in}$ ,  $g_{in}$  and  $g_{out}$ ).

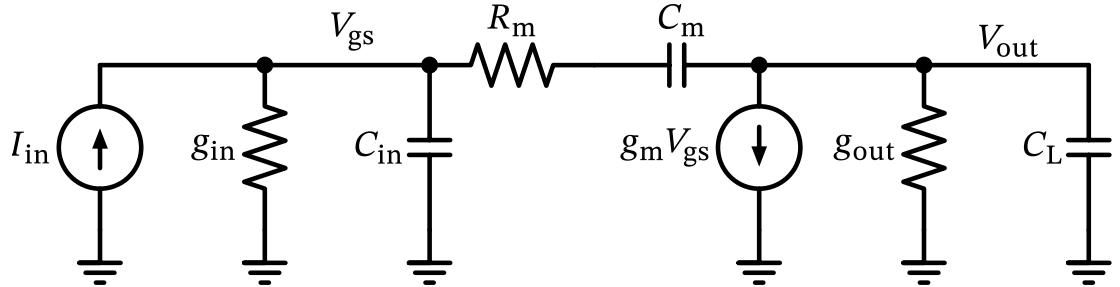


Figure 107: Small-signal model of common-source stage with Miller compensation.

In order to analyze the transfer function and thus the poles and zeros of this configuration we formulate KCL at the input and output node and the current through  $C_m$  (we set  $R_m = 0$  for now):

$$I_{in} + I_m - V_{gs}(sC_{in} + g_{in}) = 0 \quad (49)$$

$$-I_m - g_m V_{gs} - V_{out}(sC_L + g_{out}) = 0 \quad (50)$$

$$I_m = sC_m(V_{out} - V_{gs}) \quad (51)$$

Using Equation 51 in Equation 49 and Equation 50 and then calculating the transfer function we arrive at

$$\frac{V_{out}}{I_{in}} = \frac{sC_m - g_m}{(sC_m + sC_L + g_{out})(sC_m + sC_{in} + g_{in}) - (sC_m - g_m)sC_m}. \quad (52)$$

In order to check Equation 52 we can set  $sC_m = 0$  and see whether we can interpret the result:

$$\frac{V_{\text{out}}}{I_{\text{in}}} = -\frac{g_m}{(sC_L + g_{\text{out}})(sC_{\text{in}} + g_{\text{in}})} = -\frac{g_m}{g_{\text{out}}g_{\text{in}}} \frac{1}{1 + \frac{sC_L}{g_{\text{out}}}} \frac{1}{1 + \frac{sC_{\text{in}}}{g_{\text{in}}}} \quad (53)$$

We find that Equation 53 looks reasonable, as we have the correct dc gain of  $-g_m/(g_{\text{out}}g_{\text{in}})$  and two poles, one at the input and one at the output.

We now return to the more interesting case of  $sC_m \neq 0$ . We use the reasonable assumption that  $g_m \gg g_{\text{in},\text{out}}$  to simplify the algebra and result in an interpretable result. After quite a few pages of algebraic manipulations (please try for yourself!) we arrive at

$$\frac{V_{\text{out}}}{I_{\text{in}}} = -\frac{g_m}{g_{\text{out}}g_{\text{in}}} \frac{\left(1 - \frac{sC_m}{g_m}\right)}{\left(1 + s\frac{C_L + C_{\text{in}} + \frac{C_{\text{in}}C_L}{C_m}}{g_m}\right)\left(1 + s\frac{C_m \frac{g_m}{g_{\text{out}}}}{g_{\text{in}}}\right)}. \quad (54)$$

Looking at Equation 54 we can identify important changes compared to Equation 53. We have the intended low-frequency pole  $s_{p1}$  at the input where the capacitor  $C_m$  is increased by the dc gain of the common-source stage  $g_m/g_{\text{out}}$ :

$$s_{p1} = -\frac{g_{\text{in}}}{C_m \frac{g_m}{g_{\text{out}}}}$$

We further have a high frequency pole  $s_{p2}$  where the pole at the output has been shifted to higher frequencies! This is a very welcome effect called *pole splitting*, and it helps to stabilize the feedback system, as the nondominant (output) pole is shifted out in frequency while the dominant (input) pole is pulled in.

$$s_{p2} = -\frac{g_m}{C_L + C_{\text{in}} + \frac{C_{\text{in}}C_L}{C_m}}$$

Together, the movement of poles  $s_{p1}$  and  $s_{p2}$  is a great deal in terms of stability. However, not all is rosy, as we have to also look at the numerator of Equation 54. Here we see that a zero  $s_z$  has been formed, unfortunately a quite bad one. Calculating its location as

$$s_z = +\frac{g_m}{C_m} \quad (55)$$

we see that it is located in the *right half-plane* of the s-domain. Such a zero leads to a rise of the magnitude of the transfer function (this is generally not a bad thing), but the phase contribution of this zero is negative. This means that we are loosing phase margin, yet we push available gain to higher frequencies; in other words, we are degrading phase- and gain-margin!

A circuit-level interpretation of this effect is that while the Miller capacitor is wanted at the input of the amplifier (i.e., the feedback path), it also allows the input signal to pass to the output (i.e., the forward path). Since in normal operation the signal is inverted and in feed-forward mode it is not we have this unwanted effect of phase shift.

Luckily, there are several techniques to break the feed-forward path while keeping the feedback path (e.g., using a source follower to drive the output side of the Miller capacitor). For

our purposes, we use a slightly simpler technique of adding a resistor in series to the Miller capacitor (see Figure 106 and Figure 107). Doing this we can modify the location of this zero, and even push it into the left-half-plane. This is excellent news for stability, as now this zero helps to improve gain- and phase-margin!

Repeating the calculation of the transfer function  $V_{\text{out}}/I_{\text{in}}$  including  $R_m$  we see that the zero location is changed and can be calculated as (the pole locations are also slightly changed due to the addition of  $R_m$ , but we will not discuss the resulting equations here)

$$s_z = \frac{g_m}{C_m(1 - g_m R_m)} \quad (56)$$

If we do not use the resistor (i.e.,  $R_m = 0$ ) then Equation 56 collapses to Equation 55. If  $g_m R_m < 1$  then the zero stays in the right half-plane; if  $g_m R_m > 1$  then the zero moves into the left half-plane (this is what we want). If  $g_m R_m = 1$  then we have compensated the zero at it moves to  $-\infty$ ; however, in practice exact compensation is not easy to establish across conditions, so we want to move the zero into the left half-plane. Adding a bit of margin want to size

$$R_m > \frac{2}{g_m}.$$

### 13.2 Common-Mode Regulation

In fully-differential (i.e., differential inputs and outputs) OTAs we have a new issue concerning common-mode voltage control: Depending on the feedback network around the OTA we might or might not have a defined dc operating point (common-mode wise). Think of the following scenario: If implement an integrator with an OTA then the feedback network from output to input consists of a capacitor. This means that the output of the OTA is loaded very high ohmic, and any small current mismatch between  $M_4/M_7$  or  $M_6/M_8$  (see Figure 106) will cause a strong deviation of the dc operating point at the output!

We can not accept that the dc operating points in a circuit are ill defined. We thus need a way to establish the dc operating point. Using the diode-resistive load for the differential pair in Figure 106 the dc operating point there is well-defined by the diode-connected  $M_{3,5}$ . However, the output stage is different, and we need to add circuitry to also control the dc operating point there.

One well-known way is to sense the common-mode voltage using two resistors (similar to  $R_{1,2}$  in Figure 106), and compare this measured common-mode voltage to a reference voltage using an error amplifier. Then the output of the error amplifier controls the common-mode voltage, e.g., by driving the gates of  $M_{7,8}$  in Figure 106.

### ! Differential and Common-Mode Loops

When using an error amplifier to regulate a common-mode point keep in mind that you need to check the differential and common-mode stability of these various loops! This can lead to tricky situations, especially under large-signal excitation where the common-mode sensing might not work as expected!

In order to get a differential circuit stable one often has to make the common-mode loop faster than the differential loops. So simple, high-speed error amplifiers are an advantage.

In summary, stability investigations are critically important for differential circuits, and never forget to check for common-mode stability as well!

Instead of a common-mode regulation loop (and all its complications regarding stability) often a common-mode setting is sufficient (after all, a somewhat imprecise setting of the dc points is good enough). A common-mode setting has the advantage that no error amplifier is required. We will also use this approach of a common-mode loop setting in the adapted differential OTA shown in Figure 108.

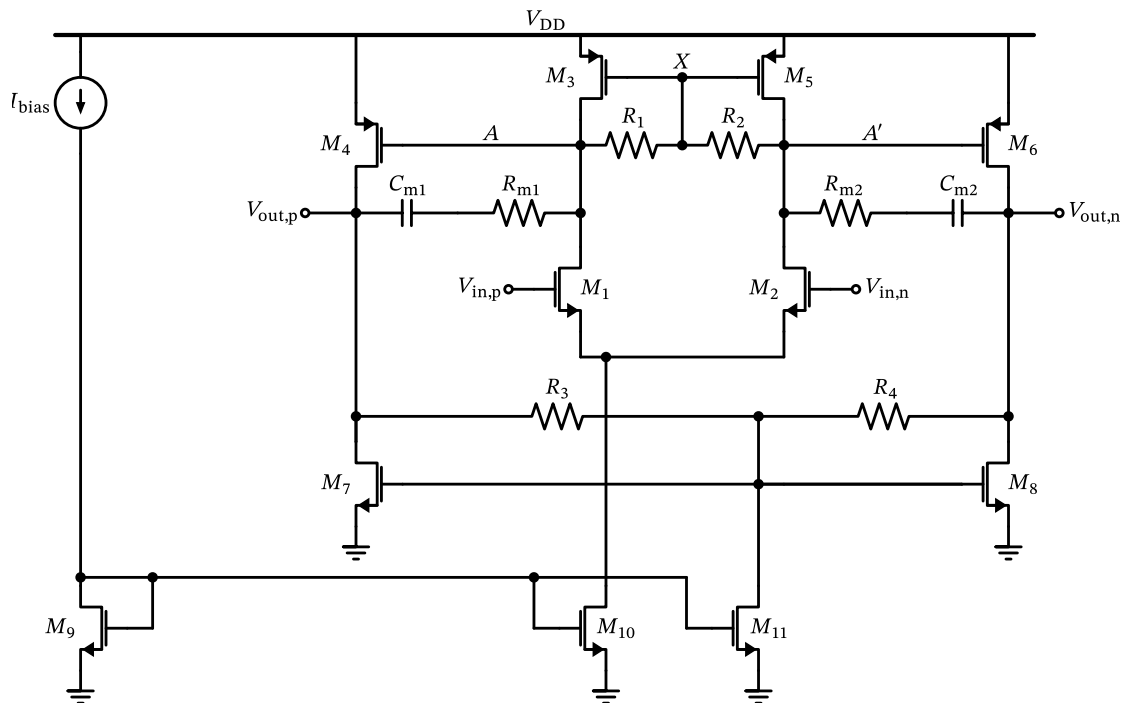


Figure 108: Differential two-stage OTA with resistive load, Miller compensation and output common-mode control.

Resistors  $R_{3,4}$  sense the output voltages and create a replica of the common-mode point (assuming  $R_3 = R_4$ ). This common-mode point is connected to the gates of  $M_{7,8}$  to essentially connect  $M_{7,8}$  like a diode (only for common-mode operation); in differential mode,  $M_7$  and  $M_8$  act as current source, like the load of the differential pair  $M_{3,5}$ . However, since we want to set the common-mode voltage at the output independently from  $V_{GS7,8}$  we also pull a current through  $R_{3,4}$  to cause  $V_{DS7,8} \neq V_{GS7,8}$ ; essentially, this is a diode connection including a voltage shift! The output common-mode voltage is then given by

$$V_{\text{out,cm}} = V_{\text{GS7,8}} + \frac{R_{3,4}I_{\text{D11}}}{2}.$$

We can realize the advantage of using the resistor/MOSFET load in the input as well as the output stage when we calculate the common-mode gain of the OTA. We realize that we can use half-circuits due to the inherent symmetry of the circuit in Figure 105. The gain of the first stage (the MOSFET-diode loaded differential pair  $M_{1,2}$ ) is given by (using Equation 13)

$$A_{\text{cm},1} \approx -\frac{1}{g_{\text{m3,5}}} \frac{g_{\text{m1,2}}g_{\text{ds10}}}{g_{\text{m1,2}} + g_{\text{ds10}}} \approx -\frac{g_{\text{ds10}}}{g_{\text{m3,5}}}. \quad (57)$$

The common-mode gain of the second stage is similarly given by

$$A_{\text{cm},2} \approx -\frac{g_{\text{m4,6}}}{g_{\text{m7,8}}}. \quad (58)$$

Combining Equation 57 and Equation 58 we arrive at (assuming that  $g_{\text{m3,5}} = g_{\text{m4,6}}$ )

$$A_{\text{cm}} = A_{\text{cm},1}A_{\text{cm},2} = \frac{g_{\text{ds10}}}{g_{\text{m7,8}}} \quad (59)$$

which is a low common-mode gain with very likely  $A_{\text{cm}} < 1$ , which is very good news for the common-mode stability!

Likewise, we can compute the differential gain of the OTA by formulating the voltage gain of the first stage as

$$A_{\text{d},1} \approx \frac{g_{\text{m1,2}}}{R_{1,2}^{-1} + g_{\text{ds3,5}} + g_{\text{ds1,2}}} \quad (60)$$

and the differential voltage gain of the second stage as

$$A_{\text{d},2} = \frac{g_{\text{m4,6}}}{R_{3,4}^{-1} + g_{\text{ds7,8}} + g_{\text{ds4,6}}}. \quad (61)$$

Combining Equation 60 and Equation 58 we arrive at the total differential voltage gain (of an **unloaded** OTA) of

$$A_{\text{d}} = A_{\text{d},1}A_{\text{d},2} = \frac{g_{\text{m1,2}}g_{\text{m4,6}}}{(R_{1,2}^{-1} + g_{\text{ds3,5}} + g_{\text{ds1,2}})(R_{3,4}^{-1} + g_{\text{ds7,8}} + g_{\text{ds4,6}})} \quad (62)$$

which can lead to significant differential voltage gain, ultimately limited by the  $g_{\text{ds}}$  of the MOSFETs  $M_{1-8}$ .

### Modify Bias Points with Currents

Keep the technique shown in Figure 108 (using  $R_{3,4}$  and  $M_{11}$ ) in mind: You can always modify a bias point by injecting a dc current into a node, or by pulling a dc current out of a node (or do both to increase or lower the quiescent current through a resistor or transistor)! Since we likely have already current mirrors in the circuit it is usually a minor effort adding MOSFETs to create these bias currents.

### 13.3 Final Differential OTA

When designing the OTA with the above mentioned techniques like Miller compensation and the common-mode setting we find that we have issues with common-mode stability. There is one issue not obvious on first sight with the MOSFET-R load of the first stage: At the node  $X$  there is significant capacitance due to the gates of  $M_{3,5}$ . This capacitance forms a lowpass response with the resistance of  $R_{1,2}$  and thus creates a low-frequency pole. This pole is in the common-mode path, and leads to a zero for the common-mode gain.

In other words: At low frequencies the common-mode gain is given by Equation 59, but at higher frequencies (above the pole at node  $X$ ) the common-mode gain increases significantly as the load resistance of the first stage increases from  $g_{m3}^{-1} \parallel g_{m5}^{-1}$  to  $g_{ds3}^{-1} \parallel g_{ds5}^{-1}$ . We need to counteract this effect by adding a capacitor in parallel to  $R_{1,2}$ , as shown in Figure 109. We use the opportunity to also add a series resistor to this capacitor to introduce an additional zero to improve phase margin.

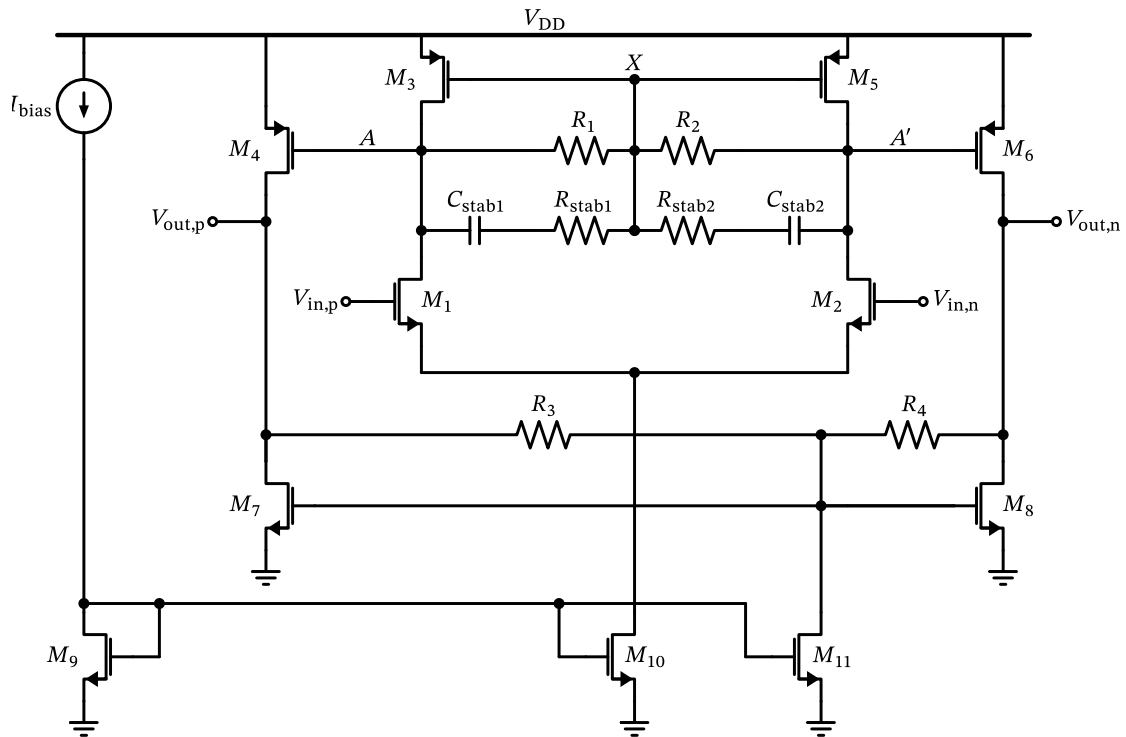


Figure 109: Differential two-stage OTA with adapted MOSFET-R load of first stage and output common-mode control by MOSFET-R load in second stage.

You can find the sizing script for the differential OTA here, as well as the circuit-level design in Xschem here. The testbench for differential and common-mode gain analysis can be found here.

The final Xschem schematics of the differential OTA and the testbench are also shown in the figures below.

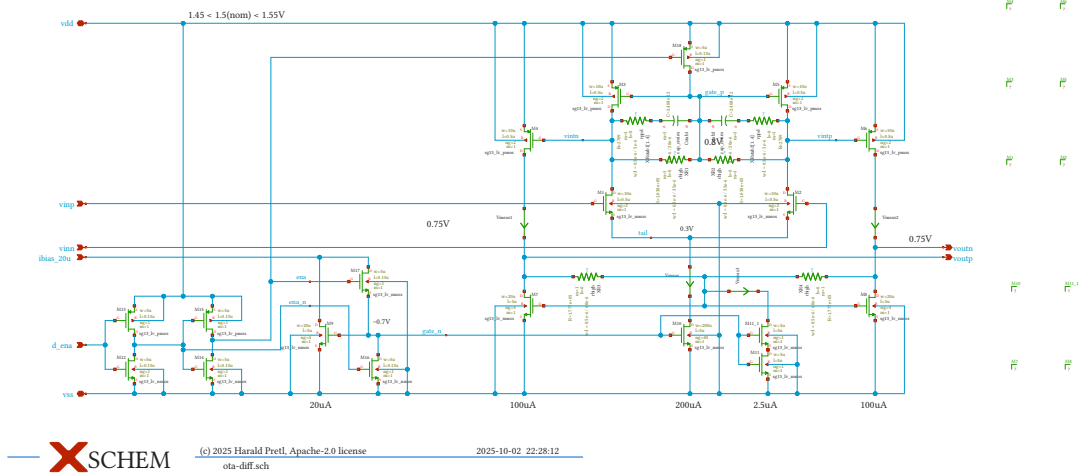


Figure 110: Differential OTA design in Xschem.

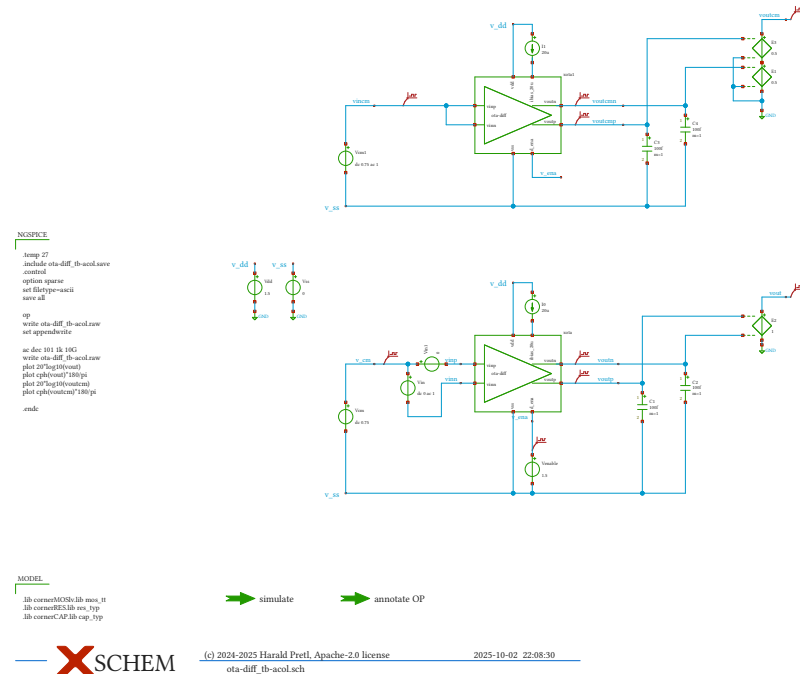


Figure 111: Simulation testbench of the differential OTA design (DM and CM gain analysis).

As you can see when you run the simulation, the differential OTA is stable for differential and common-mode gain. However, the stabilization measures resulted in a GBW which falls considerably short of the target value of 1 GHz. Here we would need to start another round of optimization, either giving up some stability margin, or increasing the power dissipation, or using a more advanced topology.

### 13.4 Differential OTA Variants

For inspiration we want to discuss two further variants of the differential OTA. The first one is shown in Figure 112 and is a telescopic OTA. The telescopic OTA is a single-stage OTA and is the differential version of the single-ended OTA shown in Figure 75. It shares its advantages and disadvantages: Stability is often not an issue (because it is single-stage), and the current consumption is low, as there is only one main current branch. The biggest disadvantage is the limited output swing, as we have to stack six MOSFETs on top of each other. Accounting for a minimum headroom per transistor of about 0.1 V, we require at least 0.6V, likely more in practice. This might be an issue in low-voltage designs.

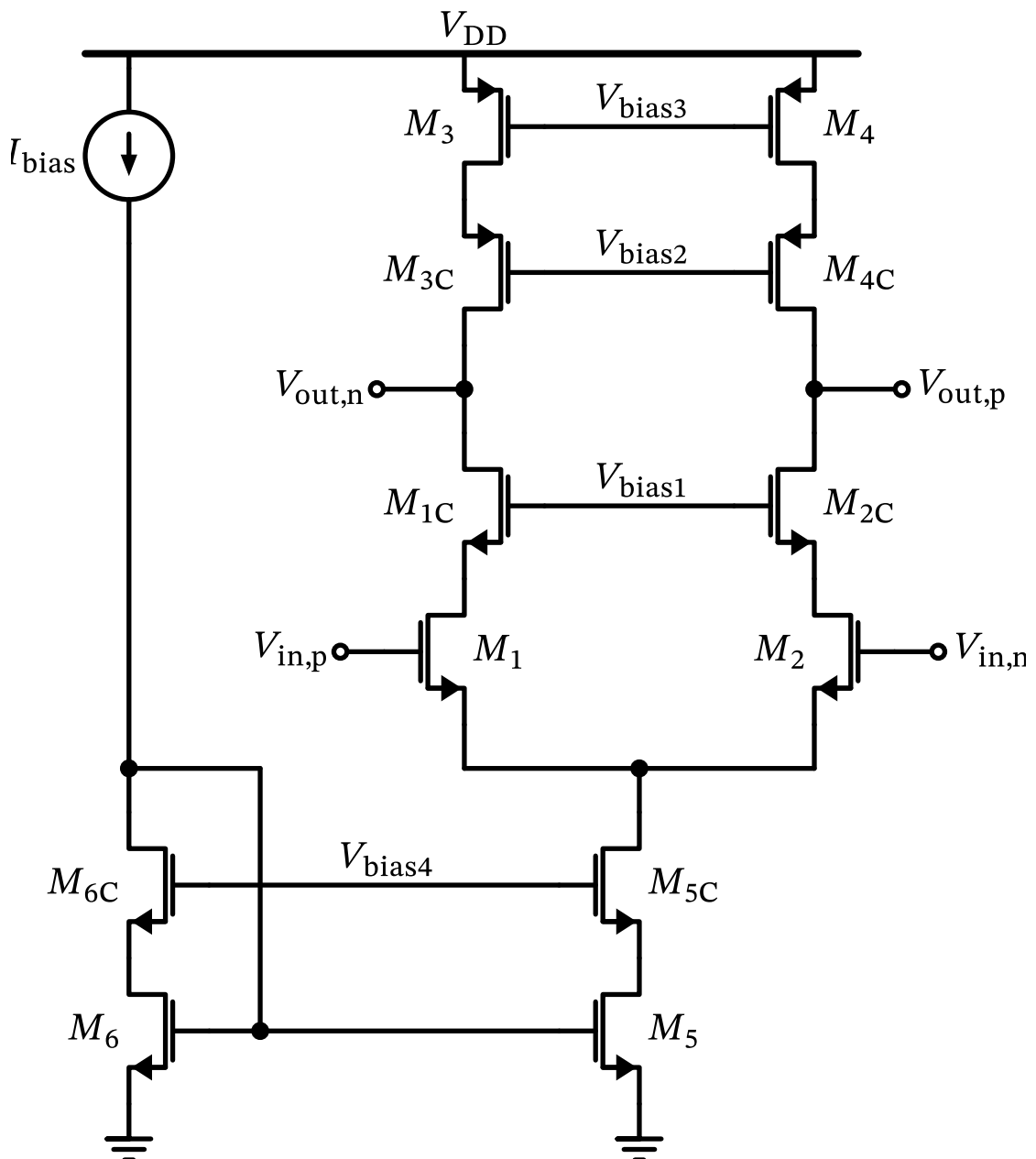


Figure 112: The telescopic differential OTA (output common-mode regulation and biasing details are not shown).

Another very popular single-stage differential OTA is the so-called *folded-cascode OTA*, shown in Figure 113. The folded-cascode OTA has a larger output swing than the telescopic OTA, as we only need to stack four MOSFETs on top of each other. However, the current consumption is higher, as we have three current branches (one for the input pair, and two for the differential cascode stage). The folded-cascode OTA is a very popular choice for high-gain, moderate-speed OTAs.

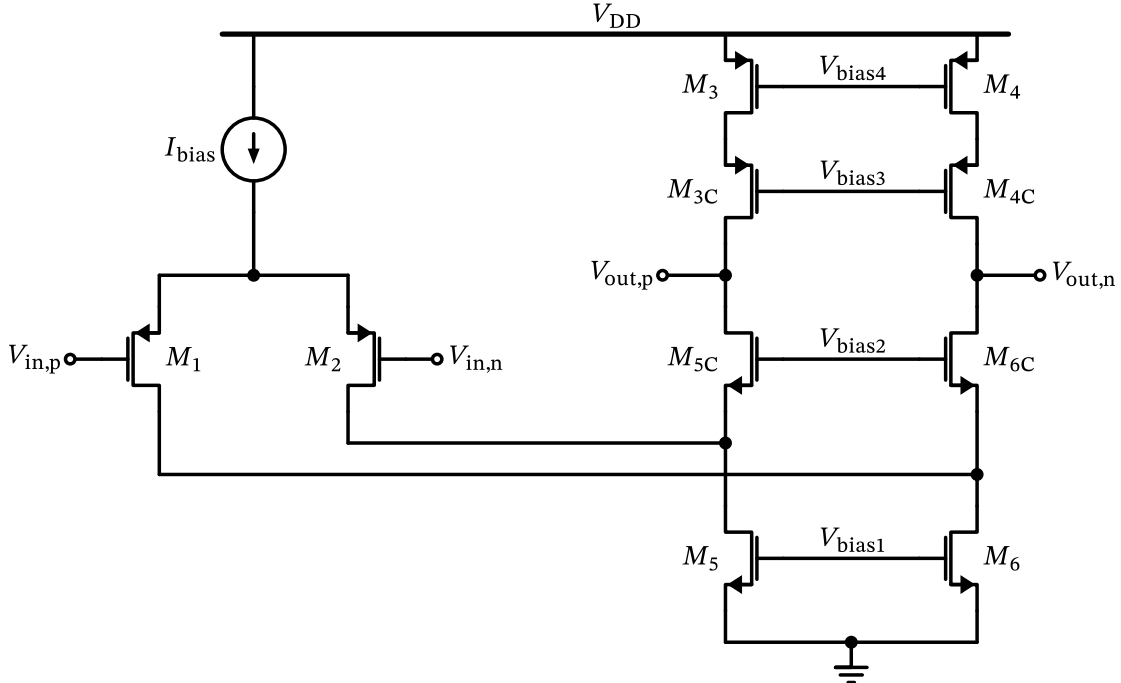


Figure 113: The folded-cascode differential OTA (output common-mode regulation and biasing details are not shown).

Note that the folded-cascode OTA has a large common-mode range at the input. In case of the shown PMOS input differential pair, the input common-mode voltage can be as low as  $V_{SS}$ . If an NMOS input stage is used, the input common-mode voltage can be as high as  $V_{DD}$ . For a rail-to-rail input stage, a combination of NMOS and PMOS input pairs can be used. Note that the bias current of the input pair needs a suitable control so that the effective input stage  $g_m$  is fairly constant over the full input common-mode range.

Note that both the telescopic OTA and the folded-cascode OTA have to be equipped with common-mode setting or regulation loops, otherwise the output common-mode voltage might be ill-defined and might drift up or down depending on bias current mismatch.

## 14 An RC-OPAMP Filter

To be added in a future release.

## 15 Summary & Conclusion

By now, you should be familiar with the use of a schematic entry tool (Xschem) and circuit simulator (ngspice). You have learned the basic performance trade-offs, and the large- and small-signal behavior of the MOSFET. You can use the  $g_m/I_D$  method to size MOSFET for

class-A operation. You can design simple amplifiers based on OTA structures. In summary, you are on a good way to become a good analog or mixed-signal circuit designer!

### ! Feedback

We hope you have enjoyed these lecture notes! If you have feedback, suggestions, additions, or corrections, please send us an e-mail, create a GitHub issue, or provide a GitHub pull request. Thank you in advance for your contributions!

### i Further Reading

For interested circuit designers, Chapter 5 of [10] is recommended as a further read. It explains additional circuits, such as the beta-multiplier reference, an OTA with a telescopic input stage, and a push-pull output stage, designs them with the  $g_m/I_D$  methodology, and simulates them in Xschem and with CACE. Hence, the design flow is the same as proposed in this course.

## 16 Appendix: Middlebrook's Method

If we want to do a closed-loop gain analysis (for stability or other investigations), we have the need to break the loop at one point, apply a stimulus, and monitor the response on the other end. By doing this we want to keep the loading (i.e. the impedance) on both ends similar to the original case. To achieve this, we break the loop at one point by inserting (1) an ac voltage source, and (2) attach an ac current source, as shown in Figure 114 and Figure 115. The derivation of this approach is presented in [15], and has the big advantage that loading is not changed compared to the closed-loop situation, and the bias points are also unchanged.

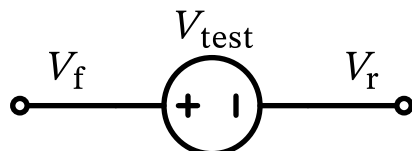


Figure 114: Middlebrook voltage loop simulation.

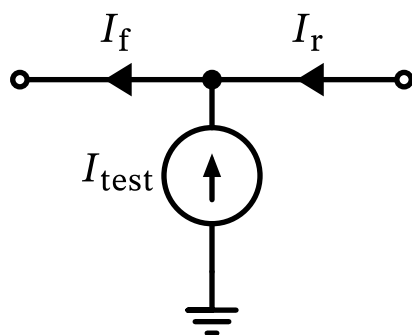


Figure 115: Middlebrook current loop simulation.

For both cases we do an ac analysis, and find the corresponding transfer functions  $T_v$  and  $T_i$  as

$$T_v = -\frac{V_r}{V_f}$$

and

$$T_i = -\frac{I_r}{I_f}.$$

Then, we can calculate the open-loop transfer function  $T(s) = H_{ol(s)}$  as

$$T(s) = \frac{T_v T_i - 1}{T_v + T_i + 2} = \frac{V_r I_r - V_f I_f}{2V_f I_f - V_r I_f - V_f I_r}.$$

The four ac quantities  $V_f$ ,  $V_r$ ,  $I_f$ , and  $I_r$  we can readily find by circuit simulation or calculation.

Please note that Middlebrook's method works well for  $|T| \gg 1$ , so it will show inaccuracies at the crossover frequency of the open-loop gain at  $T(s) \approx 0$ . An improved method (slightly more complicated) can be found in [16].

## 17 Appendix: Useful Circuit Theorems

### 17.1 Miller's Theorem

Using Miller's theorem we can find the equivalent circuit of an impedance connected between two nodes, if we know the transfer function between these nodes. The original situation is shown in Figure 116, and the equivalent circuit is shown in Figure 117.

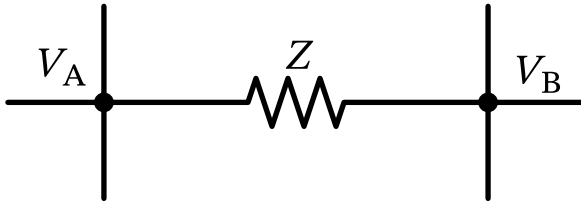


Figure 116: An impedance connected between two nodes A and B.

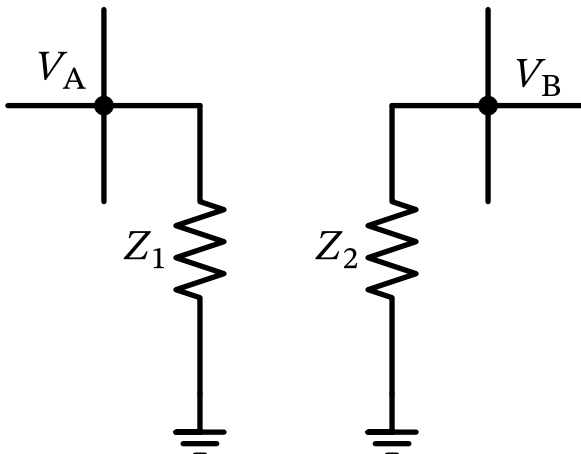


Figure 117: An equivalent circuit using Miller's theorem.

Using Miller's theorem [35] we can calculate

$$Z_1 = \frac{Z}{1 - A} = \frac{Z}{1 - V_B/V_A}$$

and

$$Z_2 = \frac{Z}{1 - A^{-1}} = \frac{Z}{1 - V_A/V_B}$$

to arrive at an equivalent circuit, given that  $A = V_B/V_A$  is the voltage gain between nodes A and B. A derivation of this theorem is relative straightforward considering the current through  $Z$  when looking into the impedance from either node A or node B and calculating an equivalent impedance causing the same current.

Note that if  $V_A = V_B$  then there is no current flow through  $Z$ , and accordingly the impedances  $Z_1 = Z_2 = \infty$ .

Miller's theorem can be quite handy when an impedance is strapped between two nodes, and we want to break this connection in a calculation, e.g., considering the effect of  $C_{GD}$  in a MOSFET.

### Miller's Secret

Note that Miller's compensation is so much more than just making a big capacitor out of a small one. There are layers upon layers of subtlety, and huge hidden benefits which can be read in [36].

## 17.2 Bode's Noise Theorem

The total integrated noise of any (no matter how complicated)  $RLC$  network (interpreted as a one-port) is given by

$$\overline{V_n^2} = kT \left( \frac{1}{C_\infty} - \frac{1}{C_0} \right),$$

where  $C_\infty$  is the capacitance looking into the network with all resistors and inductors open-circuited, and  $C_0$  is the capacitance looking into the circuit when all inductors and resistors are shorted [37].

Reference [37] is an excellent read deriving Bode's noise theorem from different angles.

## 18 Appendix: 5T-OTA Small-Signal Output Impedance

This section gives additional details to the analysis presented in Section 8.3. Here we provide the full calculation of the output impedance/conductance of the 5T-OTA for frequencies below the dominant pole, i.e., we neglect any capacitors.

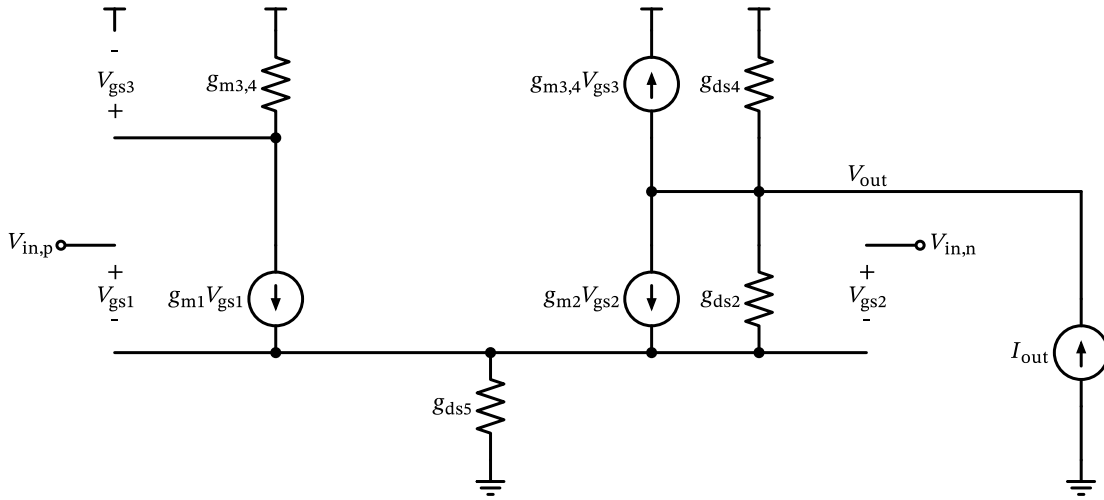


Figure 118: 5-transistor OTA small-signal model for output impedance calculations.

## 18.1 Open-Loop Configuration

For the open-loop case, the gates of  $M_1$  and  $M_2$  are tied to ground:

$$V_{\text{in},p} = V_{\text{in},n} = 0 \rightarrow V_{\text{gs}1} = V_{\text{gs}2} \quad (63)$$

KCL at the output node:

$$I_{\text{out}} - g_{\text{ds}4} V_{\text{out}} - g_{\text{m}3,4} V_{\text{gs}3} - I_{g_{\text{ds}2}} - g_{\text{m}2} V_{\text{gs}2} = 0 \quad (64)$$

KCL at the tail node:

$$g_{\text{m}1} V_{\text{gs}1} + g_{\text{m}2} V_{\text{gs}2} + I_{g_{\text{ds}2}} + g_{\text{ds}5} V_{\text{gs}2} = 0$$

Using Equation 63 we can eliminate  $V_{\text{gs}1}$  and solve for  $I_{g_{\text{ds}2}}$ .

$$I_{g_{\text{ds}2}} = -(g_{\text{m}1} + g_{\text{m}2} + g_{\text{ds}5}) V_{\text{gs}2} \quad (65)$$

Furthermore, we need an expression for  $V_{\text{gs}3}$ . Ohm's law at the transconductance  $g_{\text{m}3,4}$  will suffice.

$$V_{\text{gs}3} = -\frac{g_{\text{m}1}}{g_{\text{m}3,4}} V_{\text{gs}1} \quad (66)$$

KVL from the output node down to ground (traversing  $g_{\text{ds}2}$  and  $g_{\text{ds}5}$ ) in combination with Equation 65 gives us an expression for  $V_{\text{gs}2}$

$$V_{\text{gs}2} = -\frac{g_{\text{ds}2}}{g_{\text{m}1} + g_{\text{m}2} + g_{\text{ds}2} + g_{\text{ds}5}} V_{\text{out}} \quad (67)$$

Now, we can plug in all quantities into Equation 64. First, Equation 65 is inserted, which provide an expression for the current through the output conductance  $g_{\text{ds}2}$  of  $M_2$ :

$$I_{\text{out}} - g_{\text{ds}4} V_{\text{out}} - g_{\text{m}3,4} V_{\text{gs}3} + (g_{\text{m}1} + g_{\text{ds}5}) V_{\text{gs}2} = 0$$

Second,  $V_{\text{gs}3}$  is substituted by Equation 66. Since we have assumed a matched pair of transistors for the current mirror comprised of  $M_3$  and  $M_4$ ,  $g_{\text{m}3,4}$  perfectly cancels out of the equation, and is effectively replaced by the transconductance  $g_{\text{m}1}$  of the input transistor  $M_1$ :

$$I_{\text{out}} - g_{\text{ds}4}V_{\text{out}} + (2g_{\text{m}1} + g_{\text{ds}5})V_{\text{gs}2} = 0$$

Third, Equation 67 gives us an expression for the last remaining unknown  $V_{\text{gs}2}$ . Thus, the factor in front of  $V_{\text{out}}$  defines the conductance at the output node.

$$I_{\text{out}} - \left[ g_{\text{ds}4} + (2 \cdot g_{\text{m}1} + g_{\text{ds}5}) \frac{g_{\text{ds}2}}{g_{\text{m}1} + g_{\text{m}2} + g_{\text{ds}2} + g_{\text{ds}5}} \right] V_{\text{out}} = 0 \quad (68)$$

Before we interpret this result, we use the assumption of matched input transistors ( $g_{\text{m}1,2} = g_{\text{m}1} = g_{\text{m}2}$ ) and slightly rearrange the equation to give us more insight:

$$I_{\text{out}} - \left[ g_{\text{ds}4} + \frac{g_{\text{ds}2} \cdot (2 \cdot g_{\text{m}1,2} + g_{\text{ds}5})}{g_{\text{ds}2} + (2 \cdot g_{\text{m}1,2} + g_{\text{ds}5})} \right] V_{\text{out}} = 0 \quad (69)$$

Now, we can identify the common equation of the total resistance of two parallel resistors. However, we are dealing with conductances here, so the same equation describes the total conductance of two conductances in series, while parallel conductances are simply summed. In parallel to  $g_{\text{ds}4}$ , there is effectively the series connection of  $g_{\text{ds}2}$  and  $2 \cdot g_{\text{m}1,2} + g_{\text{ds}5}$  at work.

If we apply the general assumption of  $g_{\text{m}} \gg g_{\text{ds}}$ , only the parallel connection of  $g_{\text{ds}4}$  and  $g_{\text{ds}2}$  remains:

$$\frac{I_{\text{out}}}{V_{\text{out}}} \approx g_{\text{ds}4} + g_{\text{ds}2} \quad (70)$$

## 18.2 Closed-Loop Configuration

In contrast to the open-loop case, we keep the gate of  $M_1$  connected to ground and tie the input of  $M_2$  to the output node  $V_{\text{out}}$ :

$$V_{\text{in},n} = V_{\text{out}} \quad (71)$$

KCL at the output node:

$$I_{\text{out}} - g_{\text{ds}4}V_{\text{out}} - g_{\text{m}3,4}V_{\text{gs}3} - g_{\text{ds}2}V_{\text{gs}2} - g_{\text{m}2}V_{\text{gs}2} = 0 \quad (72)$$

We use KVL from the output node down to ground to find an expression for  $V_{\text{gs}2}$ :

$$V_{\text{gs}2} = V_{\text{out}} + V_{\text{gs}1} \quad (73)$$

KCL at the tail node:

$$g_{\text{m}1}V_{\text{gs}1} + g_{\text{m}2}V_{\text{gs}2} + g_{\text{ds}2}V_{\text{gs}2} + g_{\text{ds}5}V_{\text{gs}2} = 0 \quad (74)$$

Using Equation 73 to substitute  $V_{\text{gs}2}$  in Equation 74 we find an equation for  $V_{\text{gs}1}$ :

$$V_{\text{gs}1} = - \frac{g_{\text{m}2} + g_{\text{ds}2}}{g_{\text{m}1} + g_{\text{m}2} + g_{\text{ds}2} + g_{\text{ds}5}} V_{\text{out}} \quad (75)$$

Again, we derive the output conductance by plugging Equation 73, Equation 66 and Equation 75 step by step into Equation 72. First, we use Equation 73 to eliminate  $V_{\text{gs}2}$ :

$$I_{\text{out}} - (g_{\text{ds}4} + g_{\text{ds}2} + g_{\text{m}2})V_{\text{out}} - g_{\text{m}3,4}V_{\text{gs}3} - (g_{\text{ds}2} + g_{\text{m}2})V_{\text{gs}1} = 0$$

Second, Equation 66 also holds for the closed-loop case and lets us eliminate  $V_{gs3}$ :

$$I_{out} - (g_{ds4} + g_{ds2} + g_{m2})V_{out} - (g_{ds2} + g_{m2} - g_{m1})V_{gs1} = 0$$

Third, we use Equation 75 to eliminate the remaining unknown  $V_{gs1}$ :

$$\begin{aligned} I_{out} - (g_{ds4} + g_{ds2} + g_{m2})V_{out} \\ + (g_{ds2} + g_{m2} - g_{m1})\frac{g_{m2} + g_{ds2}}{g_{m1} + g_{m2} + g_{ds2} + g_{ds5}}V_{out} = 0 \end{aligned}$$

A simpler result can be obtained, if we neglect  $g_{ds2}$  and  $g_{ds5}$  in Equation 75 first ( $g_m \gg g_{ds}$ ) and then plug it into our main equation. Additionally, we use  $g_{m1,2} = g_{m1} = g_{m2}$  to further simplify the equation:

$$I_{out} - \left( g_{ds4} + \frac{3}{2}g_{ds2} + g_{m1,2} \right) V_{out} \approx 0$$

If we apply  $g_m \gg g_{ds}$  again we arrive at:

$$I_{out} - g_{m1,2}V_{out} \approx 0 \rightarrow \frac{I_{out}}{V_{out}} \approx g_{m1,2}$$

## 19 Appendix: Linux Cheatsheet

The most useful commands for the Linux command line are:

- `ls` to list files and directories
- `cd` to change directory (e.g. `cd analog-circuit-design/xschem`)
- `cd ..` to move one directory level down
- `mkdir` to create a new directory (e.g. `mkdir my_directory`)
- `touch` to create an empty file (e.g. `touch file.txt`)
- `rm` to remove files (e.g. `rm file.txt`)
- `rm -r` to remove recursively, for example a directory (e.g. `rm -r my_directory`)
- `cp` to copy files (e.g. `cp file.txt destination`)
- `cp -r` to copy recursively a directory (e.g. `cp -r directory destination`)
- `mv` to rename files (e.g. `mv file.txt new_name.txt`)
- `mv` to move files into other directories (e.g. `mv file.txt directory`)
- `cat` to view the contents of a file (e.g. `cat file.txt`)
- `find` to search for files and directories (e.g. `find /path -name "*.txt"`)
- `nano` to edit file (e.g. `nano file.txt`)
- `Ctrl + C` to forcefully terminate a running process
- `htop` to open the “task manager”

More advanced commands can be found under <https://www.geeksforgeeks.org/linux-commands-cheat-sheet>.

## 20 Appendix: Xschem Cheatsheet

When opening Xschem, using `Help -> Keys` a pop-up windows comes up with many useful shortcuts. The most useful are:

#### **20.0.0.1 Moving around in a schematic:**

- Cursor keys to move around
- Ctrl-e to go back to parent schematic
- e to descend into schematic of selected symbol
- i to descend into symbol of selected symbol
- f full zoom on schematic
- Shift-z to zoom in
- Ctrl-z to zoom out

#### **20.0.0.2 Editing schematics:**

- Del to delete elements
- Ins to insert elements from library
- Escape to abort an operation
- Ctrl-# to rename components with duplicate names
- c to copy elements
- Alt-Shift-l to add wire label
- Alt-l to add label pin
- m to move selected objects
- Shift-R to rotate selected objects
- Shift-F to mirror / flip selected objects
- q to edit properties
- Ctrl-s to save schematic
- t to place a text
- Shift-T to toggle the ignore flag on an instance
- u to undo an operation
- w to draw a wire
- Shift-W draw wire and snap to close pin or net point
- & to join, break, and collapse wires
- A to make symbol from schematic
- Alt-s to reload the circuit if changes in a subcircuit were made

#### **20.0.0.3 Viewing/Simulating Schematics**

- 5 to only view probes
- k to highlight selected net
- Shift-K to unhighlight all nets
- Shift-o to toggle light/dark color scheme
- s to run a simulation
- a & b to add cursors to an in-circuit simulation graph
- f full zoom on y- or x-axis in in-circuit simulation graph

## **21 Appendix: ngspice Cheatsheet**

Here is an unsorted list of useful ngspice settings and command:

### **21.1 Commands**

- ac dec|lin points fstart fstop performs a small-signal ac analysis with either linear or decade sweep

- `dc sourcename vstart vstop vincr [src2 start2 stop2 incr2]` runs a dc-sweep, optionally across two variables
- `display` shows the available data vectors in the current plot
- `echo` can be used to display text, `$variable` or `$&vector`, can be useful for debugging
- `let name = expr` to create a new vector; `unlet vector` deletes a specified vector; access vector data with `$&vec`
- `linearize vec` linearizes a vector on an equidistant time scale, do this before an FFT; with `set specwindow=windowtype` a proper windowing function can be set
- `meas` can be used for various evaluations of measurement results (see ngspice manual for details)
- `noise v(output <ref>) src (dec|lin) pts fstart fstop` runs a small-signal noise analysis
- `op` calculates the operating point, useful for checking bias points and device parameters
- `plot expr vs scale` to plot something
- `print expr` to print it, use `print all` to print everything
- `remzerovec` can be useful to remove vectors with zero length, which otherwise cause issues when saving or plotting data
- `rusage` plot information about resource usage like memory
- `save all` or `save signal` specifies which data is saved during simulation; this lowers RAM usage during simulation and size of RAW file; do `save` before the actual simulation statement
- `setplot` show a list of available plots
- `set var = value` to set the value of a variable; use variable with `$var`; `unset var` removes a variable
- `set enable_noisy_r` to enable noise of behavioral resistors; usually, this is a good idea
- `shell cmd` to run a shell command
- `show : param`, like `show : gm` shows the  $g_m$  of all devices after running an operating point with `op`
- `spec` plots a spectrum (i.e. frequency domain plot)
- `status` shows the saved parameters and nodes
- `tf` runs a transfer function analysis, returning transfer function, input and output resistance
- `tran tstep tstop <tstart <tmax>>` runs a transient analysis until `tstop`, reporting results with `tstep` step size, starting to plot at `tstart` and performs time steps not larger than `tmax`
- `wrdata` writes data into a file in a tabular ASCII format; easy to further process
- `write` writes simulation data (the saved nodes) into a RAW file; default is binary, can be changed to ASCII with `set filetype=ascii`; with `set appendwrite` data is added to an existing file

## 21.2 Options

Use option `option=val` `option=val` to set various options; important ones are:

- `abstol` sets the absolute current error tolerance (default is 1pA)
- `gmin` is the conductance applied at every node for convergence improvement (default is 1e-12); this can be critical for very high impedance circuits
- `klu` sets the KLU matrix solver
- `list` print the summary listing of the input data
- `maxord` sets the numerical order of the integration method (default is 2 for Gear)
- `method` set the numerical integration method to `gear` or `trap` (default is `trap`)

- `node` prints the node table
- `opts` prints the option values
- `temp` sets the simulation temperature
- `reltol` set the relative error tolerance (default is  $0.001 = 0.1\%$ )
- `savecurrents` saves the terminal currents of all devices
- `sparse` sets the sparse matrix solver, which can run noise analysis, but is slower than `klu`
- `vntol` sets the absolute voltage error tolerance (default is  $1\mu\text{V}$ )
- `warn` enables the printing of the SOA warning messages

## 21.3 Convergence Helper

- option `gmin` can be used to increase the conductance applied at every node
- option `method=gear` can lead to improved convergence
- `.nodeset` can be used to specify initial node voltage guesses
- `.ic` can be used to set initial conditions

## 21.4 Internal Variables

Variables can be set using `set var=value` and accessed with `$var`. Useful internal variables are:

- To set the fontsize of plots, use `xfont_size`
- To append data to an existing RAW file, use `appendwrite=1`
- Get the name of the current plot with `curplot`
- The filetype of the RAW file can be set with `filetype`, either `binary` (default) or `ascii`
- The number of threads can be set with `num_threads`
- The noise PSDs will be given in  $\text{V}^2/\text{Hz}$  or  $\text{A}^2/\text{Hz}$  when setting `sqrnoise=1` (otherwise  $\text{V}/\text{rtHz}$  or  $\text{A}/\text{rtHz}$ )

# 22 Appendix: Circuit Designer's Etiquette

## 22.1 Prolog

A consistent naming and schematic drawing style, as well as VHDL/Verilog coding scheme, is a huge help in avoiding errors and increasing productivity. Even if just one person works on a design, the error rate is lowered. If multiple persons work together in a team, a consistent working style is a big help for smooth cooperation without misunderstanding each other's intentions. Consistency also helps to reuse existing blocks. In a well-done design, the documentation is included in the schematic/source code, so there is no searching for a piece of documentation somewhere else (which is often not found anyway).

## 22.2 Pins

- Name package pins (interfacing with the outside the IC) in **UPPERCASE**, and all internal signals in **lowercase**.
- Supply voltages like VDD/VCC and ground like VSS/GND need to start with either `VDD`, `VCC`, `VSS`, `VEE` or `GND`, plus a suitable suffix. Examples: `VDD1`, `VDD_AMP`, `vdd_ldo_out`, `VSS_ANA` (uppercase means connected to a pin, lowercase means a VDD is created on-chip by, e.g., an LDO).
- Preferred are `VDD/VSS` for CMOS and `VCC/GND` for bipolar circuits. In BiCMOS circuits `VDD/VSS` are preferred, as usually, the digital content is the major part.

- Digital signals in an analog schematic should start with `di_` (for digital input) or `do_` (for digital output). Example: `di_ctrl1`. In the rare case of a bi-directional digital signal `dio_` can be used.
- Name digital signals consistently: `di_pon` is active-high, `di_pon_b` is active-low (`_b` standing for the negating “bar”); as an alternative, this last signal could be named `di_disable`. `di_reset` is an active-high reset, but often a reset is active-low, so it needs to be named `di_reset_b` (an alternative is `di_reseth`).
- In mixed-voltage designs, it might be useful to append the voltage level of a signal to avoid connecting incompatible inputs and outputs. Example: `do_comp_1v2` or `di_poweron_3v3`.
- Digital buses always have the MSB to the left and LSB to the right. Example: `do_adc[7:0]`.
- Analog signals should start with a `v` for a voltage signal or `i` for a current signal. It is often useful to include a value for bias signals or make the naming meaningful. RF signals, which are often neither voltage nor current signals, start the name with `rf_`. Examples: Signal and pin names like `ibias_30u` (30uA of bias current), `vbg_1v2` (a bandgap voltage of 1.2V), `vin_p`, `v_filt_out_n`, and `rf_lna_i` speak for themselves.
- Appending analog signals with `_i` and `_o` might be useful if a clear direction is obvious in the signal flow. If a signal is bi-directional, it is better to skip `_io`. If using `_p` or `_n` in combination with `_i` or `_o` then use `_pi/_ni` or `_po/_no`.
- Consistently use pin types `input`, `output`, or `inout` to indicate signal flow. Power supply pins are of `inout` type.

## 22.3 Schematics

- In analog schematics, add a textual note about basic circuit performance. For example, in an amplifier, note things like suitable supply range, typical and w.c. current consumption, gain, GBW, input voltage range, PSRR, and other useful information.
- If a circuit has a quirk or is particularly clever, add a note on how it works, so others can understand the function without excessive analysis (reviewing a circuit should not be a brain teaser).
- Use provided borders or drawing templates for schematics, and fill the data in, like circuit designer name, date, change history, project name, etc.
- Use a versioning system for your data, and check in often. This avoids data loss, and going back to an earlier design stage is simple. SVN is often preferable to GIT for binary data.
- Draw uncluttered clear circuits. Ideally, the circuit function is apparent by inspection **quickly**. Everyone can obscure an inverter so that it takes 5 minutes to recognize it, but this is not a good design.
- Don’t alter the standard grid setting while drawing schematics (also make sure that the pins in your drawn symbols are on the standard grid)! Off-grid schematic elements will haunt you and your colleagues forever!
- Once a schematic is finished, take the time to name component instances properly (you can use speaking names like `Rstab` or simply use `R1`, `R2`, etc.). Use iterated instances to clean up the circuit. Use wire bundles to clean up circuits where useful. A clever technique is to use bundles and iterated instances to efficiently draw large resistor ladders, for example (however, use with care).
- Avoid connection-by-name, as it makes the circuit hard to read. However, there is a fine line to not cluttering circuits. Signals with many connections (`vdd`, `vss`, `pon`, `pon_b`) are often better done with connection-by-name instead of drawing a wire.

- Some tools allow the use of colored wires, which might be used to mark signal paths, bias lines, etc. However, this should not be overdone; use it with care.
- If you add auxiliary elements like current probes, ensure they get proper treatment when creating the netlist for the LVS (some elements should be shorted, and some elements simply taken out). Ideally, only use a single schematic for simulation, LVS, etc. By using tool features this can usually be done, and avoids the need to keep multiple schematics of one block in sync.
- Use annotations in the schematics to (1) denote current levels in branches, (2) denote bias voltage levels, (3) explain the function of logic input signals, and (4) put in logic tables if not obvious.
- Add comments concerning the layout, like matching devices, certain considerations of placement, sensitive nodes, etc.
- Add simple ASCII diagrams for timing signals if useful.
- Name internal signals (signals connected to pins are anyway named like the port) in a meaningful way; this makes tracking signals in simulation or layout much easier (automatic net names like `net0032` are of not much help).
- Properly name instances, not just `I1` or `I2`; better is `amp1`, `inv2`, etc. (a descriptor in a tool output like `I1/I13/I5/net017` is not helpful; compare that to `adc1/bias/bg/vref_int`).
- On check-and-save, never ignore warnings; just fix them! They will annoy you and others forever and might flag critical design flaws.
- Name cells interpretably, ideally making the function clear already by the name. It is often useful to prefix or postfix a cell by the project name and design iteration. Example: In the project `GIGAPROJECT`, the cells which are changed in the second design step are prefixed with `g2_`, like `g2_amp_bias`. Of course, more letters as a project abbreviation are useful if a name collision is likely to happen.
- Cell names in lowercase are a good choice, as otherwise, capitalization leads to inconsistency in cell names. Use `_` to break words instead of `CamelCase`, like `amp_bias_startup`.
- When building a design, start with the hierarchy first; plan a suitable design structure, and define all interfaces. Implement simple behavioral models for every circuit block (either with controlled sources or using Verilog-A or VHDL/Verilog digital models). In this way, you can simulate the overall design early and find issues in the hierarchy or the interconnects. Then, populate the hierarchy with the detailed circuit designs in the leaf cells. At each point in the design process, you have a design that can be simulated, with some blocks as behavioral models and some blocks already designed. Try to avoid scattered circuit elements (digital or analog) in the hierarchy; it is better to push all components into the leaf cells.
- Avoid huge schematics, better break them down into smaller, maintainable, and self-contained blocks, and provide a simulation test bench for these simple blocks. In this way, later re-simulation across the hierarchy is easily possible.
- When building up the hierarchy, choose pin names and signal names as consistently as possible. Example: use the signal name `vref_int` when connecting two leaf cells with the pin names `vref_int_o` and `vref_int_i`.
- Avoid the excessive use of net breakers like small resistors, as they inhibit net tracing and can lead to simulation convergence issues. If a net breaker is needed (or a current should be probed) use a 0V dc voltage source.

## 22.4 Symbols

- Spend time drawing nice symbols! Ideally, the underlying circuit functionality is apparent by just looking at the symbol.
- Arrange the pins in a meaningful way.
- Group pins that belong together. An often useful arrangement is to locate the inputs on the left side, outputs on the right, digital control inputs at the bottom, and supplies at the top.
- Make the origin of a symbol in the top-left corner. In this way, symbols can be changed more easily, for example, by swapping out different versions of blocks.
- The cell name (and potentially library name) should be visible in the symbol, not only in the properties.

## 22.5 Design Robustness

- It is good practice to buffer incoming digital signals with a local inverter (connected to the local block supply) before connecting it to internal nodes. This improves the slew rate of the control signal and lowers the chance of unwanted cross-talk.
- Consider dummy elements for good matching, and try to make useful unit sizes of components. This will make the layout creation much smoother.
- The golden rule of good analog performance is good matching, and good matching is achieved by identical components (size, orientation, surroundings)! If the layout does not look nice (humans like symmetry), it will not perform well.
- Consider supply decoupling and bias voltage decoupling inside the cells. Often, dummy elements can be used for that. Be aware, however, of unwanted supply resonances (think bond wire L and decoupling C) and slow transients of bias nodes after disturbance.
- Always implement a proper power-down mode. Avoid floating nodes in off-mode. The better defined the on- as well as the off-mode are, the less the chance of leakage currents. Always simulate both modes (on and off), and also simulate a transient power-up of a circuit to identify issues with slow bias start or insufficient turn-off, or nasty feedback loop instabilities during transients.
- When drawing the first schematic, add parasitic capacitances to each node. If all nodes are labeled, a capacitor bank is easily put into one corner of the schematic with parasitic caps tied to the ground. Use 5fF as a starting value (and replace it later with the correct value from parasitic extraction). This accounts for some wiring parasitics in layout and helps to account for these layout impairments early in the design phase and later when simulating the schematic instead of the extracted netlist with parasitics.

## 22.6 Rules for Good Mixed-Signal and RF Circuits

- Separate analog and digital power supply, connect to package pins with multiple bond wires/bumps, and separate noisy and clean vdd/vss from each other!
- Prevent supply loops; keep vdd and vss lines close to each other (incl. bond wires and PCB traces)! This minimizes L and coupling factor k.
- Some prefer a massive (punched) ground plane, which is possible if you have enough metal levels. With a ground plane, the return path of a signal or supply line is just a few microns away.
- Use chip-internal decoupling capacitors, and decouple bias voltages to the **correct** potential (vdd or vss, or another node, depending on the circuit)!

- Use substrate contacts and guard rings to lower substrate crosstalk but use a quiet potential for connection; use triple-well if available! Connecting a guard-ring/substrate contact to a noisy supply is a prime noise injector (usually unwanted).
- Physically separate quiet and noisy circuits (at least by the epi thickness)!
- Reduce circuit noise generation as much as possible (avoid switching circuits if possible, use constant-current circuits instead, and use series/shunt regulators for supply isolation).
- Reduce sensitivity of circuits to interference (by using a fully differential design with high PSRR/CMRR, symmetrical layout parasitics, and good matching)!

## 22.7 VHDL/Verilog Coding Guide

These recommendations are specifically targeted at Verilog; however, they apply similarly to VHDL.

- Use automatic checkers (linters) to see whether your code contains errors or vulnerabilities. Commercial or open-source tools allow this, e.g., Icarus Verilog (`iverilog -g2005 -tnull FILE.v`) or Verilator (`verilator --lint-only -Wall FILE.v`).
- Write readable and maintainable code; use speaking variable names, and use a naming convention for inputs (ending with `_i`) and outputs (ending with `_o`). IO signals are using `_io`. Active-low signals have an `n` or `b` in their name (coming before the direction), like `reset_ni`. Use comments to explain the intention.
- With a synchronous reset reset-related racing conditions are often avoided. If an asynchronous reset is desirable (which is often the case), ensure the reset signals are free from race conditions.
- Module-local registers and wires could append `_w` (for Verilog `wire`) or `_r` (for Verilog `reg`) to make their function clear. This is not required in SystemVerilog where the unified type `logic` should be used.
- Use an `assign` statement for logic as this often is easier to read than an `always @(*)` block. The ternary operator `COND ? TRUE : FALSE` can help with conditional assignments and is often a better choice than a (nested) `if ... else` statement.
- Declare all outputs explicitly with either `reg` or `wire`.
- Use local parameter definitions with `localparam` in a module to make the code easier to follow. Name parameters in **UPPERCASE**.
- Take care to reset all registers to a defined state (in simulation and HW).
- Use the rule of “one file per module.” The filename shall match the module declaration.
- Use ``default_nettype none` at the beginning of a file containing a module definition. After the module you can use ``default_nettype wire`. This will add a safety net against typos in signal names.
- In a logic assign block, use `assign @(*) begin ... end` instead of spelling out the signals in the sensitivity list. Forgetting a signal could lead to serious mismatches between simulation and HW.
- Make your code flexible by making bit widths and other values parameterized using a `localparam` or module parameter.
- Be cautious of implicit type conversions and bit-width adaptions; better make explicit conversions and match bit widths in assignments.
- Use only blocking assignments (`=`) in `always @(*)` blocks, and only non-blocking assignments (`<=`) in clocked `always @(posedge ...)` blocks.

- It is recommended to follow this naming convention for latches and flip-flops: **Synchronous** set and reset should be called `set` (for setting, i.e.,  $Q=1$ ) and `res` (for resetting, i.e.,  $Q=0$ ). **Asynchronous** set and reset should be called `pre` (for presetting) and `clr` (for clearing). In this way it is immediately clear whether a control input is acting independent of the `clk` (i.e., asynchronous) or dependent on the `clk` (i.e., synchronous).

A comprehensive coding style guide for Verilog/SystemVerilog can be found [here](#), and it is highly recommended to follow it.

## 22.8 Further Reading

- Good information about drawing schematics, design testbenches, etc: <https://circuit-artists.com>
- Sutherland/Mills, *Verilog and SystemVerilog Gotchas - 101 Common Coding Errors and How to Avoid Them*, Springer, 2010
- B. Razavi, *The Analog Mind*, recurrent column in IEEE Solid-State Circuits Magazine

## Bibliography

- [1] P. R. Gray, P. J. Hurst, S. H. Lewis, and R. G. Meyer, *Analysis and Design of Analog Integrated Circuits*. Wiley, 2009.
- [2] B. Razavi, *Design of Analog CMOS Integrated Circuits*. McGraw-Hill, 2017.
- [3] W. M. C. Sansen, *Analog Design Essentials*. Springer, 2006.
- [4] C. Hu, *Modern Semiconductor Devices for Integrated Circuits*. Pearson, 2010.
- [5] Y. Tsividis and C. McAndrew, *Operation and Modeling of the MOS Transistor*. Oxford University Press, 2011.
- [6] L. W. Nagel, “SPICE2: A Computer Program to Simulate Semiconductor Circuits,” 1975. [Online]. Available: <http://www2.eecs.berkeley.edu/Pubs/TechRpts/1975/9602.html>
- [7] B. Jakoby, “Achieving signal power amplification using energetically passive devices,” *e&i Elektrotechnik und Informationstechnik*, vol. 139, no. 6, pp. 477–484, 2022, doi: 10.1007/s00502-022-01046-9.
- [8] J. C. Maxwell, *A Treatise on Electricity and Magnetism*, vol. 1. Clarendon Press, 1873.
- [9] P. G. A. Jespers and B. Murmann, *Systematic Design of Analog CMOS Circuits: Using Pre-Computed Lookup Tables*. Cambridge University Press, 2017.
- [10] S. Dorrer, “An Open-Source Adaptive Event-Based ADC for Bio-Signal Acquisition in 130\,nm CMOS.” [Online]. Available: <https://epub.jku.at/obvulihs/content/titleinfo/12118473?query=dorrer>
- [11] T. C. Carusone, D. Johns, and K. Martin, *Analog Integrated Circuit Design*. Wiley, 2011.
- [12] H. Pretl and M. Eberlein, “Fifty Nifty Variations of Two-Transistor Circuits: A tribute to the versatility of MOSFETs,” *IEEE Solid-State Circuits Magazine*, vol. 13, no. 3, pp. 38–46, 2021.
- [13] E. H. Hellen, “Verifying the diode–capacitor circuit voltage decay,” *American Journal of Physics*, vol. 71, no. 8, pp. 797–800, 2003, doi: 10.1119/1.1578070.

- [14] S. Rosenstark, “Loop gain measurement in feedback amplifiers,” *International Journal of Electronics*, vol. 57, no. 3, pp. 415–421, 1984, doi: 10.1080/00207218408938921.
- [15] R. D. Middlebrook, “Measurement of loop gain in feedback systems,” *International Journal of Electronics*, vol. 38, no. 4, pp. 485–512, 1975, doi: 10.1080/00207217508920421.
- [16] M. Tian, V. Visvanathan, J. Hantgan, and K. Kundert, “Striving for small-signal stability,” *IEEE Circuits and Devices Magazine*, vol. 17, no. 1, pp. 31–41, 2001.
- [17] M. Neag, R. Onet, I. Kovács, and P. Martari, “Comparative Analysis of Simulation-Based Methods for Deriving the Phase- and Gain-Margins of Feedback Circuits With Op-Amps,” *IEEE Transactions on Circuits and Systems I: Regular Papers*, vol. 62, no. 3, pp. 625–634, 2015, doi: 10.1109/TCSI.2014.2370151.
- [18] A. Sheikholeslami, “Noise and Distortion, Part IV [Circuit Intuitions],” *IEEE Solid-State Circuits Magazine*, vol. 17, no. 3, pp. 29–31, 2025, doi: 10.1109/MSSC.2025.3582840.
- [19] R. Sarpeshkar, T. Delbruck, and C. Mead, “White noise in MOS transistors and resistors,” *IEEE Circuits and Devices Magazine*, vol. 9, no. 6, pp. 23–29, 1993, doi: 10.1109/101.261888.
- [20] R. Widlar, “Some Circuit Design Techniques for Linear Integrated Circuits,” *IEEE Transactions on Circuit Theory*, vol. 12, no. 4, pp. 586–590, 1965, doi: 10.1109/tct.1965.1082512.
- [21] A. D. Blumlein, “Thermionic Valve Amplifying Circuit.” 1937.
- [22] B. Murmann, *Analysis and Design of Elementary MOS Amplifier Stages*. NTS Press, 2013.
- [23] B. Kamath, R. Meyer, and P. Gray, “Relationship between frequency response and settling time of operational amplifiers,” *IEEE Journal of Solid-State Circuits*, vol. 9, no. 6, pp. 347–352, 1974, doi: 10.1109/JSSC.1974.1050527.
- [24] M. Pelgrom, A. Duinmaijer, and A. Welbers, “Matching properties of MOS transistors,” *IEEE Journal of Solid-State Circuits*, vol. 24, no. 5, pp. 1433–1439, 1989, doi: 10.1109/JSSC.1989.572629.
- [25] R. J. Baker, “Bad Circuit Design 3 - Compensating an Op-Amp.” [Online]. Available: [https://cmosedu.com/cmos1/bad\\_design/bad\\_design3/bad\\_design\\_3.htm](https://cmosedu.com/cmos1/bad_design/bad_design3/bad_design_3.htm)
- [26] B. Razavi, “The Low Dropout Regulator [A Circuit for All Seasons],” *IEEE Solid-State Circuits Magazine*, vol. 11, no. 2, pp. 8–13, 2019, doi: 10.1109/mssc.2019.2910952.
- [27] B. Hosticka, “Improvement of the gain of MOS amplifiers,” *IEEE Journal of Solid-State Circuits*, vol. 14, no. 6, pp. 1111–1114, 1979, doi: 10.1109/jssc.1979.1051324.
- [28] V. V. Ivanov and I. M. Filanovsky, *Operational Amplifier Speed and Accuracy Improvement*. Kluwer Academic Publishers, 2004.
- [29] R. Widlar, “New developments in IC voltage regulators,” *IEEE Journal of Solid-State Circuits*, vol. 6, no. 1, pp. 2–7, 1971, doi: 10.1109/jssc.1971.1050151.
- [30] K. E. Kuijk, “A precision reference voltage source,” *IEEE Journal of Solid-State Circuits*, vol. 8, no. 3, pp. 222–226, 1973, doi: 10.1109/JSSC.1973.1050378.
- [31] A. Brokaw, “A simple three-terminal IC bandgap reference,” *IEEE Journal of Solid-State Circuits*, vol. 9, no. 6, pp. 388–393, 1974, doi: 10.1109/JSSC.1974.1050532.

- [32] H. Banba *et al.*, “A CMOS bandgap reference circuit with sub-1-V operation,” *IEEE Journal of Solid-State Circuits*, vol. 34, no. 5, pp. 670–674, 1999, doi: 10.1109/4.760378.
- [33] M. Eberlein, G. Panagopoulos, and H. Pretl, “A 40nW, Sub-IV Truly ‘Digital’ Reverse Bandgap Reference Using Bulk-Diodes in 16nm FinFET,” *2018 IEEE Asian Solid-State Circuits Conference (A-SSCC)*, vol. 0, pp. 99–102, 2018, doi: 10.1109/asscc.2018.8579306.
- [34] B. Razavi, “The Design of a Low-Voltage Bandgap Reference [The Analog Mind],” *IEEE Solid-State Circuits Magazine*, vol. 13, no. 3, pp. 6–16, 2021, doi: 10.1109/mssc.2021.3088963.
- [35] A. Sheikholeslami, “Miller’s Theorem [Circuit Intuitions],” *IEEE Solid-State Circuits Magazine*, vol. 7, no. 3, pp. 9–10, 2015, doi: 10.1109/mssc.2015.2446457.
- [36] C. Mangelsdorf, “Miller’s Secret [Shop Talk: What you didn’t Learn in School],” *IEEE Solid-State Circuits Magazine*, vol. 17, no. 1, pp. 21–27, 2025, doi: 10.1109/mssc.2024.3503792.
- [37] S. Pavan, “An Alternative Approach to Bode’s Noise Theorem,” *IEEE Transactions on Circuits and Systems II: Express Briefs*, vol. 66, no. 5, pp. 738–742, 2019, doi: 10.1109/TCSII.2019.2907860.